For NRC
Site Repts

DEPARTMENT OF THE INTERIOR

U.S. GEOLOGICAL SURVEY

M.C. Tynan
9/23/96

CHARACTERISTICS OF FRACTURES AT YUCCA MOUNTAIN, NEVADA: SYNTHESIS REPORT

by D.S. Sweetkind and S.C. Williams-Stroud

Administrative Report

Prepared in cooperation with the
NEVADA OPERATIONS OFFICE,
U.S. DEPARTMENT OF ENERGY, under
Interagency Agreement DE-AI08-92NV10874

Denver, Colorado

1996

102

U.S. DEPARTMENT OF THE INTERIOR
BRUCE BABBITT, SECRETARY

U.S. GEOLOGICAL SURVEY

GORDON P. EATON, Director

ADMINISTRATIVE REPORT

CONTENTS

FIGURES

TABLES

CONVERSION FACTORS AND ACRONYMS

Multiply	by	To obtain
millimeter (mm)	0.03937	inch
centimeter (cm)	0.3937	inch
meter (m)	3.281	foot
kilometer (km)	0.6214	mile

The following terms and abbreviations also are used in this report.

Ma	millions of years old
m.y.	millions of years ago

EXECUTIVE SUMMARY

A large and varied fracture data set has been collected at Yucca Mountain over the past 15 years as part of the geologic and hydrologic site characterization of a potential repository for high-level radioactive waste at Yucca Mountain, Nevada. Collection of fracture data is an integral part of the site characterization of Yucca Mountain. The fracture data are used in interpretation of the tectonic history of Yucca Mountain, in the construction of simulated three-dimensional fracture network models and in models of surface infiltration. The infiltration and fracture network models both feed into overall models of flow in the unsaturated zone at Yucca Mountain and into models of pneumatic pathways.

Data on the geometry of the fracture network developed within Miocene volcanic rocks at Yucca Mountain come from detailed maps of cleared pavements, areal surveys of natural exposures, and geologic mapping, line surveys and close-range photogrammetric mapping within a tunnel currently being excavated at the site. Digital data from all of these sources have been consolidated into a single database to facilitate quantitative analysis of fracture attributes. This report synthesizes the results from past surface fracture studies at Yucca Mountain, augmented by qualified data from the subsurface.

The biggest differences in the various available data sets are not the result of the data being qualified or non-qualified, but rather are due to the different methods of data collection. Each of the fracture data sets has its own strengths and limitations; each study resulted in the collection of different, and at times not exactly comparable, fracture characteristics. The only fracture attributes that are common to all of the data sets are orientation, trace length and the lithology in which the fracture occurs.

Despite their differences, an integration of the various data sets allows some important and fundamental generalizations to be made about the fracture network. The strength of the fracture studies at Yucca Mountain lies in the quantity and variety of data sets that provide a rare three-dimensional sampling of the fracture network. Analysis of the fracture data allows the following general conclusions to be made: 1) fracture intensity is dependent on lithology, variations in degree of welding, and on proximity to faults; 2) the connectivity of the fracture network is largely dependent on lithology and especially on the degree of welding; and 3) the width and intensity of fractured zones around faults is variable.

INTRODUCTION

Fracture studies are an integral part of the site characterization of Yucca Mountain, Nevada as a potential repository for high-level radioactive waste. The potential repository would be located in densely welded tuff within a thick sequence of variably welded Miocene ignimbrite tuff at an elevation 200-300 m above the water table (Office of Civilian Radioactive Waste Management, 1988). Most of the tuffs have very low matrix permeabilities (Montazer and Wilson, 1984), so the fracture network and faults are the primary pathways for air and water flow into and out of the potential repository. A quantitative measure of the interconnectivity of the fracture network is required in hydrologic models of fluid flow into and through the potential repository. One of the goals of fracture studies is to determine the relative importance of fractures with different characteristics, such as trace length, orientation, or aperture, to the connected fracture network. The fracture data are used in interpretation of the tectonic history of Yucca Mountain, in the construction of simulated 3-D fracture network models, and in models of surface infiltration. The infiltration and fracture network models both feed into site scale models of flow in the unsaturated zone at Yucca Mountain and in models of pneumatic pathways. The geometry of the fracture network would also affect the mechanical stability of the rock mass during and after the construction of the repository. Barton and others (1993) stated a three-fold impetus for the study of fractures: 1) to characterize the fracture network for hydrologic flow, 2) to characterize the fracture network for mechanical stability of the potential repository, and 3) to better understand the sequence of fracture formation and how it relates to the paleostress history of Yucca Mountain. In general, subsequent studies have tried to fulfill the same objectives.

GEOLOGIC SETTING

Yucca Mountain consists of a series of north-south-striking fault-bounded blocks 1 to 4 km wide (Scott, 1990). The central part of Yucca Mountain that includes the potential repository is a structurally simple homoclinal sequence of Tertiary volcanic rocks that tilts gently eastward at 5-10 degrees. This central block is bounded by the Solitario Canyon fault on the west and the Bow Ridge fault on the east (fig. 1). Both of these major faults dip steeply to the west and have cumulative displacements in the range of 100 to 200 m (Scott, 1990). Faults within the central block are typically short, discontinuous and have minor displacement (5 to 10 m). The largest

intrablock fault, the Ghost Dance fault, has up to 25 m of displacement and roughly bisects the potential repository area.

Yucca Mountain is underlain by a thick sequence of Tertiary volcanic strata. The dominant stratigraphic units at the surface and near subsurface are parts of the Miocene Paintbrush Group (Sawyer and others, 1994). This sequence of volcanic rocks is greater than 460 m thick, and consists of two densely welded pyroclastic flows, the Topopah Spring Tuff and the Tiva Canyon Tuff, separated by an interval of variably welded pyroclastic deposits (fig. 2). Both the Topopah Spring Tuff and the Tiva Canyon Tuff have been informally subdivided into a lower crystal-poor rhyolite member and an upper crystal-rich quartz latite member (Buesch and others, 1996). Both the Topopah Spring Tuff and the Tiva Canyon Tuff have been further subdivided into informal stratigraphic units (fig. 2) based on zonal variations within the welded portions of the pyroclastic flows. These zonal variations form mappable, semi-tabular bodies that reflect variations in degree of welding, development and character of lithophysae, and degree of devitrification (Buesch and others, 1996).

The stratigraphic interval within the Paintbrush Group at Yucca Mountain that extends from the base of the densely welded and devitrified portion of the Tiva Canyon Tuff downward to the top of the densely welded portion of the underlying Topopah Spring Tuff includes various interstratified pyroclastic-flow and fall deposits with a minor amount of reworked pyroclastic material (Moyer and others, 1996). This interval includes parts or all of four formations (the Tiva Canyon Tuff, the Yucca Mountain Tuff, the Pah Canyon Tuff, and the Topopah Spring Tuff) and three informally designated intervening bedded tuff units (Moyer and others, 1996). In descending stratigraphic order and using the informal stratigraphic nomenclature of Buesch and others (1996), this interval includes: the moderately welded and non- to partially welded subzones of the crystal-poor vitric zone of the Tiva Canyon Tuff (Tpcpv2 and Tpcpv1, respectively); the pre-Tiva Canyon Tuff bedded tuffs (Tpbt4); the Yucca Mountain Tuff (Tpy); the pre-Yucca Mountain Tuff bedded tuffs (Tpbt3); the Pah Canyon Tuff (Tpp); the pre-Pah Canyon Tuff bedded tuffs (Tpbt2); and the non- to partially welded and moderately welded subzones of the crystal-rich vitric zone of the Topopah Spring Tuff (Tptrv3 and Tptrv2, respectively). Stratigraphic relations of rock units within this interval are discussed in detail by Moyer and others (1996). This interval corresponds to the Paintbrush Tuff nonwelded (PTn)

hydrologic and thermal-mechanical unit (Montazer and Wilson, 1984; Ortiz and others, 1985). For the sake of brevity in this report, this interval will occasionally be referred to as the PTn hydrologic unit rather than naming all of the constituent lithostratigraphic units.

The stratigraphic interval within the Paintbrush Group above the welded portion of the Tiva Canyon Tuff includes the post-Tiva Canyon bedded tuff (Tpbt5 of Buesch and others, 1996) and a pyroclastic-flow (Tpki of Buesch and others, 1996, equivalent to tuff unit "x" of Carr, 1992). These units are rarely observed at the surface, but are visible within the ESF.

HISTORICAL OVERVIEW

Fracture data have been collected at Yucca Mountain over the past 15 years by a number of workers, motivated by a variety of goals and project requirements. Surface fracture data have been collected from the mapping of cleared exposures and the study of abundant natural exposures. In the past year, surface fracture data have been augmented by geologic mapping, line surveys and photogrammetry within the Exploratory Studies Facility (ESF), a 7.6-m diameter tunnel currently being excavated at the site (fig. 3). A brief historical synopsis of fracture data collection efforts at Yucca Mountain is presented below. A summary of the data generated by the various studies, including availability, data tracking numbers and QA status, is presented in table 1.

Pavement studies

The fracture mapping during 1984 and 1985 on pavements 100, 200, and 300 on Live Yucca Ridge and Dead Yucca Ridge (fig. 4) were the first surface-based, systematic studies designed to characterize the fracture network at Yucca Mountain (Barton and others, 1993). These pavements were followed by the clearing and mapping of pavement 500, at the east end of Live Yucca Ridge (fig. 4), in 1985, and pavement 600, in the vicinity of Drill Hole Wash (fig. 4), in 1985 and 1986. In addition to these cleared areas, pavement 400, a large natural exposure on top of Busted Butte, was mapped in 1990 (fig. 4, table 1). All of these pavements are in the same lithologic unit, the upper lithophysal zone of the Tiva Canyon Tuff. Pavement 1000, also mapped during this period, is located at the southern end of Fran Ridge (fig. 4) and is in the middle nonlithophysal zone of the Topopah Spring Tuff. The data from pavements 100, 200,

Table [illegible]mary of data included in synthesis report.

NUMBER	FRACTURE STUDY	INVESTIGATOR	DATA COLLECTION DATES	DATA AVAILABILITY	DATA TRACKING NUMBER	GOVERNING PROCEDURE	QA STATUS
1	Pavement 400	Larson, E. et al (Barton, C.)	1990	Data Package	GS910908314222.003	GP-12, R0	Non-qualified[1]
2	Pavements 100, 200, 300	Barton, C. and others	1984-85	Open File Report 93-269	GS940608314222.002	GP-12, R0	Non-qualified[1]
3	Pavements 100, 200, 300	Barton, C. and others	1984-85	Data Package	GS910908314222.003	GP-12, R0	Non-qualified[1]
4	Pavement 500	Baechle, P. and Barton, C.	1985	Data Package	GS910908314222.003	GP-12, R0	Non-qualified[1]
5	Pavement 1000	Page, R.	1985	Data Package	GS910908314222.003	GP-12, R0	Non-qualified[1]
6	Pavement 600	Throckmorton, C.	1986	Data Package	GS910908314222.001	GP-12, R0	Non-qualified[1]
7	41 uncleared outcrops	Throckmorton, C. and Verbeek, E.	1990-1991	Data Package	GS910908314222.002	GP-12, R0	Qualified
8	41 uncleared outcrops	Throckmorton, C. and Verbeek, E.	1990-1991	Open File Report 95-2	–[2]	GP-12, R0	Non-qualified[3]
9	Ghost Dance fault mapping	Braun, C., Spengler, R., and others	1992	Developed Data	GS940308314221.003	GP-12, R1; GP-01, R2	Qualified
10	Ghost Dance fault mapping	Braun, C., Spengler, R., and others	1992	Data Package	GS920708314221.002	GP-12, R1; GP-01, R2	Qualified
11	Ghost Dance fault mapping	Braun, C., Spengler, R., and others	1992	Data Package	GS921008314221.006	GP-12, R1; GP-01, R2	Qualified
12	Ghost Dance fault mapping	Braun, C., Spengler, R., and others	1992	Data Package	GS940108314221.001	GP-12, R1; GP-01, R2	Qualified
13	ESF Starter Tunnel DLS	Fahy, M. and Beason, S.	1992	Data Package	GS931008314224.006	GP-32, R0	Qualified
14	ESF Starter Tunnel FPMap	Fahy, M. and Beason, S.	1992	Map (Developed Data)	GS940208314224.002	GP-32, R0	Qualified
15	Antler Ridge Pavement	Fahy, M.	1993-1994	Data Package	GS940308314222.001	GP 12 R1	Qualified
16	Pavement P2001 (Fran Ridge)	Sweetkind, D. S.	1994	Data Package	GS950108314222.001	GP-12, R1, M1	Qualified
17	Pavement P2001 (Fran Ridge)	Sweetkind, D. S., Verbeek, E.R. and others	1994	Administrative Report	GS950508314222.004	GP-12, R1, M1	Qualified
18	Ptn section pavements	Sweetkind, D.S.	1995	Data Package	GS950508314222.003	GP-12, R1, M1	Qualified
19	Ptn section outcrops	Verbeek, E.R.	1995	Data Package	GS950608314222.005	P-12, R1, M1; HP-24	Qualified
20	Ptn section fractures	Sweetkind, D. S., Verbeek, E.R. and others	1995	Administrative Report	GS950808314222.006	P-12, R1, M1; HP-24	Qualified
21	ESF Photogrammetry	Coe, J.A.	1995	Map (Developed data)	GS960508314224.005	GP-39; GP-40	Qualified
22	Fracture study at UZ-7A pad	Williams-Stroud, S.C.	1995-1996	Data package	GS960808314222.001	GP-39; GP-12, R1, M1	Qualified
23	ESF DLS 0+60 to 4+00 m	Beason, S. and others	1994	Data Package	GS950508314224.002	GP-32, R0	Qualified
24	ESF DLS 4+00 to 8+00 m	Beason, S. and others	1995	Data Package	GS950808314224.004	GP-32, R0	Qualified
25	ESF DLS 8+00 to 10+00 m	Beason, S. and others	1995	Data Package	GS951108314224.005	GP-32, R0	Qualified
26	ESF DLS 10+00 to 16+00m	Beason, S. and others	1995	Data Package	GS960408314224.002	GP-32, R0	Qualified

[1] Data collected before NRC-approved QA program was in place.

[2] Data tracking number not applicable to non-YMP publications

[3] Non-YMP publication.

300, 400, 500, 600, and 1000 were collected prior to Nuclear Regulatory Commission approval of the U.S.G.S. quality assurance program; these data are non-qualified (table 1).

In the early 1990's, a pavement was cleared in the vicinity of the Ghost Dance fault on the south-facing slope of Antler Ridge. This pavement, called ARP-1 (fig. 4), exposes the upper lithophysal, middle nonlithophysal, and lower lithophysal zones of the Tiva Canyon Tuff. This pavement was constructed in part to verify the presence of several splays of the Ghost Dance fault that were delineated during 1:240 geologic mapping in the area (fig. 3)(Spengler and others, 1993). Fracture attributes from this pavement were collected by the detailed line survey method in 1993 and 1994 (table 1, entry 15).

Pavement P2001, located on the eastern flank of Fran Ridge (fig. 4) was mapped nearly 10 years after the first series of pavement maps were produced (Sweetkind, Verbeek, Singer, and others 1995; entry 17, table 1). Pavement 2001 exposes the upper lithophysal and middle non-lithophysal zones of the Topopah Spring tuff, providing fracture data from the rock units that would host the potential repository. The data from pavement P2001 are qualified.

Three large natural exposures of the rock units included in the PTn hydrogeologic unit were mapped as pavements in 1995 (Sweetkind, Verbeek, Geslin, and Moyer, 1995; entry 20, table 1). The three exposures are located west of Yucca Crest (fig. 4), and provide fracture data on this hydrologically important interval. The data from these exposures are qualified.

The most recent surface fracture mapping at Yucca Mountain was during 1995-1996 at the cleared exposure at the UZ-7A drill pad (fig. 4) where the middle non-lithophysal unit of the Tiva Canyon tuff is exposed (table 1, entry 22). Following the construction of the UZ-7A drill pad, a vertical wall was excavated in order to expose the area adjacent to the Ghost Dance fault. The UZ-7A exposure was mapped using close-range photogrammetry to characterize the zone of intensely fractured rock present at this locality.

Outcrop studies

Qualified fracture data from 41 uncleared outcrops were collected from 1990-1991 (entry 7, table 1) and published as a non-qualified report (Throckmorton and Verbeek, 1996; entry 8, table 1). This outcrop study included detailed descriptions of the 41 outcrop stations (figs. 3 and 4). The main impetus of the study was to characterize the fracture network in various subunits of

the Tiva Canyon and Topopah Spring Tuffs and describe the areal variability of fracture characteristics in the vicinity of Yucca Mountain.

Fracture data were collected from outcrops of rock units included in the PTn hydrogeologic unit in 1995 (table 1, entry 19; results reported in Sweetkind, Verbeek, Geslin, and Moyer, 1995, entry 20, table 1). These data were collected in the same manner as the outcrop fracture data reported in Throckmorton and Verbeek (1995), so that they provide qualitative data on termination relationships, joint sets and intensity. Fracture data were collected from these outcrops under U.S.G.S. YMP technical procedures and are qualified (entry 19, table 1).

A limited suite of data were collected for fractures encountered during 1:240 geologic mapping in the vicinity of the Ghost Dance fault (fig. 3)(Spengler and others, 1993; table 1, entries 9 through 12). Fracture orientation and roughness were recorded for several zones within the Tiva Canyon Tuff. These data are qualified.

Fracture data from the ESF

In 1993, construction of the Exploratory Studies Facility (ESF), a 7.6-m diameter tunnel currently being excavated beneath Yucca Mountain, began (fig. 3). The ESF has been excavated using a tunnel boring machine, with the exception of a short starter tunnel that was constructed using drill and blast methods. As tunneling progresses, the excavated walls of the ESF have been mapped at a scale of 1:125. Lithologic contacts, fault orientations and characteristics, shear zones and fractures greater than 1 m in length are mapped on a flat projection of the tunnel exposure. Concurrent with geologic mapping of the tunnel walls, fracture data are collected along the right rib of the tunnel using a detailed line survey (table. 1, entries 14 and 23-26). Data from the ESF are related to position along tunnel, called stationing. Each station represents 100 m, measured from the portal. At the time of writing this report, the available data from the ESF in reviewed, completed data packages included up to station 18, or the first 1.8 km of tunnel. These data include all of the Tiva Canyon Tuff, the interval between the Tiva Canyon Tuff and the Topopah Spring Tuff (the PTn hydrogeologic unit), and the crystal-rich member of the Topopah Spring Tuff.

An interval in the ESF within the crystal-rich member of the Tiva Canyon Tuff has been mapped using close-range photogrammetry (table 1, entries 21 and 22). These data were collected under USGS technical procedures and are qualified.

Fracture data from boreholes

A large number of boreholes penetrate Yucca Mountain. Borehole fracture frequency (in number of fractures per unit length) is obtained from unoriented core, downhole televiewer logs or geophysical techniques such as sonic logs. Fracture fill information is also available from some holes. The borehole data provide important information about the variability of fracture intensity with depth and lithology. Data from many of the early boreholes at Yucca Mountain were collected and interpreted by the U.S. Geological Survey (e.g. Scott and Castellanos, 1984). In recent years, however, fracture data from boreholes has been collected by Agapito Associates, Inc., under contract to Sandia National Laboratory.

The scope of this synthesis report includes surface fracture studies augmented by data from the ESF; interpretation of borehole fracture information is beyond the scope of this report. Subsurface rock structural data, including fracture data from boreholes are currently being summarized as part of a site geotechnical report (D. Kessel, Agapito Associates, Inc., written communication, 1996).

METHODOLOGY

Fracture data from Yucca Mountain can be divided into two broad subgroups: two-dimensional data where fracture observations were collected over an area, such as pavement maps, outcrop observations, and full-periphery maps in the ESF, and one-dimensional data where fracture attributes are collected along a line, such as detailed line survey. The various methodologies of data collection for both of these subgroups are described and compared below.

Data collection methodology

Cleared exposures

There are 13 surface sites at Yucca Mountain where a map of the fracture network has been produced. Ten sites are pavements or exposures that have been physically cleared by

excavation or hydraulic clearing, and three sites are natural exposures that have been mapped as pavements. The mapped pavements range in area from 300 to 1200 m^2. Fractures were mapped from air photos or by hand surveying; the number of fractures measured at each pavement range from 100 to 1200.

The earliest pavement mapping by Barton and others (1993) developed a method for mapping fracture-trace networks and measured or described eight fracture parameters: trace length, orientation, connectivity, aperture, roughness, shear offset, trace-length density and mineralization. The criteria for identification of cooling joints and tectonic joints in these early studies later became the basis for identifying fracture and joint sets in other units (Barton and Larson, 1986, Throckmorton and Verbeek, 1993). At each pavement, all fractures are mapped that exceed a specific length cutoff, typically from 0.3 to 1.5 m. Fracture attributes, including orientation, trace length, roughness, aperture, fracture filling, and fracture intersection and termination relationships, are collected for each mapped fracture (Barton and others, 1993). Several of the pavements (table 1, entries 1, 2, 3, 4, and 6) were constructed in the same lithologic unit, thus providing data on how the fracture network varies spatially within a single lithology. Two of the cleared exposures cross the Ghost Dance fault (table 1, entries 15 and 22) and provide data on changes in fracture intensity with proximity to fault zones. Pavement mapping is essentially a two-dimensional sampling of the three-dimensional fracture network.

Outcrop observation

Locally abundant bedrock exposure at Yucca Mountain makes outcrop observation of the fracture network possible. Fracture sets are identified by inspection, primarily by subdividing fractures on the basis of orientation and relative age, based on termination relationships, and average attributes for each fracture set are measured (Throckmorton and Verbeek, 1995). Information obtained includes: number of fracture sets and their relative visual prominence at the outcrop, termination (age) relationships, average orientation of each set (a representative number of fractures of each set are measured), range of trace length and trace height, and mineral filling (Throckmorton and Verbeek, 1995). The resulting data are a descriptive inventory of the fracture network in the area. Fractures in outcrops are not mapped, so the locations of individual fractures are not recorded. As a result, quantitative measures of fracture intensity or termination relationships cannot be obtained.

There are 60 outcrop stations from two fracture studies (entry 7, table 1; reported in Throckmorton and Verbeek, 1996; entry 8, table 1; and entry 19, table 1; results reported in Sweetkind, Verbeek, Geslin, and Moyer, 1995, entry 20, table 1) scattered areally across the mountain in various stratigraphic units (figs. 3 and 4). Fracture data collected during geologic mapping of a large area straddling the Ghost Dance fault (fig. 3) are also included in the outcrop data category (table 1, entries 9, 10, 11, and 12). Within the mapped area, all observed fractures greater than 2 m in length were mapped and a limited suite of fracture attributes collected (Spengler and others, 1993).

Detailed line survey

The detailed line survey (DLS) is the primary method of collecting fracture data in the Exploratory Studies Facility (ESF) (table 1, entries 13, 14, 23, 24, 25, and 26); it was also used to obtain fracture data at the ARP-1 pavement (table 1, entry 15). The DLS provides a statistical sampling of the fracture network and is a relatively rapid method for obtaining directional fracture data along a traverse (Brady and Brown, 1993). In the ESF, the location of every discontinuity longer than 0.3 m is measured along a horizontal datum line and fracture attributes including orientation, infillings, terminations, fracture origin, roughness, and aperture, are recorded. Full-periphery maps (1:125 scale) of the excavated tunnel walls provide the geologic context for interpreting the fracture data collected in the ESF using the detailed line survey method. Although the detailed line survey method is a one-dimensional sample of fracture attributes, it provides some of the same data as the two-dimensional data sets because trace lengths and termination relationships are recorded.

Close-range photogrammetry

Two sites at Yucca Mountain have been mapped and studied using close-range photogrammetric techniques (table 1, entries 21 and 22). In the field, targets are placed on the exposure to be mapped, their locations surveyed, and the exposure is photographed using a hand- or tripod-held camera to obtain blocks of overlapping stereo photographs (Coe and Dueholm, 1991a; 1991b). Once the photographs are properly oriented in an analytical photogrammetric plotter, three-dimensional fracture linework, attitudes, and attribute information can be collected. These data may then be analyzed using a Geographic Information Systems (GIS) approach where spatial data (the digitized fracture traces) are linked to attribute data (orientation, length) in a

database (Coe, 1995). For each fracture mapped, the following types of information were recorded from stereo observations: fracture trace length and orientation, trace length per unit area, lithology, presence of mineral fill, maximum wall separation, planarity, terminations, and mode of failure (shear or extension). A two-dimensional data set is produced from this data collection method, and it differs from the pavement data in that the aperture, roughness and mineral fillings cannot be precisely determined.

Strengths and weakness of different types of fracture data

Various types of fracture information are recorded for each of the collection methods discussed above. The only fracture attributes that all of the data sets share are orientation, trace length and lithology in which the fracture occurs.

Cleared exposures

Maps of cleared pavements are superior to one-dimensional fracture data as input to numerical simulations because they provide information on the termination (age) relationships and connectivity of fracture sets, provide data on fracture trace lengths, and yield fracture intensity as total trace length per unit area rather than as simple fracture frequency. However, the mapping is labor-intensive and each pavement covers only a small area. Further, half of the pavements have been constructed in the same lithologic unit, thus, the pavement data may not be representative of the fracture network as a whole.

Outcrop observation

Outcrop surveys of the fracture network allow a large amount of information to be gathered relatively quickly; typically two or three outcrop stations can be done in a day. Data from outcrop observation have the broadest areal distribution (Figs. 3 and 4) and provides fracture information on the largest number of lithologic units in this study. However, much of the data are difficult to treat statistically and important parameters such as fracture intensity are difficult to obtain from descriptive data.

Detailed line survey

The strength of the detailed line survey method is that it provides data for a very large number of fractures (more than 5000 to date from 3 kilometers of tunnel). The data are tied to lithology and location, and the nature of the exposure allows detailed identification of fault and

shear offsets. The detailed line survey is a scan-line type data set, that does not have all of the limitations of the borehole data, because trace length and termination relationship information is obtainable. The major disadvantage of detailed line survey data is the bias the collection method produces against recording low-angle fractures and high-angle fractures that parallel the tunnel alignment or the plane of the pavement.

Close-range photogrammetry

The photogrammetric method has the potential to supply a large amount of very detailed information regarding fracture orientations, trace lengths, apertures, and terminations, at strategically selected mapping sites. For example, within the ESF, close-range photogrammetry produces about fifteen times the amount of quantitative data produced by a conventional detailed line survey over the same length of tunnel. Additionally, the photogrammetric method produces a map of spatially related data, a product not obtainable from DLS. The major problem with the method is determining what features *not to map*, because of the high level of geologic detail usually visible in the photographs. Strengths of the photogrammetry method include 1) the creation of a detailed, permanent, synoptic record of exposures (stereo photographs) that can be revisited at any time; 2) the possibility to collect many different types of information that may not be practical to collect conventionally; and 3) the creation of digital records as part of the mapping process. Limitations of the method include: 1) the non-recognition and imprecise identification of mineral fillings, 2) it is relatively time intensive compared to conventional techniques, and 3) specialized equipment is required to collect the data.

Fracture data from boreholes

There are a number of difficulties in comparing borehole fracture data to fracture data collected at the surface and the ESF. Much of the available borehole fracture data come from core that is unoriented, so fracture orientations from boreholes cannot be compared statistically to fracture data from surface studies or from the ESF. Many of the boreholes have been drilled with either air or an air/foam mixture to minimize hydrologic perturbations during site characterization at Yucca Mountain. Unfortunately, these drilling practices adversely affect core recovery and promote the development of drilling-induced fractures. Borehole data do not provide information on fracture lengths or termination relationships. Fracture orientation can be

obtained from downhole televiewer logs, but the accumulation of dust generated during dry drilling makes them difficult to interpret. Borehole data are not included in this synthesis.

Comparison of data collection methods

Most of the fracture studies done at Yucca Mountain have measured all fractures above a certain length present within a prescribed area or along a prescribed scan line. The pavement mapping, detailed line survey, and photogrammetry studies all use this method of data collection. This data collection method, called a global inventory by Throckmorton and Verbeek (1995), attempts to collect fracture data in a systematic, objective manner. The resultant data set has a high degree of reproducibility and contains a large number of measurements that can be statistically manipulated. Fracture data collected by outcrop observation (entries 7 and 19, table 1) use a selective inventory (Throckmorton and Verbeek, 1995) and are subjective in nature. In the collection of these data sets, the various fracture sets are identified by inspection, primarily by subdividing fractures on the basis of orientation and relative age, based on termination relationships. Orientation, length, and roughness data are then collected from representative members of each fracture set. One of the main advantages of this method is the resulting data set can cover a wide area because the method by definition requires counting fewer fractures. Fracture sets may be described in relation to locality, stratigraphy, rock composition. A disadvantage of the selective inventory method is that the data are fundamentally descriptive in nature and are difficult to compare to the global inventory data or input into hydrologic models.

Comparison of global and selective inventories

Topopah Spring Tuff, Pavement P2001

Prior to the construction of pavement P2001 at Fran Ridge (fig. 4), two vertical pits were constructed at this location. Pit 1 is located at what is now the north end of pavement P2001 and Pit 2 at the south end. Fracture data within the pits and in the cleared areas immediately surrounding the pits were collected by C.K. Throckmorton and E.R. Verbeek using the selective inventory method. These data constitute two of the 41 uncleared outcrops (stations TOB1 and TOB2) reported in Throckmorton and Verbeek (1995; entry 8, table 1). Data from the two pits may be compared to data obained using a global inventory approach during mapping of the P2001 pavement (Sweetkind, Verbeek, Singer, and others 1995; entry 17, table 1).

Synoptic data from the two pits include the general orientations and interrelationships of the various fracture sets, but no map was created. Throckmorton and Verbeek (1995) identified three sets of cooling joints and two major sets of tectonic fractures in their observations in and around the two test pits at Fran Ridge (fig. 5). Based on the mapping of pavement P2001, Sweetkind and others (1995) also identified three sets of cooling joints that were very similar in overall orientation to those described by Throckmorton and Verbeek (1995) (table 2; fig. 5). Pavement mapping also confirmed the existence of the two tectonic fracture sets identified by Throckmorton and Verbeek (1995), but found a third set of tectonic fractures not identified during the previous work (Sweetkind, Verbeek, Singer, and others 1995) (table 2; fig. 5).

The selective inventory data from the two pits differ from the global inventory data collected during the mapping of pavement P2001 in the following ways:

1) Observations of the vertical walls of the two test pits are more likely to identify shallowly dipping surfaces. Observations made on the gently sloped pavement are biased against recognizing low-angle features (Terzaghi, 1965). Thus, the data from shallowly dipping fractures measured in the test pits define a more prominent pole concentration (fig. 5) than data from the pavement surface;

2) Throckmorton and Verbeek (1995) did not use a length cutoff in their observations; small fractures are better represented in their data set. In fact, due to the limited areal extent of their observation area, their data emphasize a different size range than the P2001 pavement data;

3) The orientation of the fracture sets in the pits were measured subjectively - measurements were only taken on fractures that fit into sets previously identified by inspection. As such, the data from the test pits are much better clustered than data from the pavement surface where all fractures were measured; and

4) The additional major set of tectonic fractures identified during the mapping of pavement P2001 is a northwest-striking set that is best exposed in the upper lithophysal zone of the Topopah Spring Tuff, a zone that is not exposed in either of the two pits vicinity (Sweetkind, Verbeek, Singer, and others 1995). Mapping of the pavement P2001 revealed that northwest-striking cooling joints and later northwest-striking tectonic joints both constitute visually prominent fracture sets represented by abundant

Table 2. Median orientation of fracture sets, pavement P2001 and test pits.

[Orientation data from the two test pits from Throckmorton and Verbeek (1995). Orientation data from pavement P2001 are from Sweetkind, Verbeek, Singer and others (1995). Interpreted joint sets are abbreviated as: C1, C2, C3, cooling joints belonging to set 1, 2, or 3, respectively; T1, T2, T3, tectonic joints belonging to set 1, 2, or 3, respectively. Subhorizontal joints, labeled SH, are foliation-parallel, have extremely rough surfaces, and were interpreted by Throckmorton and Verbeek (1995) as unloading joints. These features were not mapped at pavement P2001]

Location	Cooling Joints			Tectonic Joints			
	C1	C2	C3	T1	T2	T3	SH
Test pit 1	N28W/85SW	N80E/89SE	N62E/10SE	N01E/89NW	--	N50E/86SE	N49W/05NE
Test pit 2	N34W/84SW	N60E/67NW	--	N05E/79SE	--	--	N52W/05NE
Pavement P2001	N38W/77SW	N75E/86SE	N84E/21S	N06W/86W	N31W/84W	N55E/87SE	--

joints. The northwest-striking cooling joints are abundant in the middle nonlithophysal zone of the Topopah Spring Tuff at the extreme northern part of the pavement, near Pit 1, but are of only scattered presence elsewhere. However, the later northwest-striking tectonic joints are best developed where the northwest-striking cooling joints are absent, mostly in the upper lithophysal zone of the Topopah Spring Tuff at the south end of the pavement. The absence of the northwest-striking tectonic joints in the vicinity of the pits may be explained by the presence of the northwest-striking cooling joints that are favorably oriented to accommodate new increments of extensional strain and thus suppress the formation of new tectonic joints in their vicinity (Sweetkind, Verbeek, Singer, and others 1995).

Given the difference in the data sets described above, the overall orientation patterns between the global inventory data from pavement P2001 data and the selective inventory observations at the two test pits are remarkably similar (fig. 5, table 2). The better clustering of points and the greater number of low-angle features in the data from the test pits can be explained by the reasoning presented above. Only one additional set of fractures, the T2 tectonic set, is apparent in the data from the pavement. These fractures predominate in the upper lithophysal zone, which was not observable in the test pits.

Crystal-poor vitric zone, Tiva Canyon Tuff

The selective inventory fracture data from this zone consists of one of the 41 uncleared outcrops (station CC1) reported in Throckmorton and Verbeek (1995; entry 8, table 1) and data from outcrop observation of this unit (entry 19, table 1; reported in Sweetkind, Verbeek, Geslin, and Moyer, 1995, entry 20, table 1). These data may be compared to global inventory data from: 1) qualified data from pavement mapping of this unit (entry 18, table 1; reported in Sweetkind, Verbeek, Geslin, and Moyer, 1995, entry 20, table 1); and 3) to qualified data from this unit collected in the ESF (entries 24 and 25, table 1).

Qualified data from the ESF are generally similar to the surface data collected from this unit (compare figures 6a and 6c), although there is a relative lack of poles that plot near north or south (corresponding to roughly east-west striking planes) in the data from the ESF. While this discrepancy could be an artifact of the small number of poles plotted (112 poles, fig. 6c), there is also the likelihood that sampling bias may play a role. Fractures of this orientation would be

sub-parallel to the alignment of the ESF and the trace line of the detailed line survey (299 degrees along the north ramp of the ESF) and would be underrepresented relative to other, less biased methods of data collection.

The presence of cooling joints within the crystal-poor vitric zone of the Tiva Canyon Tuff was recently recognized by D. Sweetkind and E.R. Verbeek during qualified data collection in this unit (Sweetkind, Verbeek, Geslin, and Moyer, 1995, entry 20, table 1). Throckmorton and Verbeek (1995) do not report cooling joints in the crystal-poor vitric zone. This disparity reflects the natural evolution of understanding of the formation of cooling features in moderately to poorly welded tuff, rather than a real difference in the data. Given the similarity in orientation distributions between all of the data, it is likely that cooling joints are present at outcrop station CC1, but were not identified as such at the time (Sweetkind, Verbeek, Geslin and Moyer, 1995, entry 20, table 1). Global and selective inventory data are similar from other zones of the Tiva Canyon Tuff as well (fig. 7).

Comparison of qualified and non-qualified data

The non-qualified items included in this synthesis report are data from seven pavements (entries 1,3,4,5,6, table 1), in which data were collected between 1984 and 1990, and the non-qualified report summarizing the results of observations from 41 uncleared outcrops (entry 8, table 1), in which qualified data were collected between 1990-1991. Data from three of the pavements (100, 200, and 300) were reported by Barton and others (1993; entry 2, table 1), data from the other four pavements have never been published. None of the pavement data were formalized as a Yucca Mountain Project data package until 1996 (entries 1,3,4,5,6, table 1).

The non-qualified data from the seven pavements were collected under technical procedure YMP-USGS-GP-12, R0 (table 1). The non-qualified data were obtained using the same methodology, collecting exactly the same fracture attributes, as was later used in the collection of the qualified fracture data shown in table 1. The reason the data are not qualified is that at the time of data collection there was no NRC (Nuclear Regulatory Commission) approved QA (Quality Assurance) program in place. The investigators responsible for the collection of these non-qualified data developed the data collection methodology which they then formalized as the YMP-QA procedures for fracture data collection. For example, C.C. Barton was the

principal investigator for the seven non-qualified pavements; he prepared the portion of technical procedure YMP-USGS-GP-12 that relates to the mapping of fractures on pavements. Subsequent pavement mapping has utilized the same methodology and operated under the same technical procedure as that used to acquire the on-qualified data. Given the similarities between the methods used in the collection of the qualified and non-qualified data, no great disparities would be expected when comparing the two data sets.

Comparison of data from the Tiva Canyon Tuff, upper lithophysal zone

The non-qualified fracture data from both pavements and outcrops may be compared to qualified fracture data collected at the surface and in the subsurface from the upper lithophysal zone of the Tiva Canyon Tuff.

Non-qualified fracture data from this zone consists of six pavements (entries 1,3,4, and 6, table 1). These data may be compared to: 1) qualified data from surface geologic mapping of this unit (entries 9-12, table 1); 2) qualified data from the ESF starter tunnel (entries 13 and 14, table 1); 3) to qualified data from this unit collected in the ESF (entries 23 and 24, table 1), and 4) nine of the 41 uncleared outcrops (CPUL1 through CPUL9) reported in Throckmorton and Verbeek (1995; entry 8, table 1). This is the only unit in the Tiva Canyon Tuff where the majority of data come from the non-qualified surface observations (2088 for the non-qualified surface data, 228 for the qualified subsurface data). Fracture orientations from the qualified and non-qualified data are remarkably similar (fig. 8), given the differences in the number of poles plotted (186 for the non-qualified surface data, 1069 for the qualified surface data), the large area, and attendant variety of structural settings the data were collected from.

There appears to be no significant difference between the qualified and non-qualified fracture data. Similar orientation distributions and number of fracture sets appear to have been recorded in both non-qualified and qualified data. With the exception of the upper lithophysal zone of the Tiva Canyon Tuff, the majority of data from each lithostratigraphic unit included in this synthesis are qualified. For all of the units except the upper lithophysal zone of the Tiva Canyon Tuff, the non-qualified data could be reasonably viewed as corroborating data to the qualified.

Even given the similarities between the qualified and non-qualified data, the interpretive portion of this report will include separate sections for the two types of data. Where appropriate,

non-qualified data will be included with the qualified data for comparison and where the non-qualified data serves as corroborating or supporting data.

Data integration methodology and database construction

The various fracture studies at Yucca Mountain have resulted in a diverse and not entirely compatible collection of data sets. Even where the same fracture attribute was measured (for example, trace-length) different studies and collection methods used different measurement criteria (for example different lower-limit trace-length cutoffs) that make data difficult to compare. A further difficulty in integrating the data sets lies in comparing one-dimensional (detailed line survey) and two-dimensional (pavement maps, outcrop observations, and full-periphery maps in the ESF) sampling approaches and integrating them into an accurate representation of the fracture network.

In order to compare and synthesize data from all of the fracture studies described above, fracture data from all surface and subsurface fracture studies listed in table 1 have been consolidated into a single database. Table 3 is an example of the number of fracture attributes contained in the database. Since the types of data vary with the data collection method, all fracture characteristics which might be important to fracture network characterization are not available from all sets. The only fracture attributes that are common to all of the collection methods are orientation, trace length and the lithology in which the fracture occurs. Other attributes were common to many studies, but were recorded in different ways and had to be converted to a common format. For example, some measure of surface roughness of individual fractures was recorded for many of the studies, but several different roughness measurement schemes were used (table 4).

Fracture data from certain lithostratigraphic units were combined during analysis of the database. Lithostratigraphic units were combined where individual units that were mechanically similar had only a small amount of data collected from them (for example, the three bedded tuff intervals within the PTn hydrologic unit), or where multiple lithostratigraphic units were combined in the original data. In general, however, data were organized by lithostratigraphic unit following the usage of Buesch and others (1995) (fig. 2).

Table ample from combined fracture database.

Unique ID	Data set	Fracture	Type	Terminations	Mineral fillings	Lithology	Source	Date	QA Status
19800	ESF_nport	RRSL-F11.0	F	--	--	Tpcpul	S. Beason and others	1994	y
19801	ESF_nport	RRSL-F11.7	F	--	GROUT	Tpcpul	S. Beason and others	1994	y
19802	ESF_nport	RRSL-F16.2	F	--	CLAY/ GROU	Tpcpul	S. Beason and others	1994	y
19803	ESF_nport	RRSL-F16.8	F	--	CLAY	Tpcpul	S. Beason and others	1994	y
19804	ESF_nport	RRSL-F20.4	F	--	--	Tpcpul	S. Beason and others	1994	y
19805	ESF_nport	RRSL-F22.2	F	--	--	Tpcpul	S. Beason and others	1994	y
19806	ESF_nport	RRSL-F38.4	F	--	--	Tpcpul	S. Beason and others	1994	y

Unique ID	Easting	Northing	Elevation	Strike	Dip	Dip azimuth	Joint-set-dip	Joint-set-dip azimuth
19800	--	--	--	70	87	160	--	--
19801	--	--	--	65	90	155	--	--
19802	--	--	--	214	72	304	--	--
19803	--	--	--	235	74	325	--	--
19804	--	--	--	129	81	219	--	--
19805	--	--	--	202	79	292	--	--
19806	--	--	--	84	86	174	--	--

Unique ID	Roughness	Ends	Spacing	Trace-length	Aperture	Min.-aperture	Max.-aperture	Joint-alteration
19800	2	--	--	--	1	--	--	--
19801	3	--	--	--	0	1	--	--
19802	2	--	1	--	0	3	--	--
19803	3	--	--	--	0	3	--	--
19804	3	--	--	--	1	--	--	--
19805	2	--	--	--	6	--	--	--
19806	4	--	--	--	7	--	--	--

TABLE 4. Relationship between different descriptions of fracture roughness.

[Roughness is a qualitative description of the roughness of a fracture surface at an outcrop (Throckmorton and Verbeek, 1995). This description was used in the outcrop studies. Joint roughness coefficient (JRC) is a roughness index as measured with a carpenter's form tool (JRC defined theoretically in Barton and Choubey, 1977; field measurement techniques described in Barton and others, 1993). Roughness coefficient is used in the detailed line surveys in the ESF as a qualitative description of the roughness of a fracture surface]

ROUGHNESS	JRC	ROUGHNESS COEFFICIENT
1 - very smooth	0 - 2	R6
2 - smooth	2 - 6	R5
3 - semi-smooth	6 - 10	R4
4 - semi-rough	10 - 16	R3
5 - rough	16 - 20	R2
6 very rough	> 20	R1

Interpretation of joint origin and sequence of formation

Defining the evolution of the fracture network depends upon the identification of joint sets and their sequence of formation, both of which can be derived from descriptive fracture data and geometric analysis of pavement maps. Criteria for determining joint origin and defining fracture chronology are discussed below.

Determining joint origin

The distinction between cooling and tectonic joints in and near the potential repository is a necessary first step in understanding the evolution of the fracture network and in modeling its properties. The criteria most commonly used to distinguish cooling from tectonic joints in moderately to densely welded units of the Tiva Canyon and Topopah Spring Tuffs include the presence of tubular structures and very low roughness coefficients (Barton and others, 1984; 1993). The distinction is easiest where tubular structures are abundant, as in highly lithophysal zones of the Tiva Canyon Tuff. However, fractures identical to cooling joints in every respect may lack tubular structures, or have such structures exposed on only a portion of their area. A number of other criteria may be used in combination to recognize cooling joints that lack tubular structures including: low surface roughness (JRC of five or less); smooth, continuous traces; appreciable length; parallelism with proven cooling joints nearby; and demonstrated early age as shown through abutting relations with fractures of other sets (Throckmorton and Verbeek, 1995). In addition, where lithophysae are present in the rock, cooling joints intersect none or few of them. A combination of these criteria have been used successfully to identify probable cooling joints within various units of the Tiva Canyon Tuff (Throckmorton and Verbeek, 1995) and in the middle nonlithophysal zone of the Topopah Spring Tuff (Sweetkind, Verbeek, Singer and others, 1995). A number of fractures within poorly welded Yucca Mountain Tuff and in the crystal-poor vitric zone at the base of the Tiva Canyon Tuff possessed neither tubular structures nor extremely low surface roughness, yet were interpreted to be of cooling origin on the basis of other criteria, including smooth, continuous traces, appreciable length, and demonstrated early age (Sweetkind, Verbeek, Geslin and Moyer, 1995).

Determining joint chronology

The sequence of fracturing is determined through examination of termination relations among fractures of different sets (Kulander and others, 1979; Hancock, 1985; Pollard and Aydin,

1988). Termination of each fracture endpoint is described as blind (fracture ends within unbroken rock or in a zone of small fractures not resolvable at the scale of mapping), abutting (fracture terminates against another fracture), or crossing (fracture crosses another fracture with no interaction). In the simplest case, members of older fracture sets tend to terminate into blank rock, and younger fractures tend to abut against the older sets.

A number of factors may complicate the determination of the sequence of fracture formation including:

1) fractures of different sets may not be present in the same part of the outcrop;

2) fractures may cross each other rather than abut, so that the relative timing of the two joints is indeterminate (see Kulander and others, 1979);

3) fracture sets generally develop over a period of time, so later members of a particular set may be coeval with early members of another set;

4) fractures may undergo reactivation, slip or renewed growth during later tectonic events that can lead to ambiguous or confusing intersection relationships; and

5) the presence or absence of cooling joints has an effect on the character of the subsequent tectonic joints. When present, cooling joints have blind terminations, long trace lengths, and later tectonic joints terminate against them. Where cooling joints are absent, however, the early tectonic joints will have the greatest number of blind endings and longest trace lengths.

Determination of fracture chronology is complicated by the influence that early fractures exert over the formation and character of subsequent fractures. Early fracture sets develop within a homogeneous rock mass, whereas later sets form within a rock mass that has been subdivided by numerous planes of weakness. Some of the effects of multiple fracture generations are as follows:

(1) Joints of a given set are largest where the set was the first to form but are smaller where other, older fractures had already cut the rock. Fracture size decreases as new sets are added to the network, because new fractures simply cannot propagate very far before terminating against an already existing fracture (Barton and Larsen, 1986).

(2) Development of a given joint set commonly is suppressed wherever older joints are favorably oriented to accommodate new increments of strain. This relationship as applied to

cooling and tectonic joints occurs in the Topopah Spring Tuff (Sweetkind, Verbeek, Singer, and others, 1995) and in the Tiva Canyon Tuff (Throckmorton and Verbeek, 1995). Strain accommodation by existing fractures exerts a powerful influence on the number of joint sets that can form within a given volume of rock and is one reason why the degree of development of joint sets is so highly variable from one place to another in the Yucca Mountain area.

(3) The more abundant the existing fractures in a rock, the more irregular will be the surfaces of a succeeding joint set because of local stress perturbations in the vicinity of the older fractures. Joints of the same set can be of quite different appearance, planar in one place and irregular in another, purely as a function of previous fracture history.

(4) Late cross joints tend to be most abundant where pre-existing fractures are most closely spaced (Gross, 1993).

RESULTS OF INDIVIDUAL STUDIES

A brief synopsis of each fracture study included in this synthesis is presented below.

Pavement studies

Pavement 100

Pavement 100 is located on Live Yucca Ridge (fig. 4), and exposes the upper lithophysal zone of the Tiva Canyon Tuff (Barton and others, 1993). The pavement was mapped at a scale of 1:50 and encompasses 214 m^2. Employing a lower-limit trace-length cutoff of 0.2 m, 221 fractures were measured.

The map of pavement 100 (included in Barton and others, 1993) shows two sets of cooling joints are present at pavement 100 (table 5). Members of the best-developed set strike N. 50° E. and dip steeply to the northwest; members of this set form a prominent zone of closely spaced joints along the southeastern portion of the pavement (Barton and others, 1993). A subordinate set of cooling joints has an average strike of N. 40° W., approximately perpendicular to the NE-striking set, and fractures dip steeply to the northeast. This set is very weakly expressed.

Tectonic joints form three poorly clustered pole concentrations (Barton and others, 1993), corresponding to average fracture strikes of N. 1° W. to N. 10° E., N. 35° W., and N. 40° E (table 5). All of these sets are subvertical and are poorly expressed on the pavement map of Barton and

TABLE 5. MEDIAN ORIENTATION AND RELATIVE TIMING OF JOINT SETS, NON-QUALIFIED PAVEMENTS

Pavement	Cooling joints, NE-striking	Cooling joints, NW-striking	Tectonic joints, N-S striking	Tectonic joints, NW-striking	Tectonic joints, NE-striking
Pavement 100	Well-developed zone of closely-spaced joints, average strike of N. 50° E.	Weakly expressed, strike of N. 40° W.	North- and northwest-striking sets are present, but relative timing cannot be determined.		Poorly developed late set with northeast strike.
Pavement 200	Moderately-developed set, strike of N. 50° E.	Minor. One joint striking N. 10° W.	North- and northwest-striking sets are well developed, but relative timing is ambiguous.		Moderately well developed late set with northeast strike.
Pavement 300	Moderately-developed set, strike of N. 30° E.	Well-developed zone of closely-spaced joints, average strike of N. 45° W.	Weakly developed. Later than the northwest-striking set.	Well developed; earliest tectonic set.	Well developed late set with northeast strike.
Pavement 400	Absent	Minor. One joint striking N. 15° W.	Absent.	Well developed; earliest tectonic set and longest joints on the pavement.	Very well developed northeast-striking set. This set is followed by a number of late joints that form a complex polygonal pattern.
Pavement 500	Weakly-developed set of short joints, average strike of set is N. 20° E.	Absent	Well developed; earliest tectonic set and longest joints on the pavement.	Well developed; moderately long joints that are clearly later than the north-striking set.	Well developed late set with northeast strike.
Pavement 600	Moderately-developed set, average strike of N. 35° E.	Absent	Well developed; the dominant joint set on the pavement.	Weakly developed set, consisting of two long joints. Earlier than the north-striking set.	No late joint sets.
Pavement 1000	Well-developed joint set, average strike of N. 10° E.	Probable set of short, curved joints that strike generally east-west.	Well developed; earliest tectonic set.	Tectonic joints that formed after the north-striking set form a complex polygonal pattern.	

others (1993). Members of the northwest-striking set commonly offset the cooling joints in a right-lateral sense (Barton and others, 1993). Members of the generally north-striking set have long trace lengths, and either cross the cooling joints or terminate against them. There are no fracture interactions to constrain the relative timing between these two sets except for a single north-striking fracture that crosses a northwest-striking fracture. The northwest-striking fracture offsets several cooling joints in a right-lateral sense, but does not offset the north-striking fracture. In this case, the north-striking fracture must have post-dated the faulting along the northwest-striking fracture. The third tectonic joint set (N. 40° E.) is expressed by a few short northeast-striking joints that were clearly the latest set to form.

Pavement 200

Pavement 200 is located on Dead Yucca Ridge (fig. 4), and exposes the upper lithophysal zone of the Tiva Canyon Tuff (Barton and others, 1993). The pavement, mapped at a scale of 1:50, encompasses 260 m^2. 101 fractures were measured using a lower-limit trace-length cutoff of 0.2 m.

A single set of cooling joints is shown on the map of pavement 200 (Barton and others, 1993). Members of this set strike N. 50° E. and dip steeply to the northwest (table 5). This is the same set that dominates the cooling joints at pavement 100.

There are two main tectonic fracture sets at pavement 200 (table 5), both of which are subvertical. One set has strikes that range between N. 1° W. and N. 05° E., the second set has an average fracture strike of N. 70° W. The timing relationship between these two sets is ambiguous. In two instances, members of the northwest-striking set abut the north-striking set. However, in two other instances members of the north-striking set abut the northwest-striking set. One member of the north-striking set was reactivated as a fault relatively late; this fracture offsets all of the fractures it crosses in a right-lateral sense. An equal area net for tectonic joints at pavement 200 (Barton and others, 1993) shows a broad distribution of poles. The lack of pole concentrations results from each of the tectonic sets described above being represented by only a few fractures and from the presence of a number of small, late cross joints that range in strike direction from northeast- to east-striking.

Pavement 300

Pavement 300, like pavement 200, is located on Dead Yucca Ridge (fig. 4), and exposes the upper lithophysal zone of the Tiva Canyon Tuff (Barton and others, 1993). The pavement encompasses 221 m^2 and 248 fractures were measured. The pavement was mapped at a scale of 1:50, with a lower-limit trace-length cutoff of 0.2 m.

The map of pavement 300 (fig. 9) shows two sets of cooling joints . The best-developed set has an average strike of N. 50° W. and dips steeply to the northeast; members of this set form a prominent zone of closely-spaced joints along the southwestern portion of the pavement (fig. 9). A subordinate set of cooling joints has an average strike of N. 40° E.; fractures of this set dip steeply to the northwest. Members of this northeast-striking set are expressed much better at the nearby pavement 200.

Three sets of tectonic fracture are exposed at pavement 300 (table 5). Members of the dominant set strike between N. 50° W. and N. 70° W., subparallel to the best-developed set of cooling joints. Relative to the other tectonic joint sets, the northwest-striking joints are the longest joints, have the greatest number of blind terminations, and the other fractures consistently terminate against them - all evidence for this set being the earliest tectonic fractures. A second, weakly developed tectonic set strikes roughly north-south and is subvertical. This set consistently terminates against the northwest-striking set and is thus younger. Members of the third tectonic joint set strike between N. 40° E. and N. 55° E and dip steeply to the northwest. This set is moderately well expressed. Members of this set consistently terminate against all of the other fractures and are clearly the latest set to form.

Pavement 400

Pavement 400 is a large natural exposure of the upper lithophysal zone of the Tiva Canyon Tuff near the top of Busted Butte (fig. 4). The pavement was mapped at a scale of 1:50, with a trace-length cutoff of 0.2 m. 580 fractures were measured in an area of 1726 m^2.

A single cooling joint, striking N. 15° W, is labeled on the unpublished map of this exposure (contained in data package, entry 1, table 1). On the unpublished map there are four other fractures that are subparallel to the labeled cooling joint, all of them are very long and have blind terminations. However, at least one of these fractures has a joint roughness coefficient of

12. On the basis of roughness, these long fractures are interpreted as early tectonic joints, rather than members of the cooling joint set (table 5).

There are two principal tectonic joint sets at pavement 400 (table 5). One set, described above, trends N. 25° W.; a second set strikes between N. 50° E. to N. 65° E. Members of the northwest-striking set are characterized by long trace lengths, blind terminations, and consistent termination of other fractures against members of this set; all evidence for this set having formed relatively early. As discussed above, one of these joints is very rough, indicating that these are probably early tectonic joints rather than members of a cooling joint set. The second set of tectonic joints, striking northeast, consistently terminate against the northwest-striking set and are thus relatively younger. Much of pavement 400 is characterized by a polygonal network of small, nonsystematic joints. These joints terminate against all of the sets described above and are thus relatively late. The origin and tectonic significance of these small joints, however, are uncertain.

Pavement 500

Pavement 500 is located at the east end of Live Yucca Ridge (fig. 4), and exposes the upper lithophysal zone of the Tiva Canyon Tuff over an area of 149.7 m^2. The pavement was mapped at a scale of 1:50; 319 fractures were recorded with a lower-limit trace-length cutoff of 0.2 m.

Only a few small cooling joints are labeled on the unpublished map of pavement 500 (contained in data package, entry 4, table 1)., these have a strike of N. 20° E (table 5). There are a number of large, rough fractures of similar orientation that are probably early tectonic joints, discussed below.

Pavement 500 exposes the most complete record of tectonic joints of any of the cleared pavements in the upper lithophysal zone of the Tiva Canyon Tuff. Three well-developed sets of subvertical tectonic joints are present, along with a number of late cross joints (table 5). The three major tectonic sets include the following: a north-south-striking set (fracture strikes between N. 05° W. and N. 15° E.), a northwest-striking set (fracture strikes between N. 55° W. and N. 70° W.), and a northeast-striking set (fracture strikes between N. 20° E. and N. 35° E.). Fracture terminations between these three sets yield remarkably consistent relative timing

relationships: the north-striking fracture set was the first to form, followed by the northwest-striking set and finally the northeast-striking set. This is the only cleared exposure at Yucca Mountain that yields a clear temporal distinction between three tectonic fracture sets. Last to form were a number of minor cross joints of varying orientations.

Pavement 600

Pavement 600 is located on the southeastern end of an unnamed ridge that separates Drill Hole Wash from Teacup Wash (fig. 4). The pavement exposes the upper lithophysal zone of the Tiva Canyon Tuff. The pavement encompasses 251.2 m^2 and 327 fractures were measured. The pavement was mapped at a scale of 1:50, with a lower-limit trace-length cutoff of 0.2 m.

The unpublished map of this pavement (contained in data package, entry 6, table 1) shows one set of cooling joints mapped at this pavement, with an average strike of N. 35° E (table 5). This moderately developed set is characterized by gently curving fractures with very low surface roughness. There are also two northwest-striking joints that could be interpreted as cooling joints. These joints strike between N. 60° W. to N. 70° W., have long trace lengths, gently curving traces and cross the mapped cooling joints. However, both of these joints have joint roughness coefficients of 9 and 12, respectively. On the basis of roughness, these long joints are probably early tectonic joints, rather than members of a second cooling joint set.

The earliest possible tectonic joint set is represented by the two long joints that trend N. 60° W. to N. 70° W, discussed above. The fracture network at pavement 600 is dominated by a set of generally north-striking tectonic joints. These joints are typically very rough, have branching and anastamosing traces, and consistently terminate against the cooling joint set and early northwest-striking tectonic joints described above. There are no later sets of tectonic joints at pavement 600.

One outcrop station (station CUL8, Throckmorton and Verbeek, 1995) lies immediately adjacent to pavement 600 (figs. 3 and 4), yet the fracture sets exposed there differ significantly from those at pavement 600. Two sets of cooling joints are present at the outcrop station. The dominant set, with an average strike of N. 35° W. and featuring fractures up to 7 m in length, is not observed at pavement 600. No tectonic joint sets were identified at the outcrop station, even though they dominate at pavement 600.

Pavement 1000

Pavement 1000 is located at the southern tip of Fran Ridge (fig. 4). The pavement exposes the middle non-lithophysal zone of the Topopah Spring Tuff. The pavement encompasses 170.2 m^2 and 670 fractures were measured. The pavement was mapped at a scale of 1:50, with a lower-limit trace-length cutoff of 0.2 m.

No cooling joints are labeled on the map of pavement 1000 (fig. 10)(published in Barton and Hsieh, 1989). However, there is a set of northeast-striking fractures (average strike of N. 25° E.) that are long, gently curving, have mostly blind terminations and very low surface roughness (JRC between 1 and 3). This is probably a cooling joint set. There is possibly a second, less well-developed set of cooling joints that is expressed as a number of small, curved fractures that are approximately perpendicular to the north-striking set.

The dominant joint set at pavement 1000 is a north-striking set (strikes of N. 5-10 W.). Members of this set are long, often branch or splay, and terminate against the interpreted northeast-striking cooling joint set. These joints are interpreted to belong to the earliest set of tectonic joints (table 5). Many of the later tectonic joints at pavement 1000 form a complex polygonal pattern that is difficult to interpret (fig. 10).

Pavement P2001

Pavement P2001 is located on the east flank of Fran Ridge, 3 km to the east of the crest of Yucca Mountain (fig. 11a), and exposes the fracture network within the middle non-lithophysal and upper lithophysal zones of the Topopah Spring Tuff. The pavement encompasses 1140 m^2 and 262 fractures were measured. The pavement was mapped at a scale of 1:120, with a lower-limit trace-length cutoff of 1.5 m (Sweetkind, Verbeek, Singer, and others 1995).

An early network of cooling joints consists of three mutually orthogonal joint sets: two subvertical sets, striking northwest and northeast, and one subhorizontal set (fig. 11b, c). Three subsequent sets of tectonic fractures are all steeply dipping; the earliest tectonic fractures are oriented north-south (fig. 11d), followed by northwest-striking (fig. 11e) and finally northeast-striking sets (fig. 11f). The sequential formation of fracture sets was determined by mapped

termination relations, inferred fracture origin (cooling or tectonic joint), and fracture reactivation and offset relations (Sweetkind, Verbeek, Singer, and others 1995). Many fractures experienced renewed growth or reactivation as faults during the formation of subsequent joint sets.

Pavements in the PTn hydrologic unit

Three well-exposed outcrops of the rock units included in the PTn hydrogeologic unit have been mapped as pavements (Sweetkind, Verbeek, Geslin, and Moyer, 1995). All three mapped exposures are located in Solitario Canyon, along the western flank of Yucca Mountain and are spread over a lateral distance of 2 km (fig. 4). The three mapped exposures are named FS-1 (77 mapped fractures in a 245 m^2 area), FS-2 (79 mapped fractures in a 168 m^2 area), and FS-3 (55 mapped fractures in a 116 m^2 area) (fig. 4). Each exposure was mapped at a scale of 1:120, with a lower-limit trace-length cutoff of 1.5 m (Sweetkind, Verbeek, Geslin, and Moyer, 1995).

All three mapped areas are dominated by north-south fractures, along with subordinate numbers of northeast- and northwest-striking fractures (Sweetkind, Verbeek, Geslin, and Moyer, 1995). Overall fracture intensity of the within this interval is low and fractures are poorly connected within and between individual lithostratigraphic units. Fracture intensity in the welded crystal-poor vitric zone of the Tiva Canyon Tuff and in the Yucca Mountain Tuff approach that documented for the welded portions of the Paintbrush Group, but connectivity is poorer (Sweetkind, Verbeek, Geslin, and Moyer, 1995). Fracture intensity and connectivity for the nonwelded and bedded units in this interval is much lower than for the welded units (table 6).

ARP-1 pavement

The ARP-1 pavement is located on the south flank of Antler Ridge (fig. 4), and exposes the upper lithophysal, middle non-lithophysal, and lower lithophysal zones of the Tiva Canyon Tuff (C.A. Braun and others, written communication, 1994). The pavement straddles the main trace of the Ghost Dance fault and two small associated faults. Fracture data from this exposure were collected using detailed line surveys. East of the Ghost Dance fault, fracture data were collected from a series of parallel detailed line surveys spaced 1.5 m apart. Data were collected for fractures longer than 0.3 m that intersected a swath extending 0.3 m from either side of the

Table 6. Fracture intensity of rock units within the PTn hydrologic unit.

[Termination probability, given in percent, is calculated as number of abutting terminations divided by the total number of fracture intersections (abutting plus intersecting). Termination percentage, given in percent, is calculated as number of abutting and intersecting terminations divided by the total number of fracture endpoints. Data are from the three mapped PTn exposures FS-1, FS-2, and FS-3. Informal stratigraphic nomenclature follows the usage of Buesch and others (1995) and Moyer and others (1996). All data are qualified and are reported in Sweetkind, Verbeek, Geslin and Moyer (1995).]

LITHOSTRATIGRAPHIC UNIT	TERMINATION PROBABILITY	TERMINATION PERCENTAGE	INTERSECTIONS/m^2	FRACTURE INTENSITY	
				#/m^2	m/m^2
BT2	50	9.2	0.034	0.2	0.38
PAH CANYON TUFF	83.3	42.9	0.167	0.36	0.5
BT3	85.7	17.3	0.257	0.99	0.94
YUCCA MOUNTAIN TUFF	51	27.1	0.331	0.67	0.73
BT4	0	13.3	0.09	0.615	0.18
CRYSTAL-POOR VITRIC ZONE, TIVA CANYON TUFF	84	23.4	0.284	0.66	0.96
COLUMNAR SUBZONE OF LOWER NONLITHOPHYSAL ZONE,TIVA CANYON TUFF	87	87	2.8	3.73	–

trace line. West of the Ghost Dance fault, fracture data were collected from a series of parallel detailed line surveys spaced 3 m apart. Data were collected for fractures longer than 1.8 m that intersected a swath extending 1.8 m from either side of the trace line. In all, attributes for 577 fractures were measured over an area of 1530 m^2.

The fracture network at ARP-1 is dominated by steeply dipping fractures striking N. 5° W. to N. 25° W. (C.A. Braun and others, written communication, 1994). A smaller number of subvertical northeast-striking fractures have strikes that range from N. 50° E. through N. 70° E. A third general grouping of fractures are large, gently undulatory, shallowly dipping cooling joints with an average orientation of N. 90° E./ 6° N. There is abundant tectonic breccia present at ARP-1 and many fractures show minor amounts of offset; both are interpreted to be the result of proximity to the Ghost Dance fault (C.A. Braun and others, written communication, 1994).

Outcrop studies

Outcrop study of the Tiva Canyon Tuff and Topopah Spring Tuff

Throckmorton and Verbeek (1995) summarized fracture observations at 41 outcrop stations in eight zones of the Tiva Canyon Tuff and four zones of the Topopah Spring Tuff. The fracture observations consist of a descriptive inventory of the fracture network at each locality, with particular emphasis on defining fracture sets and interpreting their age relationships and interactions (Throckmorton and Verbeek, 1995).

Throckmorton and Verbeek (1995) identified an early network of cooling joints consisting of three mutually orthogonal joint sets: two subvertical sets, striking northwest and northeast, and one subhorizontal set. Five subsequent sets of tectonic joints were identified: four are steeply dipping, with the earliest tectonic fractures oriented north-south, followed by northwest-striking and northeast-striking sets, and a late set of cross joints that generally have east-west strikes. The fifth tectonic joint set includes gently dipping joints subparallel to compaction foliation; these joints were interpreted as unloading joints (Throckmorton and Verbeek, 1995).

The nature of the fracture network was found to vary in consistent ways with lithology. For example, cooling joints dominated the fracture network within the upper lithophysal zone of

the Tiva Canyon Tuff, but were vastly outnumbered by tectonic joints in the lower nonlithophysal zone of the Tiva Canyon Tuff (Throckmorton and Verbeek, 1995).

Outcrop study of rocks within the PTn hydrologic unit

Fracture observations were recorded at 19 outcrop stations within the PTn hydrogeologic unit (Sweetkind, Verbeek, Geslin, and Moyer, 1995). The fracture observations consisted of descriptions of the fracture network at each locality, with particular emphasis on vertical continuity of fracture sets and lithologic controls on fracturing (Sweetkind, Verbeek, Geslin, and Moyer, 1995). Fifteen of the outcrop stations are located in Solitario Canyon, along the western flank of Yucca Mountain and cover approximately the same geographic range as the PTn pavements described above (fig. 3). Four additional localities were studied, three along the southern end and eastern flank of Fran Ridge and one in Abandoned Wash (fig. 4).

Each lithostratigraphic unit within the PTn hydrogeologic has its own fracture network with characteristic fracture spacing, intensity and connectivity that are controlled by variations in lithology and degree of welding (Sweetkind, Verbeek, Geslin, and Moyer, 1995; Sweetkind and Williams-Stroud, 1995). Most of the fractures in the PTn section are stratabound and terminate at welding breaks or lithologic breaks. The welding transitions at the top and base of the PTn unit tend to limit fracture connectivity with the welded portions of the Paintbrush Group.

1:240 geologic mapping in the vicinity of the Ghost Dance Fault

Fracture attributes were collected from about 1500 fractures in conjunction with 1:240 scale geologic mapping (Spengler and others, 1993) conducted over a 0.5 km^2 area in the vicinity of the Ghost Dance fault, within the central block of Yucca Mountain (C.A. Braun and others, written communication, 1994). A limited suite of fracture attributes were recorded for fractures with exposed trace lengths greater then 1.8 m. Fracture termination relationships were not recorded, in part because colluvial cover typically obscures the fracture endpoints. These data are primarily useful for orientation analysis and are of lesser value in analyzing trace length, intensity and network connectivity.

Detailed line surveys in the Exploratory Studies Facility

This synthesis report includes fracture data up to ESF station 18+00, roughly 2700 fractures collected over 1.8 km of tunnel. These fracture data represent every lithostratigraphic unit of the Paintbrush Group down to the top of the crystal-poor member of the Topopah Spring Tuff. Important information provided by this collection method include lithologic controls on fracture frequency and continuity, and fracture frequency variations near faults or shear zones. No specific results from the detailed line surveys are summarized here, but are incorporated in the discussion to follow.

Photogrammetric studies

ESF photogrammetry

Fractures were mapped using the photogrammetric approach along a 65 m section of the Tiva Canyon Tuff exposed in the ESF (table 1, entry 21). One-hundred seventy stereo photographs were used to map 1171 fractures (J. Coe, written communication, 1996). All visible fractures with trace lengths greater than about 15 cm were mapped and fracture attributes collected (fig. 12). Seventy percent of the fractures mapped have trace lengths less than 1 m and 89 percent have trace lengths less than 2 m.

In general, fracture orientations are consistent with those observed elsewhere on Yucca Mountain. However, there is considerable variability in orientation as a function of lithology, with shallowly dipping fractures, interpreted as cooling joints, dominating in the densely welded vitrophyre near the top of the crystal-rich member of the Tiva Canyon Tuff (J. Coe, written communication, 1996). The average fracture intensity ranges from 1.85 fracture/m^2 in the densely welded vitrophyre near the top of the crystal-rich Member of the Tiva Canyon Tuff to 0.56 fracture/m^2 in the non-to-partially welded vitric unit that overlies the vitrophyre (J. Coe, written communication, 1996).

UZ-7A exposure

The 5-m high vertical cut across the Ghost Dance fault zone at the UZ-7A drill pad was mapped using the pavement method and the photogrammetry method (table 1, entry 22). Both methods were used with a lower-limit trace length cutoff of 1 m and resulted in relatively small data sets (S. Williams-Stroud, written communication, 1996). The presence of numerous short

fractures associated with the fault zone makes the use of the pavement or photogrammetric methods that use long trace length cutoffs difficult (fig. 13). At a small portion of this exposure (approximately 2.25m^2), every macroscopically visible fracture was measured. The smallest trace length in this area is 0.035 meters. Fracture intensity (in trace length per area, m/m^2) for the small measured area at the UZ-7A exposure is nearly an order of magnitude higher than for the other cleared pavements in the Tiva Canyon Tuff. Orientations of the longer fractures at the UZ-7A exposure can be generally matched to similar orientation populations observed elsewhere on Yucca Mountain.

SYNTHESIS OF FRACTURE DATA

The following sections will present a synthesis of the above studies based on an interpretation of 1) qualified data only and on 2) interpretations derived from both qualified and non-qualified data sources. The data synthesis will be structured around the types of information typically required by users of fracture data involved in numerical simulation of a three-dimensional fracture network or in hydrologic modeling, including: number of fracture sets, mean orientation of each set and dispersion about the mean, fracture trace length distribution, and a measure of fracture intensity. In addition, stratigraphic controls on fracture style and intensity, and spatial distribution of fractures will be discussed.

FRACTURE ORIENTATION

Fracture orientations based on qualified data

Qualified orientation data for fractures measured in the Paintbrush Group are shown for the crystal-rich member of the Tiva Canyon Tuff (fig. 14), the crystal-poor member of the Tiva Canyon Tuff (fig. 15), the lithostratigraphic units that comprise the PTn hydrologic unit (fig. 16), the crystal-rich member of the Topopah Spring Tuff (fig. 17), and the middle nonlithophysal zone of the crystal-poor member of the Topopah Spring Tuff (figs. 5 and 11). All fracture data are shown as lower-hemisphere, equal area projections of poles to fracture planes. The fracture orientation data from all of these units have distributions that are generally similar. In general, most of the poles to fracture planes are concentrated around the perimeter of the equal area projection, corresponding to steeply dipping fractures, with a small number of poles plotting near

the center, corresponding to gently-dipping features. None of the qualified global inventory data from the Tiva Canyon Tuff were subdivided into fracture sets, although concentrations of poles are readily apparent on several of the equal-area projections.

Fracture data from the lithostratigraphic units that comprise the PTn hydrologic unit (fig. 16) (Sweetkind, Verbeek, Geslin, and Moyer, 1995), and the middle nonlithophysal zone of the crystal-poor member of the Topopah Spring Tuff (figs. 5 and 11) (Sweetkind, Verbeek, Singer, and others, 1995) were subdivided into fracture sets on the basis of orientation, joint origin (cooling joint or tectonic joint), and relative age as determined through termination relationships. Median orientations of interpreted fracture sets from the lithostratigraphic units that comprise the PTn hydrologic unit, based on surface data (Sweetkind, Verbeek, Geslin, and Moyer, 1995), are shown in table 7. There are at least seven fracture sets identified within the lithostratigraphic units that comprise the PTn hydrologic unit: two sets of cooling joints in the both the crystal-poor vitric zone of the Tiva Canyon Tuff and in the Yucca Mountain Tuff, four sets of steeply dipping tectonic fractures, and a poorly defined set of gently dipping joints (fig. 16) (Sweetkind, Verbeek, Geslin, and Moyer, 1995). Cooling joints within the two pyroclastic flow units were the earliest joints to form, based on their long trace length, high percentage of blind endings, and the numerous other fractures that abut them. Cooling joints in both the crystal-poor vitric zone of the Tiva Canyon Tuff and in the Yucca Mountain Tuff tend to develop as crudely orthogonal joint sets with high dispersion in orientation (fig. 16; table 7). At many localities, only one of the joint sets is well developed, the other forms a weakly developed set at high angles to it. The orientation of the two sets of cooling joints differs between the two pyroclastic flows (table 7). Joints subparallel to depositional layering are present in the Yucca Mountain Tuff and the crystal-poor vitric zone of the Tiva Canyon Tuff. Some of these may be cooling joints, based on their long trace lengths and the terminations of tectonic joints against them. Other, smaller joints of gentle dip doubtless are due to unloading and constitute a minor element of these units. Data collected at the surface from these units show consistent orientations for the sets of interpreted tectonic joints (fig. 16; table 7). Pole concentrations for tectonic fractures correspond to north-, northwest- and northeast-striking sets. Rare surface structures preserved on joints of all sets show that they originated as extension rather than shear fractures (Sweetkind, Verbeek, Geslin, and Moyer, 1995).

Table 7. Median orientations of fracture sets, rock units within the PTn hydrologic unit

[Median orientations of fracture sets are calculated from combined data from mapped exposures and outcrop stations. Mean poles are calculated by vector addition of pole orientation of all planes in the set. All plunge directions are downward.]

JOINT SET	NUMBER OF POLES	TREND AND PLUNGE OF MEAN POLE	MEDIAN ORIENTATION OF FRACTURE SET
TECTONIC JOINTS			
T1	236	N93E/01	N03E/89W
T2	63	N63E/05	N27W/85S
T3	136	N118E/02	N28E/88W
COOLING JOINTS IN TIVA CANYON TUFF			
C1	39	N3E/01	N87W/89S
C2	27	N116E/06	N26E/84W
COOLING JOINTS IN YUCCA MOUNTAIN TUFF			
C1	16	N33E/01	N57W/89S
C2	11	N115E/03	N25E/87W

Data for the lithostratigraphic units that comprise the PTn hydrologic unit collected using detailed line surveys in the ESF are generally similar to the surface data. Data from surface observation are better clustered because 1) more than twice the number of fractures present in the ESF were measured at the surface, 2) a possible sampling bias is inherent in data collected from along the detailed line survey in the ESF resulting in an underrepresentation of some fracture orientations, and 3) the Yucca Mountain Tuff intercepted in the ESF was very thin (0.5 m) and nonwelded (S. Beason, written communication, 1996) resulting in an absence of cooling joints in this unit within the ESF.

Median orientations of interpreted fracture sets from portions of the upper lithophysal and middle nonlithophysal zones of the crystal-poor member of the Topopah Spring Tuff as exposed at pavement P2001 (Sweetkind, Verbeek, Singer, and others, 1995) are shown in table 2 (p. 27). Three well-defined sets of cooling joints are present. Two sets are steeply dipping and strike generally northwest and east-northeast (table 2), a third set are generally shallowly dipping surfaces that have very long trace lengths and gently undulate. The relative timing of the various cooling joints sets is often indeterminate. In general, the high-angle cooling joints cross each other or have mutually abutting relations that are indicative of similar time of formation. Occasionally, high angle cooling joints appear to terminate against the shallowly-dipping cooling joints. These abutting relationships, combined with the exceptional trace lengths of the shallowly-dipping cooling joints suggest that they may have formed slightly earlier then the two sets of steeply dipping cooling joints (Sweetkind, Verbeek, Singer, and others, 1995).

Tectonic joints form three distinct sets that strike north, northwest and northeast (table 2; figs. 5 and 11). North-striking joints at P2001 are the earliest-formed tectonic fracture set, because they are the longest tectonic fractures, have the largest percentage of blind terminations and are only truncated by preexisting cooling joints (Sweetkind, Verbeek, Singer, and others, 1995). The northwest-striking fracture set appears to generally be younger than the north-striking set at P2001. Northeast-trending tectonic fractures were the last to form and appear as short connectors between the earlier cooling and tectonic fracture sets. The orientation of tectonic joints is very similar between the lithostratigraphic units that comprise the PTn hydrologic unit and the upper lithophysal and middle nonlithophysal zones of the crystal-poor member of the Topopah Spring Tuff (compare tables 7 and 2).

At the time of writing of this report, reviewed, qualified data from the ESF were not available from the crystal-poor member of the Topopah Spring Tuff, so the surface data cannot be compared to ESF data.

Fracture orientations based on qualified and non-qualified data

Orientation data for fractures measured in the Paintbrush Group from all qualified and non-qualified sources are shown as contoured equal-area pole projections in figure 18. These contoured projections tend to emphasize concentrations of large numbers of poles. Fracture sets with fewer data points, such as shallowly-dipping joints, are less well represented. The fracture orientation data from all of these lithostratigraphic units have distributions that are generally similar to those from the qualified data only. In general, most of the poles to fracture planes are concentrated around the perimeter of the equal area projection, corresponding to steeply dipping fractures, with a small number of poles plotting near the center, corresponding to gently-dipping features.

Data from most of the lithostratigraphic units form a girdle of poles corresponding to steeply dipping fractures with northwest, north, or northeast strikes. For most units within the Tiva Canyon Tuff, a pole population corresponding to north-northwest striking planes is most common.

The upper lithophysal zone of the Tiva Canyon Tuff has additional maxima in the southeast and southwest quadrants of the equal-area net (fig. 18b). These maxima correspond to joints that were mapped and interpreted as cooling joints at pavements 100 and 300 (Barton and others, 1993) and at several outcrop localities in this unit (Throckmorton and Verbeek, 1995). A study of fractures in outcrops in the vicinity of Live Yucca and Dead Yucca ridges (fig. 4) highlighted the dominance of cooling joints in the upper lithophysal zone of the Tiva Canyon Tuff (Morgan, 1984; summarized as Barton and others, 1989).

Shallowly-dipping joints form a prominent maximum in equal area net diagram of the crystal-rich vitric zone of the Tiva Canyon Tuff (fig. 18a). These joints have been interpreted as cooling joints (J. Coe, written communication, 1996).

Much of the scatter in joint orientation on the equal area nets for the entire data set can be resolved by separating joints based on their origin. Where the method has been used, fracture

studies have had good success in resolving joint orientations from apparently very scattered pole distributions once joint origin and relative timing of formation were considered (Throckmorton and Verbeek, 1995; Sweetkind, Verbeek, Singer and others, 1995). However, all of the fracture studies did not identify joint sets or subdivide cooling joints from tectonic joints. Where tubular structures on the surfaces of cooling joints are absent, cooling joints have been interpreted using a combination of criteria including: low surface roughness (JRC of five or less); smooth, continuous traces; appreciable length; parallelism with proven cooling joints nearby; and demonstrated early age as shown through abutting relations with fractures of other sets (Throckmorton and Verbeek, 1995; Sweetkind, Verbeek, Singer and others, 1995; Sweetkind, Verbeek, Geslin and Moyer, 1995). Of this suite of criteria, low surface roughness is the most consistent differentiator between cooling joints and tectonic joints, especially in welded units. Barton and others (1993) recognized that measured fractures at pavements 100, 200 and 300 showed a bimodal distribution of joint roughness, with cooling joints having joint roughness coefficients (JRC) between zero and four, tectonic joints having a median JRC of 9. Studies of fractures in outcrops (Morgan, 1984; summarized as Barton and others, 1989) recognized the same effect.

As an attempt to distinguish joints based on their origin, joints with surface roughness of 0 to 2 are separated from joints with roughness of 3 or greater. This split is simplistic; it is possible that some extremely smooth tectonic joints may exist. Similarly, known cooling joints with may have joint roughness coefficients of up to five, and Morgan (1984) interpreted a cooling origin for certain joints with even higher roughness. The exercise merely attempts to separate the joints most likely to be of cooling origin. All fractures in the database with roughness less than 3 were plotted on equal-area projections (fig. 19). The orientations of these fractures are compared with features definitively identified as cooling joints in the individual studies (fig. 19).

The contoured equal area nets for the smooth joints and for the fractures actually recorded as cooling joints in the data sets both show broad, diffuse girdles of orientations with few well-defined maxima (fig. 19). This is mostly the result of the overlapping of orientations of cooling join sets from individual pyroclastic flows where the joints formed at the time of flow deposition and the orientation of joint sets are unique to each of the flow units.

The number and orientation of tectonic fracture sets are generally similar between the Tiva Canyon Tuff (Throckmorton and Verbeek, 1995), portions of the Topopah Spring Tuff (Sweetkind, Verbeek, Singer, and others, 1995) and in the intervening bedded and non-welded units (Sweetkind, Verbeek, Geslin, and Moyer, 1995). In general, there appear to be three broad orientation groupings of tectonic joint sets, north-striking, northwest-striking, and northeast-striking (fig. 20). The contoured plots show this quite well (fig. 20). The most prominent maximum is for N-S striking joints (fig. 20a). Subordinate maxima for NE and NW striking joints are also present. The fractures with joint roughness coefficients greater than two and the fractures identified by the observer to be tectonic joints produce very similar orientation distributions (fig. 20a and 20b).

TRACE LENGTH

Qualified data

Understanding the distribution of fracture size (observed as trace length) is a critical descriptive element of the fracture network. The range of distribution of fracture sizes is an important consideration in the construction of discrete fracture network models. Geometric models of fracture network, such as fractal scaling models, also require knowledge of the distribution in fracture sizes.

Fracture length data are affected by the size of the area of observation, either a natural exposure or a cleared pavement, and the lower-limit trace length cutoff used during fracture mapping. As a result, trace length distributions may be truncated artificially at the long end by the limits of exposure and in the small size range by the lower-limit cutoff used.

Available qualified data from surface mapping suggest that within the limited size range measured (minimum length cutoff measured 1.5 m, maximum length measured approximately 15 m), that it is reasonable to approximate fracture trace length distributions with curves that have the general shape of exponential or power-law curves (fig. 21). Similar shaped distributions occur for the ESF detailed line survey data where the fracture trace length cutoff goes down to 0.3 m (fig. 22) and for close-range photogrammetry along a 60-m stretch of the ESF where fractures were measured down to .15 m. Fracture trace length distributions for individual lithostratigraphic units within the ESF show the same general shape but are less regular in units

where only a small number of fractures (50 or less) were measured. This suggests that fracturing is sufficiently variable that rather large data sets are required to obtain realistic distributions.

Analysis of fracture size by set from surface mapping suggests that fracture size tends to decrease as new sets were added to the network (Sweetkind, Verbeek, Geslin and Moyer, 1995). Fractures decrease in size because new fractures simply could not propagate very far before terminating against an already existing fracture (Barton and Larsen, 1986). The fracture data from both the mapped exposures and the outcrop stations in lithostratigraphic units within the PTn interval show this general pattern: cooling joints and early tectonic joints in general have the longest trace lengths, later joints have generally shorter trace lengths. However, cooling joints tend to exist as dominant and subordinate sets, so all cooling joints are not necessarily long, even though they can be shown to have formed early based upon abutting relations. Another complication is that all fracture sets are not developed at any given locality, so that the earliest set to form locally may be relatively late in the overall sequence. In some instances, tectonic joints may have been the earliest fractures to have developed locally and have the longest trace lengths and greatest proportion of blind endings. Local variations in the development of different fracture sets could explain much of the variability of the trace length data from the individual lithostratigraphic units in the ESF data.

Qualified and non-qualified data

Trace lengths for cooling joints and tectonic joints from the entire database are shown in figure 23. The only significant addition from the qualified data set discussed above are the nonqualified pavements. Similar to the analysis of qualified data alone, available data from surface and subsurface mapping suggest that within the limited size range measured (minimum length cutoff measured 1.5 m, maximum length measured approximately 15 m), it is reasonable to approximate fracture trace length distributions with curves that have the general shape of exponential or power-law curves (fig. 23). A simple query of the entire data set based on fracture roughness indicate no significant difference in the distribution of fractures most likely to be cooling joints versus those likely to be tectonic joints (fig. 24). In this case, the shape of the trace length distribution is mostly affected by the minimum trace length cutoff used for the individual

study, for example, the trace length cutoff for the Ghost Dance fault mapping data set was 1.8 meters (fig. 24).

FRACTURE INTENSITY

Qualified data

Fracture data from Yucca Mountain can be divided into two broad subgroups: two-dimensional data where fracture observations were collected over an area, such as pavement maps, outcrop observations, and full-periphery maps in the ESF, and one-dimensional data where fracture attributes are collected along a line, such as detailed line survey. One of the most difficult aspects to compare between the two broad types of data is fracture intensity. Fracture intensity for two-dimensional data can be reported as fracture trace length per unit area (units of m/m^2), number of fractures per unit area ($1/m^2$), or number of fracture intersections per unit area ($1/m^2$) (table 8). Intensity for one-dimensional data can only be measured as number of fractures per meter (1/m). These various measures of fracture intensity are shown for qualified data in table 8.

Different lower-limit trace-length cutoffs make difficult statistical comparisons of data collected by different methods. The shape of fracture trace length distributions at Yucca Mountain are generally consistent with a power-law or exponential model to these distributions (for example, figs. 21 and 22). Therefore, use of a smaller lower-limit trace-length cutoff results in the measurement of increasing numbers of fractures in a given area, which directly affects fracture intensity as reported in fracture trace length per unit area (units of m/m^2) or number of fractures per unit area ($1/m^2$) (table 9). Both qualified pavement and photogrammetry data and data from non-qualified pavements show the same type of decreases in calculated fracture intensity with increases in minimum trace length cutoff (table 9). Thus, realistic comparison of fracture intensity can only be made from data sets that used the same minimum trace length cutoff.

The effect of trace length cutoff on calculated fracture intensity is shown for two-dimensional data sets data (pavement maps and ESF photogrammetry) in figure 25. If intensity (in trace length per area, m/m^2) is calculated using all measured fractures at a particular exposure, regardless of lower-limit trace-length cutoff, the fracture intensity for the control area

Ta . Comparison of fracture intensity and network ge ry, Paintbrush Group.

[Fracture intensity is calculated as number per area, #/m^2, and trace length per area, m/m^2, for two dimensional data and number per meter, #/m, for one dimensional data. Intersection intensity is calculated as number of intersections per area, #/m^2, for two dimensional data and number of intersections per unit fracture trace length, #/m, for one dimensional data. Termination percentage, given in percent, is calculated as number of abutting and intersecting terminations divided by the total number of fracture endpoints. Numerical values for each of the above parameters are coded by data collection method, as follows: plain type for data collected by the pavement method; data collected by detailed line surveys (DLS) within the ESF in brackets; and bold type for data collected by close-range photogrammetry within the ESF. Lower-limit trace length cutoffs are 0.3 m and 0.15 m for the DLS and photogrammetry, respectively. Lower-limit trace length cutoffs for pavements are given in the footnotes.]

LITHOLOGIC UNIT	FRACTURE INTENSITY			INTERSECTION INTENSITY		TERMINATION PERCENTAGE
	#/m^2	m/m^2	#/m	#/m^2	#/m	
Bedded tuff[1]	0.20	0.38	[0.38]	0.03	0.18 [0.1]	9.2 [18.4]
Nonwelded to partially welded pyroclastic flow[1]	0.67	0.73	[0.47]	0.33	0.44 [0.1]	27.1 [23.3]
Poorly to moderately welded vitric zone, Tiva Canyon Tuff[1]	0.66	0.96	[1.23]	0.28	0.3 [0.32]	23.4 [38.4]
Moderately to densely welded Tiva Canyon Tuff						
Crystal-rich member[2]	1.00	0.98	0.74 [1.2]	0.29	1.02	15.20
Upper lithophysal zone[3]	0.80	2.03	[1.79]	0.73	0.59 [0.23]	29 [22.8]
Middle nonlithophysal zone	—	—	[2.64]	—	— [0.56]	— [60.7]
Moderately to densely welded Topopah Spring Tuff						
Upper lithophysal zone[4]	0.26	0.64	[1.23]	0.10	0.18 [0.25]	20.40
Middle nonlithophysal zone[4]	0.73	1.70	[3.73]	1.40	0.78 [0.71]	79.7 [56.7]

[1] Pavement data are derived from maps of three natural exposures of the interval separating the Tiva Canyon Tuff from the Topopah Spring Tuff (D. Sweetkind, unpubl. data). Non- to partially-welded pyroclastic flows include the Pah Canyon and Yucca Mountain Tuffs (Sawyer et al., 1993). Lower-limit trace length cutoff is 1.5 m.

[2] Data are from ESF photogrammetry strip. Lower-limit trace length cutoff is 0.15 m.

[3] Pavement data (Non-qualified) are derived from maps of pavements 100, 200, and 300 (Barton et al., 1993). Lower-limit trace length cutoff is 0.2 m.

[4] Pavement data are derived from map of pavement P2001, Fran Ridge. Lower-limit trace length cutoff is 1.5 m.

TABLE 9. RELATIONSHIP OF FRACTURE INTENSITY TO TRACE LENGTH CUTOFF

[Sum of the measured trace lengths, number of mapped fractures, and minimum trace length cutoff used are shown for each mapping study a first entry for each study. Calculated intensity, number of fractures, and total fracture trace length are computed by arbitrarily varying the minimum trace length cutoff. Non-qualified data from the upper lithophysal zone of the Tiva Canyon Tuff are included for comparison]

	Lower-limit trace Length cutoff	Total area of pavement (in m^2)	Total measured fracture trace length (in m)	Intensity (m/m^2)	Number of fractures measured
ESF photogrammetry, crystal-rich member of Tiva Canyon Tuff					
	0.3	1170	1145	0.98	1170
	1	1170	730	0.62	338
	1.5	1170	551	0.47	191
	1.8	1170	466	0.4	139
Pavement P2001, middle nonlithophysal zone, Topopah Spring Tuff					
	1.5	500	507	1.01	131
	1.8	500	481	0.96	115
Pavement 100, upper lithophysal zone, Tiva Canyon Tuff					
	0.2	214	508	2.35	221
	1	214	457	2.13	139
	1.5	214	402	1.88	99
	1.8	214	383	1.79	84

at the UZ-7a exposure, along the Ghost Dance fault, is nearly an order of magnitude higher than for the other exposures (fig. 25a). If intensity instead is calculated using only fractures greater than 1.5 m in length (the smallest common lower-limit trace-length cutoff), the calculated fracture intensity at all exposures decreases, and the apparent fracture intensity at the UZ-7A exposure is similar to the other exposures (fig. 25b). As in table 9, data from non-qualified pavements 100, 200 and 300 show the same type of decreases in calculated fracture intensity with increases in minimum trace length cutoff as do the qualified data (fig. 25). A large lower-limit trace length cutoff used during mapping minimizes the contribution of short fractures in calculations of fracture intensity. In cases where short trace length fractures have a high percentage of blind terminations, they may not be important to the hydrologic network. However, in the case of highly fractured rocks near fault zones, where observations indicate a high degree of connectivity, short trace length fractures may constitute an important component of the fracture network.

Comparing data that were collected using the same trace length cutoff, fracture intensity is controlled largely by the lithologic units; the bedded tuffs have much lower fracture intensities than the pyroclastic flows (table 8). The relationship between fracture character and zonal variations within the flows is often less clear, but the poorly welded, vitric tops and bottoms of the flows have generally lower fracture intensity than the densely welded interiors (table 8).

Fracture intensity, or frequency, for one-dimensional data sets is given in number of fractures per meter (#/m). Fracture frequency is calculated for fractures in various lithostratigraphic units using data from the ESF detailed line survey (fig. 25c). The relative fracture frequencies follow the same general relative pattern as the 2-dimensional sets shown in table 8, with the intensity of the bedded tuff units being considerably lower than that for the welded tuff units. Figure 25d compares the detailed line survey data from the ESF to the pavement data set collected by the detailed line survey method at ARP-1. Fracture frequency for both sets of data has been calculated using the lower-limit trace length cutoff used at ARP-1, which was 1.8 meters. Fractures intensity for ARP-1 is similar, but slightly higher than for the same units within the ESF, perhaps due to the fact that ARP-1 is along the Ghost Dance fault.

FRACTURE CONNECTIVITY

Fluid flow through a fracture network depends in part on how well the fractures are interconnected. Fracture connectivity, in turn, is dependent upon fracture size and orientation distributions, fracture density, and the fracture system geometry, particularly the distribution of intersection types, all of which can be measured or described through field observations and geometric analysis of the resulting pavement maps. Complex fracture networks are typically well-connected since the development through time of multiple fracture sets promotes fracture interaction. Abundant cooling joints and early tectonic joints limited the amount of available area for subsequent fractures to propagate, thus many late fractures simply connect early-formed fractures.

Barton and others (1993) represented fracture connectivity within a unit as ratios of three types of fracture terminations or interactions. Fractures may (1) terminate in the rock matrix as a blind or dead end; (2) they may cross each other as an intersection or X termination, or (3) they may abut each other, at a T or Y termination. The relative proportions of these termination types in an exposure maybe expressed as ratios using the terms of termination probability and termination percentage. Termination probability, the likelihood that a fracture will abut an earlier formed fracture, is calculated as the number of abutting intersections divided by the total number of fracture intersections (abutting and intersecting). Termination percentage, the likelihood that a fracture will intersect another fracture rather than end blindly, is calculated as the number of abutting and crossing terminations divided by the total number of fracture endpoints.

Fracture connectivity must be integrated with intensity in an evaluation of the potential flow properties of a fractures network; well-connected fractures may still yield very few continuous pathways given low fracture densities. One such combination of connectivity and intensity is intersection intensity. Intersection intensity is calculated as the number of fracture intersections per area ($\#/m^2$) for the two-dimensional data. For one-dimensional data (detailed line survey) intersection intensity is reported in terms of number of fracture intersections per unit fracture trace length (table 8). The calculation of intersection intensity is dependent on both fracture intensity and on network geometry. For example, a network consisting of many subparallel fractures would yield a low intensity by this measure. In general, however, this

measure of intensity yields values that are quite consistent for both one-dimensional and two-dimensional fracture measures (table 8).

Qualified data

Geometric analysis of the qualified pavement and photogrammetry data has yielded data on fracture intensity, fracture intersection intensity and termination probabilities (table 8). Table 8 shows values for various types of intensity and connectivity measures for qualified data from pavement, detailed line survey and photogrammetry studies. Fracture intensity appears to be directly related to the degree of welding of the lithostratigraphic unit. Fracture intensity within the bedded and nonwelded to poorly welded units is much lower than in the surrounding densely welded units (table 8). The highest termination percentage is in the non-lithophysal zones of both the Tiva Canyon and Topopah Springs Tuffs, with the values obtained from pavements slightly higher than those derived from the ESF data. The non-welded bedded tuff deposits have the lowest termination percentage; in this case the value from the pavement data is lower than the value from the ESF detailed line survey. Data from the ESF photogrammetry study within the crystal-rich member of the Tiva Canyon Tuff yield relatively high fracture intensities, but relatively low termination percentage. These data may be explained by a predominance of short, subparallel fractures, many of which are probably cooling joints (fig. 12).

Qualified and non-qualified data

Inclusion of non-qualified data allows pavement data from the upper lithophysal zone of the Tiva Canyon Tuff to be compared with the qualified pavement data (fig. 26). In general, fracture intensity, intersection intensity and termination percentage are comparable to those from qualified data in moderately to densely welded pyroclastic units (table 8). The non-qualified data from the upper lithophysal zone of the Tiva Canyon Tuff are consistent with the trends defined based on the qualified data - that the degree of welding has the greatest effect on the overall character of the fracture network. Fracture intensity and network connectivity within nonwelded and poorly welded units is again much lower than in the surrounding welded units (fig. 26, table 8). Fracture intensity increases with degree of welding within the welded pyroclastic flows (fig. 26) due to the presence of cooling joints and because increasing brittleness of the rock favors an

increase in the number of tectonic joints. Network connectivity increases markedly in the welded portions of pyroclastic flows (fig. 26) due to the presence of multiple joint sets and to the presence of cooling joints that are typically large and act as important connectors of the network.

STRATIGRAPHIC CONTROLS ON FRACTURE NETWORK PROPERTIES

There are a number of primary controls on fracture character within the Paintbrush Group that are related to stratigraphy, upon which any later tectonic signature is superimposed. Variations in lithology across depositional boundaries, and variations in welding, devitrifcation and lithophysae development within welded pyroclastic flows of the Paintbrush Group control fracture network properties such as intensity and network connectivity. The controls on fracture character within the Paintbrush Group are discussed below.

Welding variations

Fracture characteristics in the pyroclastic flows are primarily controlled by variations in the degree of welding. Fracture intensity and network connectivity within nonwelded and poorly welded units are much lower than in the surrounding welded units (table 8; fig 26). Fracture intensity and network connectivity increase markedly in the welded portions of pyroclastic flows due to the presence of multiple joint sets. Greater degree of welding promotes the formation of both cooling and tectonic joints. In addition, typically long cooling joints act as important connectors of the network. For example, the welded units have a significant number of fractures with trace lengths in the range of 5 to 10 meters (fig. 21), whereas the non-welded units tend to have few fractures longer than approximately 5 meters.

Cooling joints have been identified in every zone of the Tiva Canyon Tuff and Topopah Spring Tuff that are at least moderately welded. Cooling joints are also present in the Pah Canyon Tuff and Yucca Mountain Tuff where these units are welded; cooling joints are absent in the non-welded PTn units (Sweetkind, Verbeek, Geslin and Moyer, 1995). Cooling joints within the Topopah Spring and Tiva Canyon Tuffs often consist of two orthogonal sets that are steeply dipping, resulting in a rectangular pattern of joints (see for example, figs. 9 and 11). The joints of one set typically dominate in length and abundance over those of the other. Less frequently, a third, subhorizontal set of cooling joints is present. These joints are generally shallowly dipping

surfaces that are subparallel to flattening foliation, have very long trace lengths and gently undulate. The shallowly dipping cooling joints are more common at particular stratigraphic intervals, for example, near the contact between the middle nonlithophysal and upper lithophysal zones of the Topopah Spring Tuff (Sweetkind, Verbeek, Singer and others, 1995). Cooling joints within the columnar subzone of the lower nonlithophysal zone of the Tiva Canyon Tuff form a hexagonal network of that subdivide the rock into abundant, crude, vertical columns 2-5 m high. Cooling joints that bound the columns extend only short distances upward and downward into the surrounding rock units (Sweetkind, Verbeek, Geslin and Moyer, 1995).

Fracture intensity also increases with degree of welding within the welded pyroclastic flows because increasing rigidity of the rock favors an increase in the number of tectonic joints. Formation of tectonic fractures is limited to some extent by the development of cooling joints - the cooling joints tend to accommodate extensional strains through reactivation and also limit the amount of free space available for tectonic joints to propagate. Still, late joint sets are most common in the welded flow units, and the number and size of tectonic fractures increase as the degree of welding increases.

Pumice content and clast size

Where primary depositional features such as pumice and lithic clasts have not been obliterated by welding, they can act as a control on fracture development. The fracture characteristics of nonwelded pyroclastic flows and interstratified fall and reworked pyroclastic deposits within the Paintbrush Group are controlled primarily by changes in pumice content and clast size (Sweetkind, Verbeek, Singer, and others, 1995; Sweetkind and Williams-Stroud, 1995). Increasing pumice content is correlated to decreasing fracture intensity. Clast size has a lesser role in determining fracture character, but coarser units are not as fractured as fine-grained deposits.

Increasing pumice content is correlated to decreasing fracture intensity in nonwelded portions of the Paintbrush Group (Sweetkind, Verbeek, Geslin and Moyer, 1995). Among the nonwelded units, recognizable sets of fractures are most common in the basal, nonwelded portion of the crystal-poor vitric zone of the Tiva Canyon Tuff and in nonwelded Yucca Mountain Tuff, both of which generally contain 15 percent or less of pumice clasts (Moyer and others, 1996).

Nonwelded units with 30-70 percent pumice clasts, which includes most of the bedded tuffs and nonwelded flows between the base of the Yucca Mountain Tuff and the top of the Topopah Spring Tuff, are much more sparsely fractured, and definable sets are lacking at many localities (Sweetkind, Verbeek, Geslin and Moyer, 1995). Many of the fractures terminate at compositional boundaries, such as the contacts with pumice-rich airfall deposits. Pumiceous tephra deposits containing 80 percent or more of pumice clasts generally are unfractured except for sparse weathering joints (Sweetkind, Verbeek, Geslin and Moyer, 1995).

High pumice density appears to interfere with fracture propagation. As a result, fracture trace lengths are shorter, fewer fractures from each set are present, and there are a greater proportion of blind fracture terminations (Sweetkind, Verbeek, Geslin and Moyer, 1995). Brittle, pumice-poor rocks develop tectonic joints because they fail at low strains by fracture. Pumice-rich units are apparently able to accommodate strain without brittle failure, possibly through such mechanisms as compaction and rotation of glass shards, and volume reduction of pumice fragments. In response to extensional stresses, fractures would be expected to initiate in the relatively more brittle units and propagate into the surrounding units. Often the only tectonic joints seen in the pumice-rich bedded tuffs in the Paintbrush Group are those that propagated into them from other units above or below (Sweetkind, Verbeek, Geslin and Moyer, 1995).

The effect of clast size is difficult to separate from other important controls on fracture network development. Nevertheless, increasing clast size appears to inhibit the development of fractures (Sweetkind, Verbeek, Geslin and Moyer, 1995). Comparison of the three pumiceous airfall tephras within the Paintbrush Group (informal subunits units Tpbt3a, Tpbt3d, and Tpbt4, of Moyer and others, 1996) reveals that the finest-grained of the three (informal unit Tpbt4) consistently contains the most fractures. Similar relationships between joint development and grain size are known in sedimentary rocks, particularly sandstones and conglomerates (Price, 1966).

Lithophysal zones

The development of lithophysae inhibits fracture propagation, resulting in decreases in joint length and continuity, and increases in surface roughness and trace irregularity. Tectonic fractures in highly lithophysal rock are short - most cannot be followed as continuous surfaces

for more than three meters. The joints also become more difficult to follow visually, their surfaces become rougher and pockmarked by abundant lithophysal cavities, and their traces become more irregular. In many cases, the fractures appear to link lithophysae. All of these properties reflect the difficulty of propagating a smoothly continuous fracture through a rock containing numerous large voids.

A good example of the effect of lithophysae on fracture development is seen at pavement P2001 at Fran Ridge (fig. 4). The rock units exposed at this pavement include both the upper lithophysal and middle non-lithophysal zones of the Topopah Spring Tuff and the transition zone in between. The overall style of fractures at Pavement P2001 differs markedly as a function of lithology (Sweetkind, Verbeek, Geslin and Moyer, 1995). Fractures within the middle non-lithophysal zone tend to be planar or arcuate with low surface roughness; fractures within the upper lithophysal zone are sub-planar but extremely rough. On average, fractures in the middle non-lithophysal zone are significantly longer than fractures in upper lithophysal zone. At pavement P2001, fracture intensity varies from a high of 1.7 m/m^2 in the middle non-lithophysal zone to a low of 0.54 m/m^2 in the upper lithophysal zone (table 8). These changes in fracture character occur abruptly at the lithologic contact (Sweetkind, Verbeek, Geslin and Moyer, 1995).

Fracture data from lithophysal and nonlithophysal zones within the Tiva Canyon Tuff show similar, but less distinct, trends to those seen in the Topopah Spring Tuff. Fracture intensity from the upper lithophysal zone of the Tiva Canyon Tuff, collected by detailed line survey within the ESF, is only about 30 percent lower than calculated fracture intensity from the underlying middle non-lithophysal zone (table 8). The reason that the fracture intensity in these two zones is relatively similar lies in the greater abundance of cooling joints in the upper lithophysal zones of the Tiva Canyon Tuff. Cooling joints are thought to have formed prior to or during lithophysae development (Morgan, 1984; Barton, 1984; Barton and others, 1984). Thus cooling joints are able to grow as long, smooth, continuous features, unimpeded by the presence of lithophysal cavities. Cooling joints are common in the upper lithophysal zone of the Tiva Canyon Tuff, but are relatively rare in the upper lithophysal zone of the Topopah Spring Tuff. Both units probably have similar numbers of tectonic joints, but the lack of cooling joints in the upper lithophysal zone of the Topopah Spring Tuff results in an aggregate fracture intensity that

is very different than the underlying middle non-lithophysal zone. These two zones have subequal intensities in the Tiva Canyon Tuff (table 8).

VERTICAL CONTINUITY OF THE FRACTURE NETWORK

The fluid-flow properties of the fracture network within the Paintbrush Group are dependent upon the vertical continuity of the fracture network and the degree to which the fractures within each lithostratigraphic unit are interconnected. Fracture connectivity within the Paintbrush Group as a whole is limited by the Paintbrush Tuff nonwelded (PTn) hydrogeologic unit (Montazer and Wilson, 1985; Moyer and others, 1996), an interval of nonwelded, bedded tuffs that has moderate to high porosity and permeability, largely stratabound fracture networks and very low fracture intensity. Fracture connectivity within the welded portions of the pyroclastic flows is dependent on the degree of communication between fracture networks within individual zones.

Connectivity within the welded units

The relationship between fracture network properties such as intensity and connectivity and the zonal variations within the welded portions of the pyroclastic flows is often obscure. Except for the welding transitions at the tops and bottoms of the flows, all of the zonal variations within the Tiva Canyon Tuff and Topopah Spring Tuff are developed in densely welded tuff (Buesch and others, 1996). Thus, differences between zones cannot be related to degree of welding, but must be controlled by other factors including lithophysae content, degree of vapor phase recrystallization, and crystal and lithic clast content. Outcrop observations were carried out in order to begin to characterize the fracture network of various zones within the welded flow units (Throckmorton and Verbeek, 1995), but there has never been a surface or subsurface data collection effort to attempt to characterize the vertical connectivity of the fracture network within the welded flow units. However, other types of evidence suggest that overall connectivity is high within the welded units, including: 1) pressure changes in boreholes associated with the opening of the ESF (J. Rousseau, written communication, 1996); 2) pathways analysis of simulated fracture network in the Tiva Canyon Tuff (L. Anna, written communication, 1996).

Connectivity within the bedded and nonwelded units

Overall fracture intensity for lithostratigraphic units that comprise the Paintbrush Tuff nonwelded (PTn) hydrogeologic unit is low and fractures are poorly connected within and between lithostratigraphic units (table 8). Each of the units in this interval appears to have its own fracture network - in many cases, poorly developed - with characteristic fracture spacing, intensity and termination style units (Sweetkind, Verbeek, Geslin and Moyer, 1995). Fracture intensity in the welded crystal-poor vitric zone of the Tiva Canyon Tuff and in the Yucca Mountain Tuff approach that documented for the welded portions of the Paintbrush Group, but connectivity is poorer (fig. 26, table 8). Fracture intensity and connectivity for the nonwelded and bedded PTn units is much lower than for the welded units (Sweetkind, Verbeek, Geslin and Moyer, 1995) (fig. 26).

The fracture networks for most of the lithostratigraphic units that comprise the Paintbrush Tuff nonwelded (PTn) hydrogeologic unit are dominantly stratabound. For instance, the fracture network within the pre-Pah Canyon bedded tuffs (informal unit Tpbt2 of Moyer and others, 1996) is completely stratabound and has no connection to the surrounding units (Sweetkind, Verbeek, Geslin and Moyer, 1995). Most of the fractures in the lithostratigraphic units of this interval terminate at welding transitions or compositional breaks. A significant number of fractures in the Yucca Mountain Tuff extend a short distance upward or downward into the surrounding bedded units. In response to extensional stress, fractures must have initiated in the relatively more brittle Yucca Mountain Tuff and propagated outward into the surrounding units. Lithologic changes also are responsible for the termination of stratabound fractures within the pre-Yucca Mountain bedded tuffs (informal unit Tpbt3 of Moyer and others, 1996). Many fractures within this unit terminate at lithologic contrasts, such as contacts with pumice-rich units.

Connectivity across welding transitions

The welding transitions at the base of the Tiva Canyon Tuff and the top of the Topopah Spring Tuff tend to limit fracture connectivity within the Paintbrush Group. Fractures often terminate abruptly at these welding transitions and vertical connectivity is thus limited, even though fracture connectivity within the welding zone may be high. Cooling joints of the

columnar subzone of the lower nonlithophysal zone of the Tiva Canyon Tuff terminate downward into a network of small, irregular cooling joints in the upper part of the crystal-poor vitric zone (Sweetkind, Verbeek, Geslin and Moyer, 1995). Both cooling and tectonic joints in the crystal-poor vitric zone of the Tiva Canyon Tuff have limited vertical extents and terminate downward into poorly welded tuff that has significant matrix porosity and permeability (Moyer and others, 1996). A similar relationship between fracture character and degree of welding exists within the more abrupt welding transition at the top of the Topopah Spring Tuff.

SPATIAL DISTRIBUTION OF FRACTURE ORIENTATION

A determination of the manner in which fracture characteristics, such as orientation and length, and network characteristics, such as intensity, change over the repository area is a potentially important input for hydrologic modeling. Unfortunately, such analysis is made difficult by the data available. This type of analysis would ideally be made with a number of data points from the same unit - this is not available.

Qualified data sets that were collected over a large enough area to show any spatial pattern include: 1) fracture data collected in conjunction with 1:240 geologic mapping in the vicinity of the Ghost Dance fault (Spengler and others, 1993); 2) fracture study areas within the PTn unit; and 3) data collected at the 41 uncleared outcrop stations.

The 1:240 geologic mapping in the vicinity of the Ghost Dance fault (Spengler and others, 1993) recorded the location of more than 1500 fractures and cooling joints. These data are shown in map view in figure 27. Cooling and tectonic joints were not explicitly listed in the original data, but joint roughness data were collected for each joint. Using the roughness criterion, the fractures were divided into groups with a joint roughness coefficient (JRC) of two or less, possibly corresponding to cooling joints, and JRC of three or more, possibly corresponding to tectonic joints (fig. 28). The 30 m (100 foot) squares in figure 27 show the distribution of fractures in a portion of the area mapped, with the approximate location of the Ghost Dance fault trace (30 m grid is after Spengler and others, 1993; approximate trace of the Ghost Dance fault is from W. Day and others, written communication, 1996). No systematic increase can be seen in the number of fractures closer to the fault. Ground cover has a very critical effect on any interpretations of spatial changes in orientation or fracture intensity that

could be made from these data. The distribution of fractures in this data set is an absolute artifact of the collection method; visible fractures were mapped without an attempt to quantify the degree of exposure. As a result, the number of fractures in each square has little significance for fracture intensity.

An evaluation of the orientations of fractures from the 1:240 mapping is also limited to qualitative approach. Figure 28 shows the orientations of joints with roughness < 3 and joints with roughness > 2 for the Ghost Dance fault mapping data set. Many of these data were collected from the crystal-poor member of the Tiva Canyon Tuff; the orientation maxima show many similarities to data from these units collected elsewhere on Yucca Mountain (fig. 15). Both the possible cooling joints and the possible tectonic joints have most of their planes oriented 5 to 10 degrees west of north (fig. 28).

Rose diagrams of strike distributions from all the surface data sets except the fracture data collected in conjunction with 1:240 geologic mapping are shown at their locations on the map in figure 29. Most of the rosettes (51) are for outcrop data sets; 13 are from mapped pavements, and two are fracture mapping from the ESF (ESF photogrammetry and ESF starter tunnel. The rosettes are subdivided by lithostratigraphic unit as follows:

- red, crystal-rich member of the Tiva Canyon Tuff;
- green, upper lithophysal zone of the crystal-poor member of the Tiva Canyon Tuff (non-qualified data from pavements 100, 200, 300, 400, 500 and 600 are shown for comparison);
- light blue, middle nonlithophysal zone, crystal-poor member of the Tiva Canyon Tuff;
- orange, lower lithophysal and nonlithophysal zones of the crystal-poor member of the Tiva Canyon Tuff;
- black, lithostratigraphic units that comprise the PTn hydrologic unit, including the crystal-poor vitric zone of the Tiva Canyon Tuff, the Yucca Mountain Tuff, the Pah Canyon Tuff, and intervening bedded tuffs; and
- purple, the Topopah Spring Tuff.

The six rosettes from exposures in the crystal-rich member of the Tiva Canyon Tuff (shown in red, fig. 29) give the appearance of a possible influence of dominant structures on fracture orientation. The three outcrop stations in the northwest part of the map have joint trends

that are subparallel to the Pagany Wash fault. However, cooling joints, one set of which is roughly parallel to the Pagany Wash fault, dominate the network in these three outcrops (Throckmorton and Verbeek, 1995). Throckmorton and Verbeek (1995) observed one tectonic joint set in only the CUC1 outcrop station, which roughly parallels the trend of the fault. If there is any tectonic influence in the orientation of fractures at these locations, it may be one of the Pagany Wash fault reactivating, and accentuating, preexisting cooling features. The two outcrop stations in the crystal-rich member of the Tiva Canyon Tuff along Yucca Crest are also dominated by cooling joints; the dominant joint strikes are not parallel to the trend of the Solitario Canyon fault, but are approximately at right angles to it.

The rosette from the ESF photogrammetry study (fig. 29) shows a preference of strikes around a plane roughly parallel to the Bow Ridge Fault. However, the photogrammetry strip is located about 200 m west of the Bow Ridge fault, so the structural association is not clear.

The outcrops in the upper lithophysal zone of the Tiva Canyon Tuff (green in fig. 29) show a dominance of northwest and northeast strikes. These directions correspond to those of cooling joints that are very prominent in this zone (Morgan, 1984; summarized as Barton and others, 1989; Barton and others, 1993; Throckmorton and Verbeek, 1995). The expression of the tectonic joints in most of the outcrops in this zone is poor (Throckmorton and Verbeek, 1995). The rosettes for the non-qualified pavements have a broader distribution of orientations than the outcrop stations, primarily as a result of different sampling methodologies, but show a similar dominance of northwest and northeast strikes. The narrow range of strikes for pavement 600 is the exception.

The two pavements in middle non-lithophysal zone of the Tiva Canyon Tuff are dominated by north-south fractures (fig. 29). Both of these pavements cross the Ghost Dance fault. The face of the UZ-7A exposure is oriented east-west, suggesting the possibility of bias against fractures in this orientation. However, data from other locations suggest that east-west striking fractures are not common in the middle nonlithophysal zone of the crystal-poor member of the Tiva Canyon Tuff, the zone exposed at the UZ-7A drill pad. Many outcrops in this zone show the same dominance of north-south strikes, often with an additional set striking to the northeast or northwest (Throckmorton and Verbeek, 1995).

Fracture orientations within this interval of the lithostratigraphic units that comprise the PTn hydrologic unit (Sweetkind, Verbeek, Geslin and Moyer, 1995) do not appear to vary significantly over approximately a 600 m distance from north to south (shown as black rosettes in fig. 29). All three mapped exposures (labeled FS-1, FS-2, and FS-3 in fig. 4) are dominated by north-south fractures, along with subordinate numbers of northeast- and northwest-trending fractures. Outcrop stations over this same north-south extent show similar orientation trends to the mapped exposures (fig. 29). The variability in fracture orientation within this interval have been interpreted to be a function of variations in degree of welding and compositional variation, not of a systematic north-south change in fracture pattern (Sweetkind, Verbeek, Geslin and Moyer, 1995).

The outcrops and pavement study areas in the Topopah Spring Tuff (shown in purple, fig. 29) occur mainly along Fran Ridge. Many of the strike rosettes for this unit have multiple clusters of orientations, some at nearly right angles. At pavement P2001 and many of the outcrop localities, this unit is dominated by cooling joints (Sweetkind, Verbeek, Singer and others, 1995; Throckmorton and Verbeek, 1995). In contrast, non-qualified data from pavement 1000, shown for comparison, has dominantly north-striking fractures, probably of tectonic origin (table 5).

Much of the variability seen in joint orientations across Yucca Mountain may be attributed to cooling joints. Cooling joints appear as a system of joint sets in all of the welded units with considerable variability of their orientations from individual data sets (for example, fig. 16). The north-south trend that is seen in many of the rosettes (fig. 29) probably corresponds to one of the major sets of tectonic fractures (Throckmorton and Verbeek, 1995). The different data collection methods between the pavements and the outcrops (global inventory for pavements versus selective inventory for outcrops) makes their comparison problematic. The same joint sets may be present in both types of data sets, but because all fractures above a certain trace length are measured for pavements, the rosette pattern will be more diffuse, and some important orientations may not appear to contribute significantly to the overall distribution. The only group of data sets for which the pavements and the outcrops really do show a strong correlation between the sets as well as for a major structure is the group of PTn outcrops and pavements along Solitario Canyon. Despite the fact that the pavement data sets have significantly more

fractures than the outcrop sets, the rosette pattern remains tight, indicating a similar sampling from both collection methods.

DISCUSSION OF SYNTHESIS RESULTS

Impact of non-qualified data on conclusions

With the exception of the upper lithophysal zone of the Tiva Canyon Tuff and the middle nonlithophysal zone of the Topopah Spring Tuff, all of the data from each lithostratigraphic unit included in this synthesis are qualified. Even in the above cases, there appears to be no significant difference between the qualified and non-qualified fracture data. The only aspect of the synthesis that depends heavily on non-qualified data is an analysis of fracture orientation in the upper lithophysal zone of the Tiva Canyon Tuff (in part reported in Barton and others, 1993). Similar orientation and number of fracture sets appear to have been recorded in both non-qualified and qualified data. The non-qualified data could be reasonably viewed as corroborating data to the qualified.

Sequential formation of fractures and paleostress evolution

Small-scale structural features may be used as indicators of portions of the stress history at Yucca Mountain. Extension joints are useful as recorders of paleostress because the relationship between joint orientation and components of the principal stresses is known (e.g., Griggs and Handin, 1960; Engelder and Geiser, 1980). Thus, the observable sequential development of fracture sets relates to systematic changes in the local or regional stress field. Subsequent to their formation, many joints at Yucca Mountain have been reactivated as small faults. In some cases, the timing and/or sense of motion on these faulted surfaces can be determined and these data used to integrate the joint history with the overall structural evolution of the mountain.

Evidence for sequential formation of fractures

North-striking joints appear to be the earliest-formed tectonic fracture set, because they are the longest tectonic fractures, have the largest percentage of blind terminations and are only truncated by preexisting cooling joints. In certain places, the northwest-striking fracture set appears the post-date the north-striking set (Throckmorton and Verbeek, 1995). At some

localities the northwest-striking fracture set has consistent termination relations against the north-striking set (Throckmorton and Verbeek, 1995; Sweetkind, Verbeek, Singer, and others, 1995). There are rare examples of north-south striking fractures that appear to have renewed growth at their tips in the northwest-striking direction, yielding a bent or even sigmoidal overall fracture shape (Throckmorton and Verbeek, 1995). In many locations, however, the age relationship between the north-striking and northwest-striking sets is not clearly defined. The two sets often have ambiguous or contradictory termination relationships, and in some instances, the northwest-striking set appears to be the older. In contrast to the fracturing sequence reported by Throckmorton and Verbeek (1995), there is no clear evidence that the northwest-striking set is consistently later than the north-striking set. In general, the two fracture sets appear to be roughly coeval. Northeast-striking tectonic joints consistently terminate against cooling joints and the two sets of tectonic fractures described above (Throckmorton and Verbeek, 1995; Sweetkind, Verbeek, Singer, and others, 1995; Sweetkind, Verbeek, Geslin, and Moyer, 1995). Thus, the northeast-striking tectonic joints formed relatively late in the sequence.

A number of small, irregular, variably oriented joints are present within the Paintbrush Group. These joints consistently terminate against all of the joint sets described above, and are thus the latest joints to form. Many of these late joints have been interpreted to be the result of erosional unloading (Throckmorton and Verbeek, 1995; Sweetkind, Verbeek, Singer, and others, 1995). Late joint sets, particularly those formed upon erosional unloading of previously fractured rock, typically have variable orientations. The most systematic of the late joints are east-striking fractures that appear as short connectors between the earlier cooling and tectonic fracture sets. The east-striking joints formed about perpendicular to whatever older joints were present and thus show a fairly wide strike dispersion of 45 degrees; local strikes tend to cluster near N. 90° E. where north-striking joints are dominant but about N. 60° E. where instead the northwest-striking set is better developed. Regardless of orientation, the geologic significance of the late east-striking cross joints remains the same: they are an expression of minor extensional strains not accommodated by pre-existing fractures as the rocks underwent progressive decompression during erosional unloading (Gross, 1993).

Joint orientation and paleostress history

Systematic sets of extension joints (joints that originate as tensional openings, rather than shear fractures) reflect components of the stress field from which they formed. Each joint set is interpreted to represent a distinct episode of jointing and an associated stress field. The major tectonic joint sets in general are vertical to subvertical (for example, figs. 5, 11 and 16). For each joint set, two components of the stress field at the time of fracture can be defined: the minimum compressive stress, σ_3, perpendicular to the median fracture plane; and the maximum horizontal compressive stress, σ_{hmax}, parallel to fracture strike. The maximum compression in the horizontal plane (σ_{hmax}) is not necessarily equivalent to either of the principal compressive stresses σ_1 or σ_2. Thus for vertical to subvertical fractures, fractures may have been generated in a "normal" stress field (σ_1 roughly vertical) or in a "strike-slip" stress field (σ_1 roughly horizontal).

Throckmorton and Verbeek (1995) interpreted the sequential development of subvertical north-striking, northwest-striking, and northeast-striking fracture sets as products of noncoaxial regional extension during basin-range faulting. In their model, each of the fracture sets represents a distinct phase of regional extension, requiring the regional direction of maximum horizontal compressive stress to first have rotated counterclockwise, from σ_{hmax} about north-south to about N. 30° W., between the north-striking and northwest-striking events; and then clockwise, from about N. 30° W. through north again and thence to about N. 40° E., between the northwest-striking and northeast-striking events.

Geologic evidence throughout the Yucca Mountain region indicates dominantly east-west directed extension during the deposition of the Paintbrush Group, with little evidence for a separate phase of northeast-southwest extension. Faulting on north-striking, block-bounding faults, which had extension directions compatible with the opening of north-striking fractures, began prior to eruption of the Paintbrush Group, and continued during and after the deposition of the Paintbrush Group (Scott, 1990). Fault-slip analysis in nearby areas to the north record continuous east-west directed extension until around 8.5 Ma (Minor, 1995). Offset relations and measured slip lineations on faulted joints at pavement P2001 at Fran Ridge suggest that at this locality extensional strain was expressed first in the formation of the north-striking joints and,

with continued extension, as localized normal faulting along the same joints. Because joints form at very low resolved stress, it is likely that north-striking fractures formed throughout the time represented by the deposition of the Paintbrush Group, in response to east-west directed extension.

Evidence for continuous east-west directed extension and lack of consistent evidence of the relative age of the north-striking and northwest-striking tectonic fracture sets suggests it is unlikely that the regional direction of maximum horizontal compressive stress rotated counterclockwise, from σ_{hmax} about north-south to about N. 30° W., between the time of formation of the two fracture sets. It is more likely that the northwest-striking fractures formed during the same period of time as the north-striking fracture. Formation of northwest-striking fractures could be the result of locally rotated σ_3 directions within a regime of regional east-west directed extension. For example, initiation of sinistral slip on major, block-bounding faults (Scott, 1990; Simonds and others, 1995) could favor the formation of northwest-striking extension fractures within the fault-bounded blocks (Dyer, 1988).

Recent work on concurrently active normal and strike-slip faults in the southern Great Basin indicate that adjacent faults having disparate slip vectors need not require temporal changes in the stress field (Wesnousky and Jones, 1994; Morris and others, 1996). The work suggests that given relative magnitudes of the principal stresses where $\sigma_1=\sigma_2>>\sigma_3$, a complex record of normal, oblique, and strike-slip events might could arise from a relatively simple stress history. Alternatively, roughly concurrent motion along normal and strike-slip faults could result from the interplay between active Basin and Range extension and initiation of strike-slip motion along the Walker Lane zone (Bellier and Zoback, 1995). Variability in the relative importance of these two stress regimes could explain the perplexing and often ambiguous relative timing relationships between the north-striking and northwest-striking fractures.

Northeast-striking tectonic joints are a consistently late joint set, based on termination relationships with all other cooling joints and tectonic joints at Yucca Mountain (Throckmorton and Verbeek, 1995; Sweetkind, Verbeek, Singer, and others, 1995; Sweetkind, Verbeek, Geslin, and Moyer, 1995). Northeast-striking extension joints are consistent with the present-day direction of σ_{hmin} (equivalent to σ_3 for subvertical fractures), as determined from hydrofracture

tests and orientations of borehole breakouts (Haimson and others, 1974; Springer and others, 1984; Stock and others, 1985; Stock and Healy, 1988) and from earthquake fault plane solutions and inversion of slip vectors on active faults in the region (Rogers and others, 1983; Bellier and Zoback, 1995). Fault-slip analysis in nearby areas to the north record dominantly east-west directed extension until 8.5 to 9 Ma (Minor, 1995), after which time, the extension direction shifted towards the present-day orientation. It is likely that the northeast-striking tectonic joints formed since the shift at 8.5 to 9 Ma to the present-day extension direction.

Relationship of joints to faulting

Fracture style and intensity near fault zones

The only surface data sets that present the possibility of being able to analyzed for systematic changes in fracture intensity and style near fault zones are the fracture data collected during 1:240 mapping in the vicinity of the Ghost Dance fault (Spengler and others, 1993), the UZ-7A fracture study, and data from the ARP-1 pavement. Data for all three sets were collected by different methods, so comparisons between them are problematic.

The UZ-7A exposure is highly fractured in the hanging wall of the fault (fig. 13). The middle non-lithophysal zone of the Tiva Canyon Tuff is exposed in the hanging wall of the Ghost Dance fault. True fracture intensity (measured with no trace length cutoff) is extremely high, nearly 12 m/m^2 and for most of the fractures all apertures are open. Connectivity is also high in the hanging wall. The width of the intensely fractured zone of the hanging wall is about 50 meters wide. The study does not include fracture mapping in the foot wall, so no interpretations can be made about fracture style or intensity east of the Ghost Dance fault. The style of fracturing in the hanging wall does not change within 50 meters of the fault, resulting in a broad zone of influence by the fault on the fracture network at this locality.

The ARP-1 pavement maps (fractures measured by detailed line survey method) have closer trace lines in the foot wall (1.8 m apart) than in the hanging wall (3.2 m apart). In addition, the trace length cutoffs are different for both sides of the fault; 0.3 m on the foot wall, and 1 m on the hanging wall. The one-dimensional fracture intensity measure, fractures per meter results in a much higher intensity for the foot wall. Descriptions and locations of the shear zones observed along the trace lines for ARP-1 do not show an increase in frequency of either

faults or shear zones closer to the Ghost Dance fault (C.A. Braun and others, written communication, 1995). The width of the exposure of the hanging wall at ARP-1 is less than 100 meters; the edge of the zone of increased deformation is not visible due to the ground cover.

In the ESF, the relationship between fault occurrence and number of fractures per meter of trace line is variable (fig. 30). There are a relatively higher number of fractures around some of the faults in the ESF detailed line survey, but not for all lithologies.

The relationship between fracture intensity and fault zones in the ESF varies considerably. The fracture frequency and trace length histograms in figure 30 have some minor correlation between the peaks for total trace length and number of fractures per 10 m of trace line. Fracture intensity appears to increase within a narrow range near fault zones, but the increase in fracture frequency 10 meters on either side of the Bow Ridge fault is smaller than the variation in frequency in stretches of the trace line where there is little to no faulting. The total trace length of fractures summed over 10 m trace line increments show no increase near the Bow Ridge fault (fig. 30b). The irregular variation of the trace length by station in the ESF for the Tiva Canyon Tuff does not correlate to the presence of faults, suggesting that the long trace lengths may be due to cooling joints.

On the surface, clusters of cooling joints appear to be present in the pavements. Of the pavements in the upper lithophysal zone of the Tiva Canyon Tuff, areas of closely spaced cooling joints appear in two out of the six pavements (table 5). In both of the pavements in the Topopah Spring tuff, areas of closely spaced cooling joints is present (fig. 5). The spacing of the pavements in the upper lithophysal zone of the Tiva Canyon Tuff containing the closely spaced cooling joints suggests that these areas of closely spaced cooling joints could occur at least 30 meters apart, that is, having a spacing greater than the width of the pavements, since they are not seen on each pavement. The spacing between peaks in trace length per 10 m trace line in the ESF detailed line survey data (fig. 30) is 20 to 30 m, possibly of the same distance apart as the cooling joint clusters in the pavements.

In the ESF, the a relationship between fracture intensity and fault zones cannot be seen around the Bow Ridge fault because of the differing lithologies adjacent to the fault (fig. 30). The foot wall of the fault is the competent middle nonlithophysal zone of the Tiva Canyon Tuff, and in the hanging wall is the non-welded to poorly welded post-Tiva Canyon bedded tuff.

There is a slight increase in fracture frequency for the 10 m interval on either side of the fault for both lithologies (fig. 30a), but the trace lengths for those intervals do not change for either lithology near the fault (fig. 30b).

The intensity of fracturing at P2001 is about half that seen at pavement P1000 at the southern tip of Fran Ridge (Sweetkind, Verbeek, Singer, and others 1995). The proximity of P1000 to major structures is probably responsible for the increase in fracture intensity. Pavement 1000 is located at the southern tip of Fran Ridge (fig. 4), very close to large splays of the Paintbrush Canyon Fault that bound Fran Ridge to the west (Scott and Bonk, 1984). Highly broken outcrops of lower lithophysal zone of the Topopah Spring Tuff at the southern end of Fran Ridge probably also reflect the zone of influence of the large faults. Pavements 2001 and 1000 may represent end-members in the possible range of fracture network properties within the middle non-lithophysal zone of the Topopah Spring Tuff.

Links between discontinuous faults and the fracture network

The fracture network developed within the welded pyroclastic flows of the Paintbrush Group is an important mesoscopic fabric element that has profoundly influenced the style of faulting at Yucca Mountain. The fracture network consists of multiple joint sets that include both early cooling joints and later tectonic joints. The multiple fracture sets form an interconnected network that subdivide the mountain into innumerable fracture-bounded blocks. The fracture network, especially the sets of large cooling joints, acts as a significant pre-existing weakness in the rock mass.

The fracture network has accommodated extensional strain over broad zones through distributed slip along many reactivated joints. Evidence for reactivation of joints includes the presence of thin breccia zones along cooling joints and observable slip lineations along joint surfaces. Cooling joints originally formed as tensional openings, having just face separation, not shear. However, thin selvages of tectonic breccia are often present along the trace of the cooling joint. The presence of tectonic breccia along these surfaces indicates they have been reactivated and accommodated later slip.

Detailed observations of the fracture network at the cleared exposure P2001 at Fran Ridge indicate the common presence of joints reactivated as small faults. Slip is most common on northwest-striking cooling joints and north- to northwest-striking tectonic joints. Dominantly

dip-slip normal movement is indicated where gently dipping cooling joints and early tectonic joints are offset across these reactivated features. Small grabens showing centimeter-scale offsets are evident locally.

Slickenside striae are observed on reactivated joints of several orientations at pavement P2001, but are most visually evident on the gently northeast- to southeast-dipping cooling joints that divide the pavement into a series of low ledges. Slickenside striae are common in mineral phases deposited on cooling joint surfaces; suggesting that slip occurred well after cooling joints had already formed in the rock. The orientation and morphology of the striae allow slip vectors to be calculated for the faulted joints. Slip directions along the cooling joint surfaces are fully compatible with the opening directions and stress state during formation of the subsequent tectonic joint sets. Offset relations between successive fracture sets indicate that many fractures experienced renewed growth or reactivation as faults during the formation of subsequent joint sets. During faulting, local strains were accommodated within blocks of rock isolated between reactivated cooling joints by brecciation and the development of numerous minor tectonic fractures. It is likely that extensional strain was expressed first in the formation of the joint sets and then shortly thereafter as localized normal faulting along the same joints.

Faults within the central part of Yucca Mountain are typically short, discontinuous and have minor displacement (1 to 10 m). Many of these minor faults represent the localization of slip along pervasive preexisting weaknesses in the rock mass. One well-studied example is the northwest-striking Sundance fault zone with a trace length of 750 m, a maximum width of about 70 meters, and up to 10 m of aggregate dip-slip separation (Potter and others, 1995). However, total displacement across the fault zone is the summation of numerous 1- to 2-m contact offsets along small, discontinuous, discrete fault segments (Potter and others, 1995). The trend of each fault segment corresponds to one of the dominant orientations of cooling joints exposed on this portion of the mountain (Morgan, 1984; Barton and others, 1989; 1993). Each of these fault segments is probably a reactivated cooling joint (Sweetkind and others, 1996).

Elsewhere at Yucca Mountain, mapped offsets of lithostratigraphic contacts are accompanied by the presence of numerous irregular small blocks showing evidence for minor slip and/or rotation and by pervasive brecciation along fracture sets and as isolated breccia bodies

(Potter and others, 1995; 1996). Stratigraphic offset in these areas is accomplished through distributed slip over a broad zone, rather than by movement along a single structure.

Fractures are a network of preexisting weaknesses in the volcanic rock at Yucca Mountain that allows transfer of extensional strain between structures (Potter and others, 1995; 1996). Stratigraphic offset associated with small, discontinuous faults may die out as fault offset is distributed over a wide zone within the fracture network (Sweetkind and others, 1996). It is likely that some of these discontinuous faults are themselves reactivated cooling joints (Potter and others, 1995).

Predicting fracture distribution at depth based on surface studies

The process of synthesizing all the available fracture data has allowed us to develop some criteria for prediction of fracture characteristics at depth from surface studies. General controls on the fracture network were derived from surface studies, which were performed predominantly in the Tiva Canyon Tuff. The controls of fracture intensity that are dependent on factors such as welding relationships and/or presence or absence of lithophysae are directly applicable to the Topopah Springs Tuff.

The biggest obstructer for predicting fracture character for the subsurface from surface data is the difference in the type of data collected. The detailed line survey provides a large number of observations, but the values that can be compared are not available for most of the surface data sets. The most promising parameter would be number of intersections/trace length, but because this value is available for so few data sets, the weak correlation makes direct comparisons difficult.

Implications for hydrologic models

One of the primary uses of the Yucca Mountain fracture data is to provide constraints to the hydrologic flow models. The fracture network information obtained from the pavements provides the required geometry in two dimensions for developing a synthetic fracture network. Additional constraints are required in order to extrapolate to a 3-dimensional grid for the models, or to determine whether a 1-dimensional data set is viable. The validity of the assumption of a linear relationship between fractures/per meter (1-d), fracture trace length/area (2-d), fracture

area/volume can be tested with a fracture data set that contains observations for at least two of the intensity parameters. Unfortunately, because most of the fracture data was collected for varied purposes at different times, the unified parameter set is not present as the data are now recorded. As the data now stand, it still can provide a range of values for fracture intensity, and connectivity that greatly enhance the chances that the model can represent a possible real scenario.

The areal distribution of fracture characteristics is only obtainable from the fracture database in a qualitative form. A distribution of fracture intensity and connectivity that could provide the inputs for a flux value map could be made from the type of data obtained from pavements. The majority of the pavement data are in the upper lithophysal zone of the Tiva Canyon Tuff, and the range of values could be assigned across the repository area to the geologic map, but in all there are not enough pavements in different lithologies to provide the value in a quantitative manner. The widest distribution of data sets is the outcrop data, which does not contain quantitative connectivity and trace length information.

CONCLUSIONS

The integration of the different data sets and comparison of various parameters that measure the same types of attributes allows the following conclusions to be made:

1. Fracture intensity seems to increase only very near faults (10 m near the Bow Ridge, 50 m near the Ghost Dance fault at UZ-7A), although only this conclusion is based only on observations at these two locations. There is an increase in number of short trace length fractures and connectivity at UZ-7A near the Ghost Dance fault. Generalizations about all the faults cannot be made based on this data.

2. Fracture orientation is influenced by proximity to major intrablock structures in some instances. The UZ-7A data set and ARP-1 show a tight clustering of strikes roughly parallel to the Ghost Dance fault. In other localities, the tight clustering of strikes has no apparent relationship to faults.

3. The biggest controlling factor for fracture characteristics is lithology. Trace length, connectivity, and orientations are more consistent within lithologic units than by location. The average variability across units is stronger than the variability within lithologic units and fracture

intensity is generally highest for the welded non-lithophysal units and lowest for the non-welded bedded tuff units. In general, fracture intensity correlates with the thermo-mechanical units.

5. The biggest differences in the data analysis is not a result of qualified vs non-qualified data, but rather is due to the different methods of data collection. The various fracture studies at Yucca Mountain have resulted in a diverse and not entirely compatible collection of data sets. The only fracture attributes that are common to all of the data sets are orientation, trace length and the lithology in which the fracture occurs. Some data sets do not contain trace length, whether they are qualified or not, preventing any comparison based on that parameter. Even where the same fracture attribute was measured (for example, trace-length) different studies and collection methods used different measurement criteria (for example different lower-limit trace-length cutoffs) that make data difficult to compare. A further difficulty in integrating the data sets lies in comparing one-dimensional (line survey) and two-dimensional (pavement maps, outcrop observations, and full-periphery maps in the ESF) sampling approaches and integrating them into an accurate representation of the fracture network.

6. There are consistent relative changes in fracture character by lithology, but the nature of the data does not allow assignment with certainty of absolute values to any lithologies, largely because of the different constraints used in different data collection methods. The comparisons of intensity and connectivity should be given in a range of values.

7. Fracture trace length cutoff has a significant effect on fracture intensity measures.

8. Spatial variability in the fracture network are mostly the result of variations by lithology, irregular distribution of cooling joints, and, to a lesser extent, associated with proximity to faults.

REFERENCES

Barton, C.C., Howard, T.M., and Larsen, E., 1984, Tubular structures on the faces of cooling joints - A new volcanic feature (abs.): EOS, Transactions of the American Geophysical Union, v. 65, p. 1148.

Barton, C.C., and Hsieh, P.A., 1989, Physical and hydrologic flow properties of fractures: Field trip guidebook T385: International Geologic Congress, 28th, Washington, D.C., American Geophysical Union, 36 p.

Barton, C.C., and Larsen, E., 1986, Pattern of development of fracture networks (abs.): Geological Society of America Abstracts with Programs, v. 18, no. 6, p. 536.

Barton, C.C., Page, W.R., and Morgan, T.L., 1989, Fractures in outcrops in the vicinity of drill hole USW G-4, Yucca Mountain, Nevada--Data analysis and compilation: U.S. Geological Survey Open-File Report 89-92, 133 p.

Barton, C.C., Larsen, E., Page, W.R., and Howard, T.M., 1993, Characterizing fractured rock for fluid-flow, geomechanical, and paleostress modeling: Methods and preliminary results from Yucca Mountain, Nevada: U.S. Geological Survey Open-File Report 93-269, 62 p.

Barton, N. R., and Choubey, V., 1977, The shear strength of rock joints in theory and practice: Rock Mechanics, v. 10, p. 1-54.

Bellier, O., and Zoback, M.L., 1995, Recent state of stress change in the Walker Lane zone, western Basin and Range province, United States: Tectonics, v. 14, p. 564-593.

Buesch, D.C., R.W. Spengler, T.C. Moyer, and J.K. Geslin, 1996, Revised stratigraphic nomenclature and macroscopic identification of lithostratigraphic units of the Paintbrush Group exposed at Yucca Mountain, Nevada: U.S. Geological Survey Open File Report 94-469, 52 p.

Brady, B.H.G., and Brown, E. T., 1993, Rock mechanics for underground mining (2nd. ed.), London, Chapman and Hall, 571 p.

Carr, W.J., 1992, Structural models for western Midway Valley based on RF drillhole data and bedrock outcrops (Appendix A), *in* Gibson, JD., Swan, F.H., Wesling, J.R., Bullard, T.F., Perman, R.C., Angell, M.M., and DiSilvestro, L.A., Summary and evaluation of existing geological and geophysical data near prospective surface facilities in Midway Valley, Yucca Mountain Project, Nye County, Nevada: Sandia National Laboratory SAND90-2491, 27 p.

Coe, J.A., 1995, Close-range photogrammetric geologic mapping and structural analysis, Henderson Mine, Empire, Colorado: unpublished M.S. thesis, Colorado School of Mines, Golden, Colorado, 192 p.

Coe, J.A., and Dueholm, K.S., 1991a, Geologic mapping of tunnels using photogrammetry--control point configuration: U.S. Geological Survey Open-File Report 90-37, 36 p.

Coe, J.A., and Dueholm, K.S., 1991b, Geologic mapping of tunnels using photogrammetry--target and camera positioning: U.S. Geological Survey Open-File Report 90-49, 15 p.

Dyer, R., 1988, Using joint interactions to estimate paleostress ratios: Journal of Structural Geology, v. 10, p. 685-699.

Engelder, T. and Geiser, P., 1980, On the use of regional joint sets as trajectories of paleostress fields during the development of the Appalachian Plateau, New York: Journal of Geophysical Research, v. 85, p. 6319-6341.

Griggs, D., and Handin, J., 1960, Observations on fracture and a hypothesis of earthquakes, *in* Griggs, D., and Handin, J., eds., Rock Deformation (A Symposium), Memoir, Geological Society of America, v. 79, p. 347-364.

Gross, M.R., 1993, The origin and spacing of cross joints: examples from the Monterey Formation, Santa Barbara coastline, California: Journal of Structural Geology, v. 15, no. 6, p. 737-751.

Haimson, B.C., Lacomb, J., Jones, A.H., and Green, S.J., 1974, Deep stress measurement in tuff at the Nevada Test Site: Advances in Rock Mechanics, v. IIa, National Academy of Sciences, Washington, D.C., p. 557-561.

Hancock, P.L., 1985, Brittle microtectonics: principles and practice: Journal of Structural Geology, v. 7, p. 437-457.

Kulander, B.R., C.C. Barton, and S.L. Dean, 1979, The application of fractography to core and outcrop fracture investigations: U.S. Department of Energy Report METC/SP-79/3, 179 p.

Minor, S.A., 1995, Superimposed local and regional paleostresses--fault-slip analysis of Neogene Basin-and-Range faulting near a middle Miocene caldera complex, Yucca Flat, southern Nevada: Journal of Geophysical Research, v. 100, p. 10,507-10,528.

Montazer, P. and Wilson, W.E., 1984, Conceptual hydrologic model of flow in the unsaturated zone, Yucca Mountain, Nevada: U.S. Geological Survey Water Resources Investigation Report 84-4345, 55 p.

Morgan, T.L., 1984, Fracture characterization in the Tiva Canyon Member, Paintbrush Tuff, Yucca Mountain, Nevada: unpubl. M.S. thesis, Colorado State University, Fort Collins, Colorado, 179 p.

Morris, A., Ferrill, D.A., and Henderson, D.B., 1996, Slip-tendency analysis and fault reactivation: Geology, v. 24, p. 275-278.

Moyer, T.C., Geslin, J.K., and Flint, L.E., 1996, Stratigraphic relations and hydrologic properties of the Paintbrush Tuff nonwelded (PTn) hydrologic unit, Yucca Mountain, Nevada: U.S. Geological Survey Open File Report 95-397, 151 p.

Office of Civilian Radioactive Waste Management, 1988, Site Characterization Plan Overview, Yucca Mountain Site, Nevada Research and Development Area, Nevada: Washington, D.C., U.S. Department of Energy, DOE/RW-0198, 164 p.

Ortiz, T.S., Williams, R.L., Nimick, F.B., and South, D.L., 1985, A three-dimensional model of reference thermal/mechanical and hydrological stratigraphy at Yucca Mountain, southern Nevada: Sandia National Laboratories Report SAND84-1076, Albuquerque, NM.

Petit, J.P., 1987, Criteria for the sense of movement on fault surfaces in brittle rocks: Journal of Structural Geology, vol. 9, no. 5/6, p. 597-608.

Pollard, D.D., and Aydin, A., 1988, Progress in understanding jointing over the past century: Geological Society of America Bulletin, v. 100, p. 1181-1204.

Potter, C.J., Day, W.C., Sweetkind, D.S., and Dickerson, R.P., 1996, Fault styles and strain accommodation in the Tiva Canyon Tuff, Yucca Mountain, Nevada: EOS, Transactions, American Geophysical Union, 1996 Spring AGU meeting, in press.

Potter, C.J., Dickerson, R.P., and Day, W.C., 1995, Nature and continuity of the Sundance fault, Yucca Mountain, Nevada: U.S. Geological Survey Administrative Report to the U.S. Department of Energy, 26 p., 3 plates.

Price, N., 1966, Fault and joint development in brittle and semi-brittle rock: Oxford, England, Pergamon Press, 176 p.

Rogers, A.M., Harmsen, S.C., Carr, W.J., and Spence, William, 1983, Southern Great Basin seismological data report for 1981 and preliminary data analysis: U.S. Geological Survey Open-File Report 83-669, 243 p.

Sawyer, D.A., Fleck, R.J., Lamphere, M.A., Warren, R.G., Broxton, D.E., and Hudson, R., 1994, Episodic caldera volcanism in the Miocene southwestern Nevada Volcanic Field: Revised stratigraphic framework, $^{40}Ar/^{39}Ar$ geochronology, and implications for magmatism and extension: Geological Society of America Bulletin, v.106, p. 1304-1318.

Scott, R.B., 1990, Tectonic setting of Yucca Mountain, southwest Nevada, in Wernicke, B.P., ed., Basin and Range extensional tectonics near the latitude of Las Vegas, Nevada: Boulder, Colorado, Geological Society of America Memoir 176, p. 251-282.

Scott, R.B., and Bonk, Jerry, 1984, Preliminary geologic map of Yucca Mountain, Nye County, Nevada, with geologic sections: U.S. Geological Survey Open File Report 84-494: scale 1:12000.

Scott, R.B., and M. Castellanos, 1984, Stratigraphic and structural relations of volcanic rocks in drill holes USW GU-3 and USW G-3, Yucca Mountain, Nye County, Nevada: U.S. Geological Survey Open File Report 84-491, 121 p.

Scott, R.B, Spengler, R.W., Diehl, S., Lappin, A. R., and Chornack, M.P., 1983, Geologic character of tuffs in the unsaturated zone at Yucca Mountain, southern Nevada: in Role of the unsaturated zone in radioactive and hazardous waste disposal; Mercer, J.W., Rao, P.S.C., and Marine, I.W., eds.,: Ann Arbor Science Publishers, Ann Arbor, Michigan, p. 289-335.

Simonds, F.W., Whitney, J.W., Fox, K.F., Ramelli, A.R., Yount, J.C., Carr, M.D., Menges, C.M., Dickerson, R.P., and Scott, R.B., 1995, Map showing fault activity in the Yucca Mountain area, Nye County, Nevada: U.S. Geological Survey Miscellaneous Investigations Map I-2520, scale 1:24,000.

Spengler, R.W., Braun, C.A., Linden, R.M., Martin, L.G., Ross-Brown, D.M., and Blackburn, 1993, Structural character of the Ghost Dance fault, Yucca Mountain, Nevada: High Level Radioactive Waste Management, Proceedings of the Fourth International conference, American Nuclear Society, v. 1, p. 653-659.

Springer, J.E., Thorpe, R.K., and McKague, H.L., 1984, Borehole elongation and its relation to tectonic stress at the Nevada Test Site: Lawrence Livermore National Laboratory Report UCRL-53528, 43 p.

Stock, J.M., Healy, J.H., Hickman, S.H., and Zoback, M.D., 1985, Hydraulic fracturing stress measurements at Yucca Mountain, Nevada, and relationship to the regional stress field: Journal of Geophysical Research, v. 90, no. B10, p. 8691-8706.

Stock, J.M., and Healy, J.H., 1988, Stress field at Yucca Mountain, Nevada, in Carr, M.D., and Yount, J.C. (eds.), Geologic and hydrologic investigations of a potential nuclear waste disposal site at Yucca Mountain, southern Nevada: U.S. Geological Survey Bulletin 1790, p. 87-94.

Sweetkind, D.S., Potter, C.J., and Verbeek, E.R, 1996, Interaction between faults and the fracture network at Yucca Mountain, Nevada: EOS, Transactions, American Geophysical Union, 1996 Spring AGU meeting, in press.

Sweetkind, D.S., Verbeek, E.R., Geslin, J.K, and Moyer, T.C., 1995, Fracture character of the Paintbrush Tuff nonwelded hydrologic unit, Yucca Mountain, Nevada, U.S. Geological Survey Administrative Report to the U.S. Department of Energy, 202 p.

Sweetkind, D.S., Verbeek, E.R., Singer, F.R., Byers, F.M., Jr., and Martin, L.G., 1995, Surface fracture network at pavement P2001, Fran Ridge, near Yucca Mountain, Nye County, Nevada: U.S. Geological Survey Administrative Report to the U.S. Department of Energy, 130 p.

Sweetkind, D.S., and Williams-Stroud, S., 1995, Controls on the genesis of fracture networks, Paintbrush Group, Yucca Mountain, Nevada: EOS, Transactions, American Geophysical Union, vol. 76, p. F597.

Terzaghi, R.D., 1965, Sources of error in joint surveys: Géotechnique, v. 15, p. 287-304.

Throckmorton, C.K., and Verbeek, E.R., 1995, Joint networks in the Tiva Canyon and Topopah Spring Tuffs of the Paintbrush Group, southwestern Nevada: U.S. Geological Survey Open File Report 95-2, 179 pp.

Wesnousky, S.G., and Jones, C.H., 1994, Oblique slip, slip partitioning, spatial and temporal changes in the regional stress field, and the relative strength of active faults in the Basin and Range, western United States: Geology, v. 22, p. 1031-1034.

APPENDIX

A summary of the fracture characteristics of each unit of the Tiva Canyon Tuff and of the Topopah Spring Tuff studied by Throckmorton and Verbeek (1995) is presented below in order to facilitate comparison of data from outcrop studies with the other data sets. Stratigraphic nomenclature follows that of Buesch and others (1996), except for the unit upper lithophysal zone-middle non-lithophysal zone, undifferentiated (Tpcpum), that follows the usage of W. Day and others (written communication, 1996).

Tiva Canyon Tuff, Crystal-rich member

Mixed pumice subzone (Tpcrn2): At the single outcrop station in this unit (Station CCR1, Throckmorton and Verbeek, 1995) two steeply dipping cooling joint sets were observed. Members of both sets had lengths of at least 3-5 m, and spacing of 1-2 m. Observations during 1:6000 mapping within the central block of Yucca Mountain suggest that the well-developed joint network in Tpcr2 does not extend downward very far into the underlying Tpcrn1.

Crystal-transition subzone (Tpcrn1): At two outcrop stations, the unit is characterized by long cooling joints (1-10 m) of diverse orientations. Many of these joints extend only a meter or less into the underlying upper lithophysal zone, but at one locality one of the cooling joint sets existed in both units. During 1:6000 mapping within the central block of Yucca Mountain, the unit was commonly observed to contain a number of small, low-angle joint surfaces that give this unit a ledgy appearance in outcrop.

Tiva Canyon Tuff, Crystal-poor member

Upper lithophysal zone (Tpcpul): This unit is characterized by consistently well developed cooling joints that generally form as two sets of steeply dipping fractures that are roughly orthogonal. The two sets form a prominent rectangular pattern observable at most of the cleared pavements in this unit (e.g. Barton and others, 1993), and at nine outcrop localities studied by Throckmorton and Verbeek (1995). These joints are commonly large (from 3 m in length to greater than 10 m in length). Spacing is variable, with a tendency for the cooling joints to occur as swarms of closely spaced (0.5-1 m) joints separated by zones of more widely spaced joints (2-3 m). The relative expression of each set is extremely variable over short distances. Commonly, one set of joints is weakly expressed relative to the other. A number of tectonic joint sets, often 1-2 m in length are common in this unit as well. These joints commonly abut the earlier cooling joints.

Middle non-lithophysal zone (Tpcpmn): This unit is characterized by abundant short (1-2 m or less), curving fractures of diverse orientation. Most joint surfaces are smooth, making the distinction between cooling joints and tectonic joints difficult. In rare cases where this unit and the overlying upper lithophysal zone are well exposed, cooling joint sets identified in the upper lithophysal unit can be seen to exit in the middle non-lithophysal zone as well.

Upper lithophysal zone, middle non-lithophysal zone, undifferentiated (Tpcpum): At three outcrop stations on Isolation Ridge (Throckmorton and Verbeek, 1995), the unit has characteristics of both the upper lithophysal zone and the middle non-lithophysal zone. Cooling joints are evident, either as a single, widely spaced set or as two sets that form a rectangular pattern. Also present are numerous fractures of diverse orientations that are difficult to assign to sets.

Lower lithophysal zone (Tpcpll): At the single outcrop station on Isolation Ridge (Throckmorton and Verbeek, 1995), there is a single cooling joint set (1-6 m lengths, 0.1-3 m spacing) and two sets of tectonic joints that are smaller (0.2-0.4 m) with variable spacing.

Lower non-lithophysal zone (Tpcpln): Where not obscured by a network of small, anastomosing fractures, the upper part of this unit is characterized by a network of tectonic joints, commonly 1-3 m long and relatively closely spaced (<2 m) (based on 9 outcrop stations, Throckmorton and Verbeek, 1995, most of which were probably in rock that was transitional into the overlying lower lithophysal zone). Near the top of the lower non-lithophysal zone, cooling joint sets become more prominent and easy to identify and appear to be continuous with the overlying lower lithophysal zone. Throughout most of the lower non-lithophysal zone, cooling joints are difficult to identify because tubular structures are all but absent and roughness is not definitive. Locally developed in this zone, and in the lower part of the lower lithophysal zone, is a network of very short, curved, anastomosing fractures that break the rock mass into 2-4 cm. fragments (the hackly subzone of Buesch and others, 1996). The pervasive hackly fracturing may be a cooling phenomenon.

Columnar subzone of the lower non-lithophysal zone (Tpcplnc): This unit is characterized by a hexagonal network of cooling joints that subdivide the rock into abundant, crude, vertical columns 2-5 m high. Column diameters of 0.2-1 m are common. Cooling joints that bound the columns extend only short distances upward into the lower non-lithophysal zone and downward into the crystal-poor vitric zone.

Vitric zone (Tpcpv): This zone, which includes the top of the PTn hydrogeologic unit, has the greatest range in welding character of any zone of the Tiva Canyon Tuff, going from densely welded at the top to nonwelded at the base, over an interval of 7-9 m. This change in welding is mirrored by changes in material properties and fracture characteristics. Cooling joints are abundant and commonly outnumber tectonic joints in the densely welded tuff at the top of the zone. These joints are large, and although their full dimensions are rarely exposed, exposed lengths of 1.5-3 m (5-10 ft) and exposed heights of 0.6-1 m (2-5 ft) are typical. The regular cooling joints that characterize the overlying columnar subzone of the lower non-lithophysal zone of the Tiva Canyon Tuff generally die out within a few meters of entering the densely welded top of the vitric zone. Lower in the zone the cooling joints gradually decrease in abundance downward. The base of the moderately welded portion of the vitric zone generally marks the lowermost extent of the cooling-joint network within the Tiva Canyon Tuff. Tectonic joints tend to be small and of modest abundance at the top of the vitric zone, larger and much more abundant throughout the middle of the vitric zone, and sharply decrease in abundance in the poorly welded lower portion of the zone.

Topopah Spring, crystal-rich member

Vitric zone (Tptrv) The four outcrops described in this zone are dominated by cooling joints with exposed lengths ranging from 0.2 m to more than 11 meters. Four sets are identified, with two pairs of sets at nearly right angles to each other. The tectonic fractures are shorter in length (mostly < m), with one set nearly parallel to the most prominent cooling joint set. Unloading joints and stress relaxation joints are common in this unit.

Non-lithophysal zone (Tptrn) At the one locality described in this unit, the fracture network is similar to that observed in the exposures of the crystal-rich vitric zone (Tptrv). There

are 3 sets of cooling joints and 2 sets of tectonic joints, all of which are poorly expressed, but the tectonic joints dominate the fracture network.

Topopah Spring, crystal-poor member

Middle non-lithophysal zone (Tptpmn) The two outcrops described from this unit are test pits #1 and #2 located in the Fran Ridge pavement, and were described before the pavement was cleared. Three mutually perpendicular cooling joint sets are present with three additional joint sets interpreted to be tectonic in origin. The gently-dipping cooling joints set shows tubular structures. The orientation of the tectonic joint set that strikes nearly north-south is continuous with the longest cooling joints, is distinguished from cooling joints by their roughness and irregular surfaces. Some of the tectonic joints also have long trace lengths (up to 12m), so that their interpretation as cooling vs tectonic joints is somewhat equivocal. An additional set of gently dipping joints is present at the two localities that has rough surfaces, irregular shape, no tubular structures and transects lithophysal cavities. This set is interpreted to be late joints formed from erosional unloading.

Vitric zone (Tptpv) Cooling joints the most well-expressed fracture set at the one outcrop described in the vitric zone of the crystal-poor member of the Topopah Spring Tuff. Exposed lengths of the cooling joints range from 1-2 m, with some as long as 4m. Two nearly perpendicular sets are observed, the second less well-expressed, but are interpreted to be cooling joints based on the devitrification rinds found in both sets and the orientation relationships. A tectonic joint set at this locality is expressed as mostly tight, high-angle joints in the range of 0.2 to 0.6 m in length.

FIGURE CAPTIONS

Figure 1. Generalized map of regional block-bounding faults near Yucca Mountain. Location of faults after Simonds and others (1995).

Figure 2. Generalized stratigraphic section of the Paintbrush Group. Group and Formation names after Sawyer and others (1994). Member designations, zonal subdivisions, and unit abbreviations are informal, after Buesch and others (1996). Thickness of lithostratigraphic units are from well G-3 (Scott and Castellanos, 1984) and are intended to be schematic; actual thicknesses are variable. The interval labeled bedded tuff, plus the overlying crystal-poor vitric zone of the Tiva Canyon Tuff, corresponds to the PTn hydrologic unit. The uppermost parts of the Paintbrush Group, including the vitric top of the Tiva Canyon Tuff, post-Tiva Canyon bedded tuff and a pyroclastic-flow (Tpki of Buesch and others, 1996), are not shown.

Figure 3. Map of the central part of Yucca Mountain, Nevada. Generalized location of dominant faults after Day and others (W. Day, written communication, 1996). The location of fracture study areas in the vicinity of the potential repository are shown. Additional fracture study areas in outlying locations are shown in fig. 4.

Figure 4. Location map for pavements and outlying fracture study areas. Generalized location of dominant faults after Scott and Bonk (1984) and Day and others (W. Day, written communication). Mapped pavements are labeled; outcrop stations within the area shown on fig. 3 are not shown in this figure.

Figure 5. Comparison of data from Fran Ridge pavement P2001. Fig. 5a is a lower-hemisphere, equal area projection of poles to fracture planes at the two test pits at the Fran Ridge site. Data are collected by selective inventory method, reported in Throckmorton and Verbeek (1995). Median orientation of joint sets are labeled as follows: cooling joint sets for each pit are labeled C1, C2 and C3; tectonic joint sets are labeled T1, and T3; subhorizontal joints are labeled SH. Fig. 5b is a lower-hemisphere, equal area contour plot of poles to fracture planes at Fran Ridge pavement P2001. Data are from Sweetkind, Verbeek, Singer and others (1995). Median orientation of joint sets are labeled as follows: cooling joint sets are labeled C1, C2 and C3; tectonic joint sets are labeled T1, T2 and T3.

Figure 6. Comparison of data from the crystal-poor vitric zone, Tiva Canyon Tuff. Lower-hemisphere, equal area projections of poles to fracture planes. Contours as percent total per 1 percent counting area. A. Qualified selective inventory data from a single outcrop station (reported in Throckmorton and Verbeek, 1995). B. Qualified data from mapped exposures and outcrop observation (Sweetkind, Verbeek, Geslin and Moyer, 1995). C. Qualified subsurface data, from detailed line survey within the ESF.

Figure 7. Comparison of data from middle nonlithophysal zone, Tiva Canyon Tuff. Lower-hemisphere, equal area projections of poles to fracture planes. A. Qualified selective inventory data from four outcrop stations (reported in Throckmorton and Verbeek, 1995). B. Qualified

data from mapped exposures (ARP-1 and UZ-7A) and fracture data collected in conjunction with 1:240 geologic mapping in the vicinity of the Ghost Dance fault (Spengler and others, 1993). C. Qualified subsurface data, from detailed line survey within the ESF.

Figure 8. Comparison of qualified and non-qualified data, upper lithophysal zone, Tiva Canyon Tuff. Lower-hemisphere, equal area projections of poles to fracture planes. A. Non-qualified data from nine outcrop stations (from Throckmorton and Verbeek, 1995) and six cleared pavements (in part reported in Barton and others, 1993). B. Qualified data from mapped exposures (ESF starter tunnel) and fracture data collected in conjunction with 1:240 geologic mapping in the vicinity of the Ghost Dance fault (Spengler and others, 1993). C. Qualified subsurface data, from detailed line survey within the ESF.

Figure 9. Photograph and map of pavement 300, Dead Yucca Ridge. Location of pavement 300 is shown on figure 4. A) Aerial photograph of pavement, length of the tail of north indicator arrow is three meters. B) Geologic map of pavement 300 (from Barton and others, 1993). The map and photograph do not exactly correspond because photograph is of a sloping surface whereas the map portrays fractures on the horizontal plane.

Figure 10. Photograph and map of pavement 1000, southern end of Fran Ridge. Pavement is in the Topopah Spring Tuff. Location of pavement is shown on figure 4. A) Aerial photograph of pavement, length of the tail of north indicator arrow is three meters. B) Geologic map of pavement 300 (from Barton and Hsieh, 1989). Map explanation is shown on fig. 9.

Figure 11. Mapped fracture relations at pavement P2001, Fran Ridge. A. Location of P2001 relative to Yucca Mountain. B. Equal area projection of poles to fracture planes plotted on the lower hemisphere. Six fracture sets are identified; three sets of cooling joints (C1-C3) and three sets of tectonic joints (T1-T3). Contours as percent of total per 1 percent area; contour intervals are 2, 4, 6 and 8 percent. C. Simplified map of P2001 showing distribution of the three cooling joint sets. Exposed surfaces of fractures of the shallowly dipping C3 set are depicted as cross-hatched areas. Vertical pits at the north and south ends of the pavement, 8 m and 3 m deep, respectively, expose the fracture network in the third dimension. Figures D., E., and F. highlight the subsequent development of the three tectonic fracture sets T1, T2, and T3, respectively. Fractures belonging to each of the sets are shown in each map as bold lines, superimposed on the network of previously formed fractures. Figure is summarized from Sweetkind, Verbeek, Singer and others (1995).

Figure 12. Photogrammetry site in the ESF at Yucca Mountain. Location is shown on figure 3. A. Simplified map of fracture relations. All data were collected using photogrammetric methods. The tunnel floor occurs at the top and bottom of the map; the centerline, at the top of the tunnel, occurs in the center of the map. Informal stratigraphic nomenclature, including member designation, zonal subdivisions, and unit abbreviations are after Buesch and others (1996). The stratigraphic units mapped at this locality are at the top of the Tiva Canyon Tuff, just above the top of the stratigraphic section shown in figure 2. Double line running across top of map is the location of the detailed line survey. B. Distribution of median trace length as a function of wall separation. C. Fracture intensity, in number of fractures per square meter, for each of the mapped stratigraphic units

and for the entire map area (all units). D. Density contour plot of attitudes of fractures for the entire map area.

Figure 13. Comparison of results of data collection at UZ-7A exposure. A. Map of the UZ-7A exposure, showing fractures greater than 1 m in length. Location of the "control area", where fractures down to 0.035 m long were measured, is outlined by a dashed line. B. Photo of Ghost Dance fault at UZ-7A exposure. C. Photo of "control area". D. Detail of fractures in "control area". E., F., and G. Orientations and trace length distributions of fractures from the "control area" (fig. 12E), from fractures longer than 1 m mapped using photogrammetry over the entire exposure (fig. 12F), and from fractures longer than 1 m mapped using the pavement method over the entire exposure (fig. 12G).

Figure 14. Qualified fracture orientation data, crystal-rich member, Tiva Canyon Tuff. Lower-hemisphere, equal area projections of poles to fracture planes. A. Qualified surface data, from fracture data collected in conjunction with 1:240 geologic mapping in the vicinity of the Ghost Dance fault (Spengler and others, 1993). B. Qualified subsurface data, from detailed line survey within the ESF. C. Qualified subsurface data, from ESF photogrammetry (J. Coe, written communication, 1996).

Figure 15. Qualified fracture orientation data, crystal-poor member, Tiva Canyon Tuff. Lower-hemisphere, equal area projections of poles to fracture planes. A. Upper lithophysal zone. B. Middle nonlithophysal zone. C. Lower lithophysal zone. D. Lower nonlithophysal zone. Qualified surface data are from mapped exposures (ESF starter tunnel, ARP-1 and UZ-7A) and from fracture data collected in conjunction with 1:240 geologic mapping (Spengler and others, 1993). Qualified subsurface data, from detailed line survey within the ESF. Non-qualified data are shown for comparison purposes.

Figure 16. Qualified fracture orientation data from lithostratigraphic units within the PTn hydrologic unit. Lower-hemisphere, equal area projections of poles to fracture planes. A. Qualified surface data; contours as percent total per 1 percent counting area (from Sweetkind, Verbeek, Geslin and Moyer, 1995). B. Qualified subsurface data, from detailed line survey within the ESF.

Figure 17. Qualified fracture orientation data, crystal-rich member, Topopah Spring Tuff. Lower-hemisphere, equal area projections of poles to fracture planes. Qualified subsurface data, from detailed line survey within the ESF.

Figure 18. Qualified and non-qualified fracture orientation data, Paintbrush Group. Lower-hemisphere, equal area projections of poles to fracture planes. Contours as percent total per 1 percent counting area.

Figure 19. Fracture orientation diagrams for smooth fractures and cooling joints. Lower-hemisphere, equal area projections of poles to fracture planes and rose diagrams of fracture strikes for qualified and non-qualified data, Paintbrush Group. A. Orientation of possible

cooling joints; identified as having a joint roughness coefficient of two or less. B. Orientation of joints definitively identified as cooling joints by the observer.

Figure 20. Fracture orientation diagrams for rough fractures and tectonic joints. Lower-hemisphere, equal area projections of poles to fracture planes and rose diagrams of fracture strikes for qualified and non-qualified data, Paintbrush Group. A. Orientation of possible tectonic joints; identified as having a joint roughness coefficient of three or higher. B. Orientation of joints definitively identified as tectonic joints by the observer.

Figure 21. Trace length distribution for qualified data. A. Trace length histograms, pavement P2001, Fran Ridge (Sweetkind, Verbeek, Singer and others, 1995). B. Trace length histograms, lithostratigraphic units that comprise the PTn hydrologic unit (Sweetkind, Verbeek, Geslin and Moyer, 1995). Data in both figures are subdivided by the number of fracture endpoints exposed. Trace length distributions are effectively truncated to the left due to the 1.5 m (5 feet) minimum length cutoff that was employed during the mapping.

Figure 22. Trace length histograms for qualified ESF data, Paintbrush Group. Lower-limit trace length cutoff is 0.3 m.

Figure 23. Trace length histograms, surface fracture data, Paintbrush Group. Both qualified and non-qualified data are shown. Lower-limit trace length cutoff is variable, so the distributions are variably truncated to the left.

Figure 24. Trace length histograms for smooth and rough joints.. A. Trace lengths of possible cooling joints; identified as having a joint roughness coefficient of less than three (JRC<3), from fracture data collected in conjunction with 1:240 geologic mapping in the vicinity of the Ghost Dance fault (Spengler and others, 1993) B. Trace lengths of possible tectonic; identified as having a joint roughness coefficient of three or more (JRC>2), from fracture data collected in conjunction with 1:240 geologic mapping in the vicinity of the Ghost Dance fault. C. Trace lengths for smooth fractures (JRC<3) from all qualified and non-qualified fracture data, Paintbrush Group. D. Trace lengths for rough fractures (JRC>2) from all qualified and non-qualified fracture data, Paintbrush Group. E. and F. Cooling joints (E.) and tectonic fractures (F.) definitively identified by the observer, from all qualified and non-qualified fracture data, Paintbrush Group.

Figure 25. Fracture intensity from qualified data sets. A. Fracture intensity, as fracture trace length per unit area (units of m/m^2), for two-dimensional data. Minimum trace length cutoff varies by data set, as shown. Non-qualified data from pavements 100, 200, and 300 are shown for comparison. B. Fracture intensity, as fracture trace length per unit area (units of m/m^2), for two-dimensional data normalized to 1.5 m trace length cutoff for all data sets. C. Fracture frequency (number of fractures per meter) from detailed line survey in the ESF. Minimum trace length cutoff is 0.3 m. D. Fracture frequency (number of fractures per meter) from detailed line survey in the ESF and at pavement ARP-1. Fracture frequency is calculated for the ESF data using a minimum trace length cutoff of 1.8 m for comparison to pavement ARP-1.

Figure 26. Correlation of fracture network properties to degree of welding, Paintbrush Group. Both qualified and non-qualified data are shown. A. Geometric analysis of fracture terminations from cleared pavements in the Paintbrush Group, subdivided by degree of welding. B. Changes in fracture intensity and termination relationships with degree of welding in the Paintbrush Group. Intensity is reported in terms intersection intensity, the number of fracture intersections per area ($\#/m^2$).

Figure 27. Locations of fractures for a portion of the Ghost Dance fault mapping area. A. Distribution of possible tectonic fractures. Rough fractures (joint roughness coefficient, JRC, greater than 2) are shown for a portion of the 1:240 scale map area (Spengler and others, 1993), with the approximate location of the Ghost Dance fault trace shown (trace of fault from W. Day and others, written communication, 1996). B. Distribution of possible cooling joints. Smooth fractures (joint roughness coefficient, JRC, of 2 or less) are shown for a portion of the 1:240 scale map area (Spengler and others, 1993), with the approximate location of the Ghost Dance fault trace shown (trace of fault from W. Day and others, written communication, 1996).

Figure 28. Orientation of smooth and rough fractures collected in conjunction with 1:240 geologic mapping. A. Lower-hemisphere, equal area projections of poles to fracture planes and rose diagrams of fracture strikes for possible cooling joints; identified as having a joint roughness coefficient of two or less. B. Lower-hemisphere, equal area projections of poles to fracture planes and rose diagrams of fracture strikes for possible tectonic joints; identified as having a joint roughness coefficient of three or more.

Figure 29. Strike distributions for surface fracture study areas and ESF photogrammetry. Qualified and non-qualified data are shown. Strike rosettes are subdivided by lithostratigraphic unit as follows: red, crystal-rich member of the Tiva Canyon Tuff; green, upper lithophysal zone of the crystal-poor member of the Tiva Canyon Tuff; light blue, middle nonlithophysal zone, crystal-poor member of the Tiva Canyon Tuff; orange, lower lithophysal and nonlithophysal zones of the crystal-poor member of the Tiva Canyon Tuff; black, lithostratigraphic units that comprise the PTn hydrologic unit, including the crystal-poor vitric zone of the Tiva Canyon Tuff, the Yucca Mountain Tuff, the Pah Canyon Tuff, the non- to partially welded and moderately welded subzones of the crystal-rich vitric zone of the Topopah Spring Tuff, and intervening bedded tuffs; and purple, the Topopah Spring Tuff.

Figure 30. Fracture frequency and trace lengths in the ESF. Data are from detailed line survey. Location is shown in meters from the ESF portal. A. Number of fractures per 10 meters of trace line. B. Total trace length of fractures per 10 meters of trace line. Stratigraphic abbreviations explained in fig. 2.

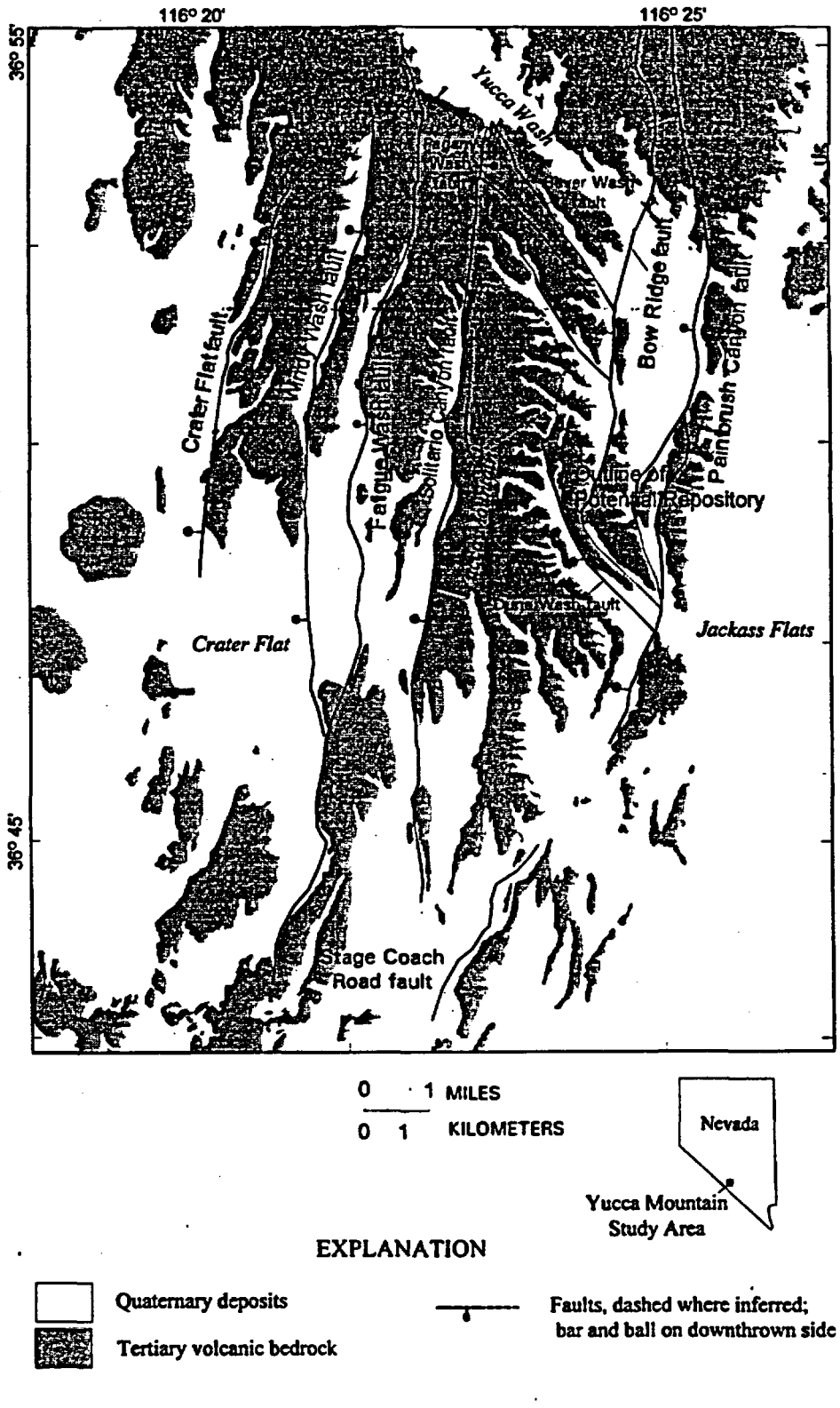
116° 20'
116° 25'
36° 55'
36° 45'
Yucca Wash
Beaver Wash fault
Bow Ridge fault
Paintbrush Canyon fault
Crater Flat fault
Windy Wash fault
Fatigue Wash fault
Solitario Canyon fault
Outline of Potential Repository
Drill Wash fault
Crater Flat
Jackass Flats
Stage Coach Road fault
0 1 MILES
0 1 KILOMETERS
Nevada
Yucca Mountain Study Area
EXPLANATION
Quaternary deposits
Tertiary volcanic bedrock
Faults, dashed where inferred; bar and ball on downthrown side

Figure 1

Generalized stratigraphy of the Paintbrush Group

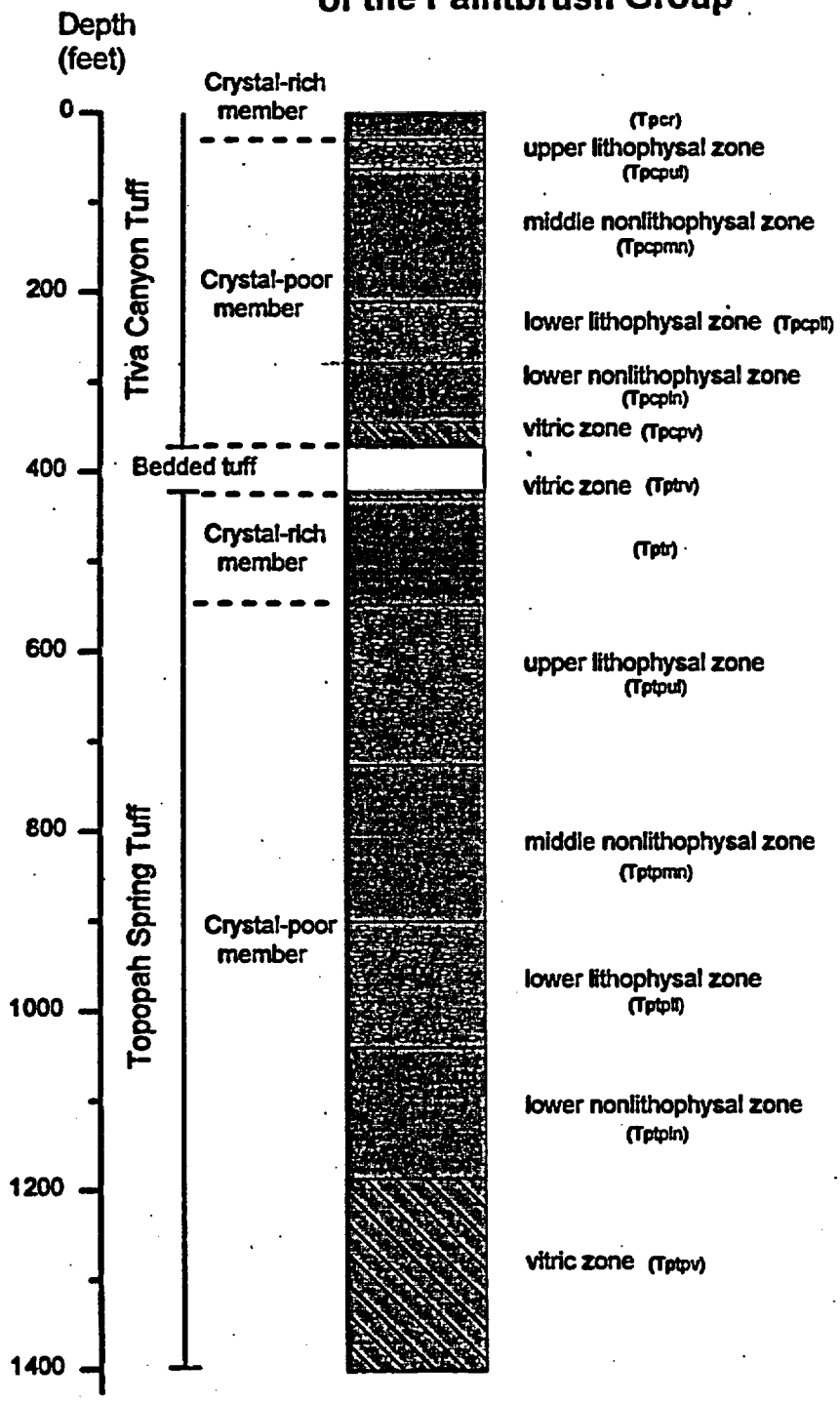

EXPLANATION OF SYMBOLS

Pyroclastic flow: devitrified, moderately to densely welded

Pyroclastic flow, lithophysal zone: devitrified, moderately to densely welded

Pyroclastic flow: vitric, densely welded to nonwelded

Bedded tuff: Interval includes two poorly welded pyroclastic flows and interbedded nonwelded pyroclastic fall and reworked material

Figure 2.

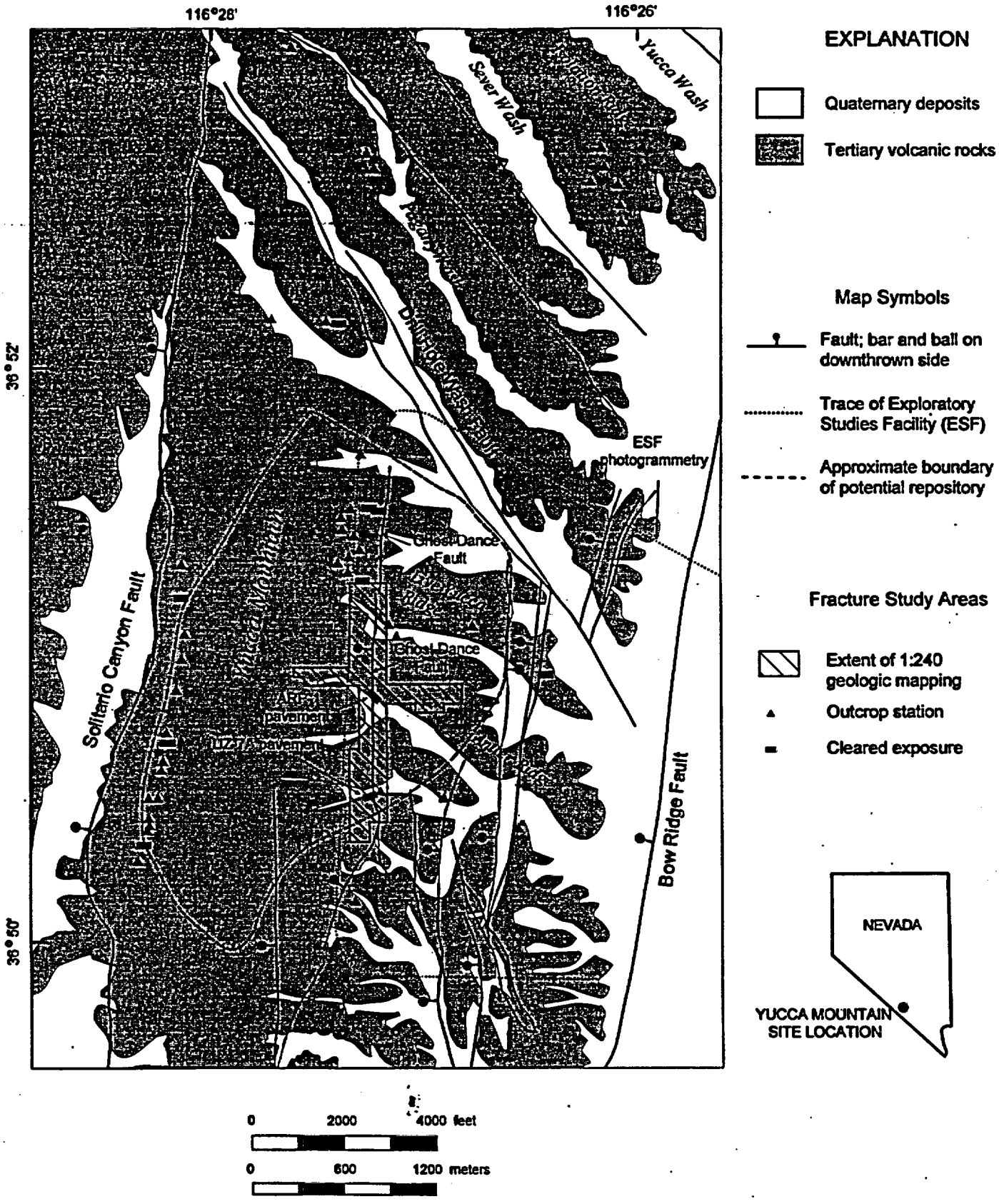
116°28'
116°26'
36°52'
36°50'
Sever Wash
Yucca Wash
Drill Hole Wash Fault
ESF
photogrammetry
Ghost Dance
Fault
Fran Ridge
Ghost Dance
Fault
Busted Butte
Solitario Canyon Fault
Bow Ridge Fault
0
2000
4000 feet
0
600
1200 meters
EXPLANATION
Quaternary deposits
Tertiary volcanic rocks
Map Symbols
Fault; bar and ball on downthrown side
Trace of Exploratory Studies Facility (ESF)
Approximate boundary of potential repository
Fracture Study Areas
Extent of 1:240 geologic mapping
Outcrop station
Cleared exposure
NEVADA
YUCCA MOUNTAIN
SITE LOCATION

Figure 3.

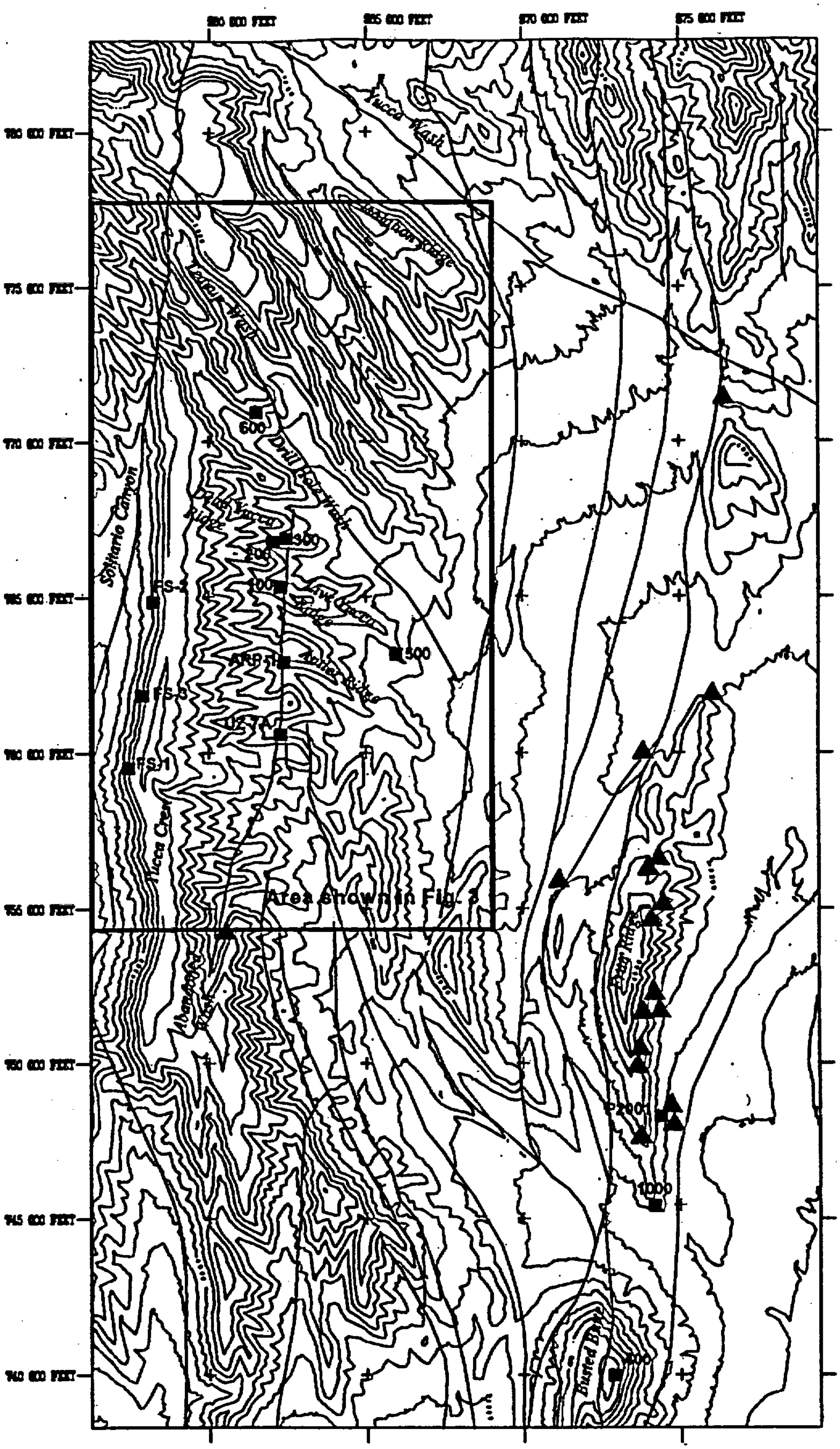

EXPLANATION

Map Symbols

Trace of major fault

Fracture Study Areas

Cleared exposure

Outcrop station outside area shown in fig. 3.

Contour interval 100'

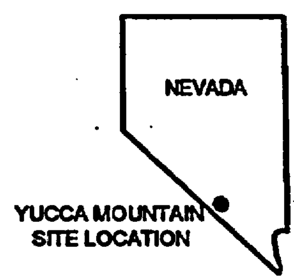

Figure 4.

A. TEST PIT DATA

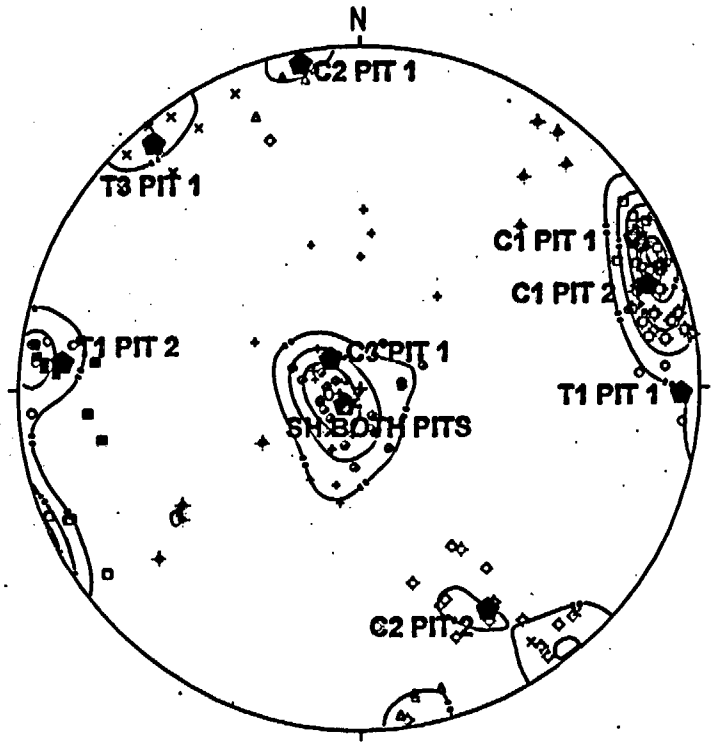

139 poles. Contours as percent of total per one percent area, contour intervals are 2, 4, 6, 8 and 10%.

SYMBOL LEGEND, FIG 9A

COOLING JOINT SETS
- C1 Pit 1
- C2 Pit 1
- C3 Pit 1
- C1 Pit 2
- C2 Pit 2
- C3 Pit 2

TECTONIC JOINT SETS
- T1 Pit 1
- T3 Pit 1
- T1 Pit 2
- SH, both pits
- Median set orientation, test pits

SYMBOL LEGEND, FIG 9B
- Mapped tectonic joints, P2001
- Mapped cooling joints, P2001
- Median set orientation, P2001

B. PAVEMENT DATA

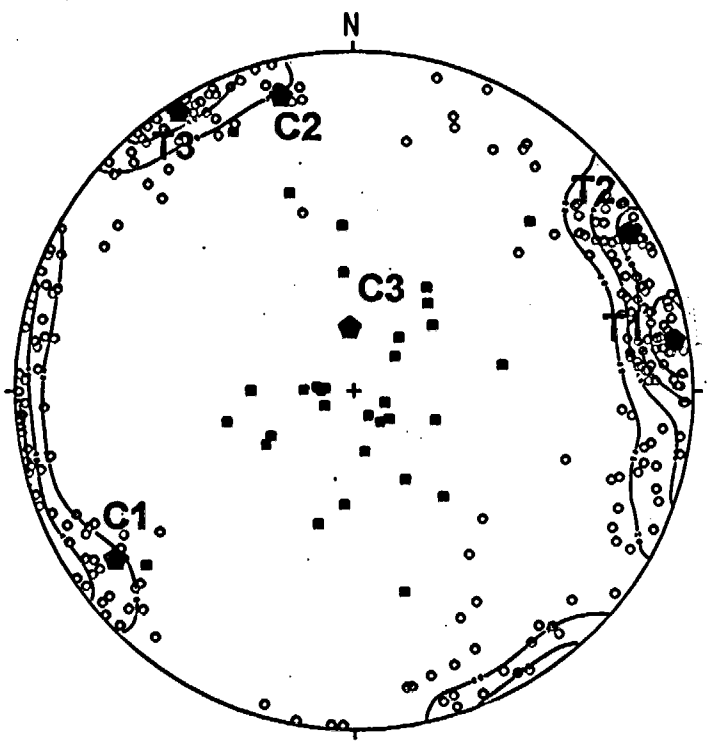

284 poles. Contours as percent of total per one percent area, contour intervals are 2, 4, 6, 8 and 10%.

FIGURE 5

TIVA CANYON TUFF
CRYSTAL-POOR VITRIC ZONE

A.

Outcrop
station CC1

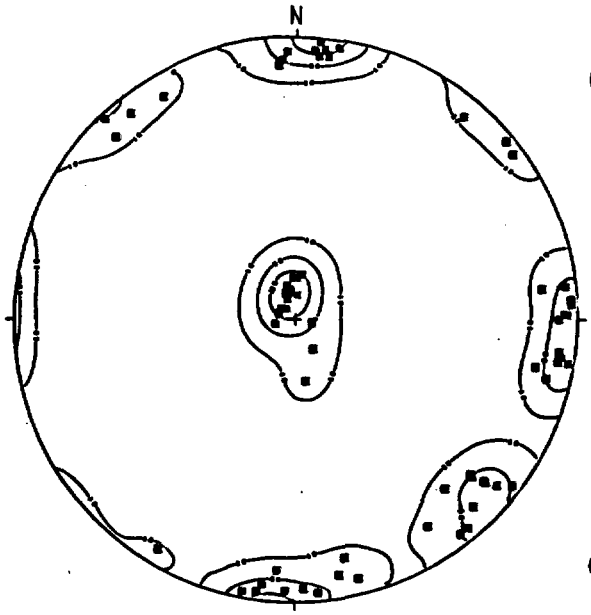

70 POLES

CONTOURS ARE 1, 5 AND 10%

B.

Qualified outcrop
and pavement data

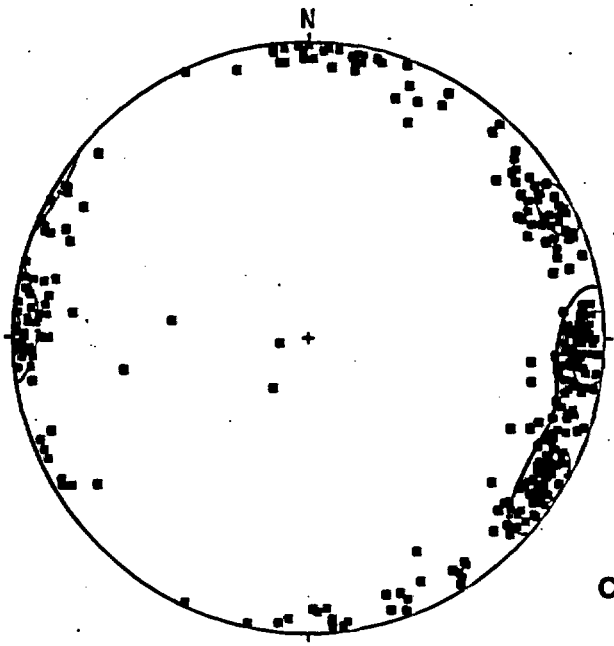

320 POLES

CONTOURS ARE 5 AND 10%

C.

Qualified
subsurface data

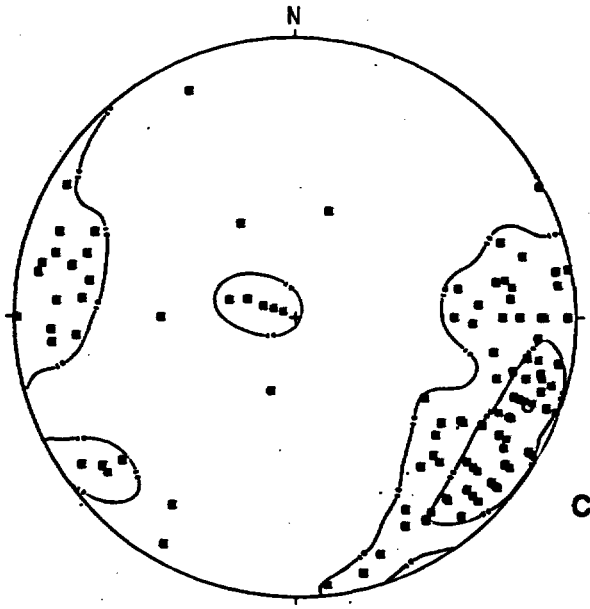

112 POLES

CONTOURS ARE 1, 5 AND 10%

Figure 6.

Tiva Canyon Tuff - Middle Nonlithophysal Zone

A. Qualified surface data (selective inventory)

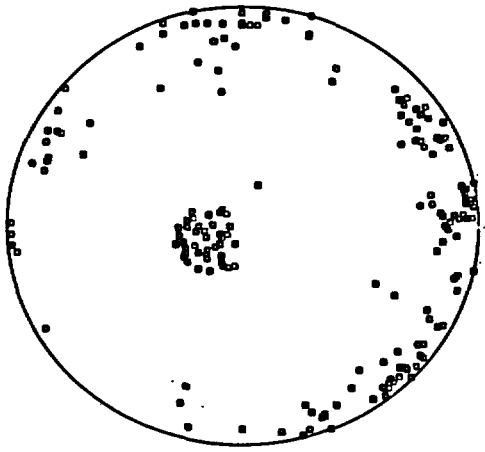

Number of points = 186

B. Qualified surface data (global inventory)

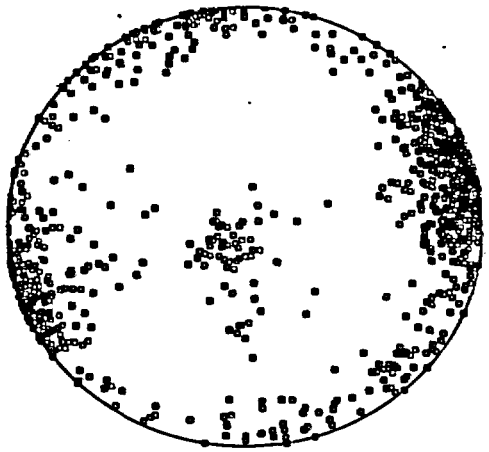

Number of points = 1069

C. Qualified subsurface data

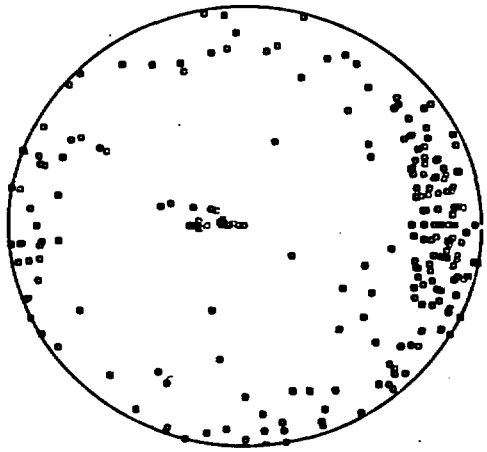

Number of points = 267

Figure 7

Tiva Canyon Tuff - Upper Lithophysal Zone

A. Non-qualified pavement data

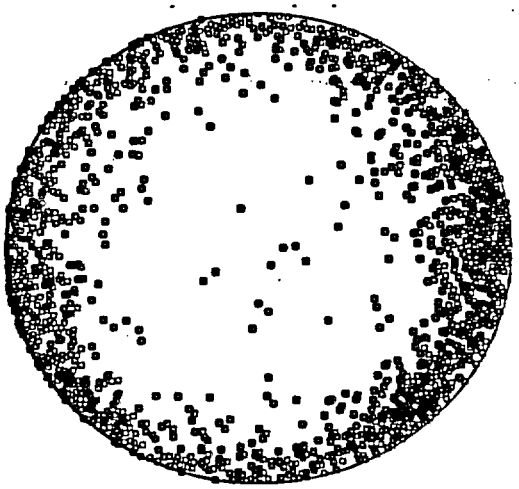

Number of points = 2088

B. Qualified outcrop data

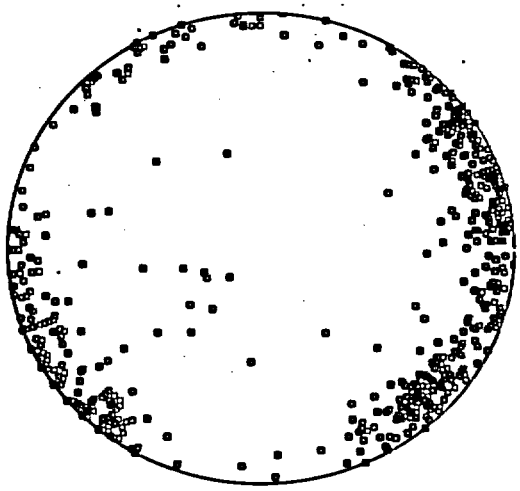

Number of points = 591

C. Qualified subsurface data

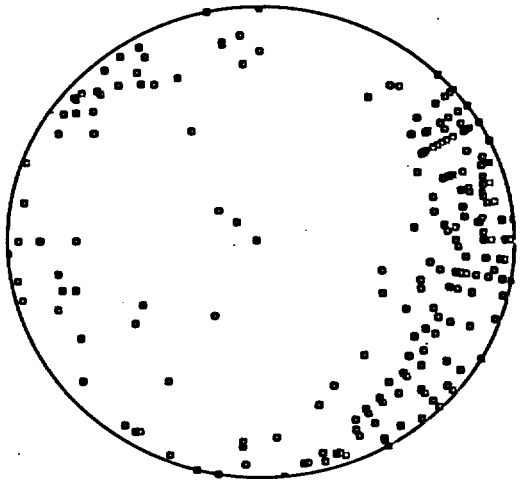

Number of points = 228

Figure 8

A.

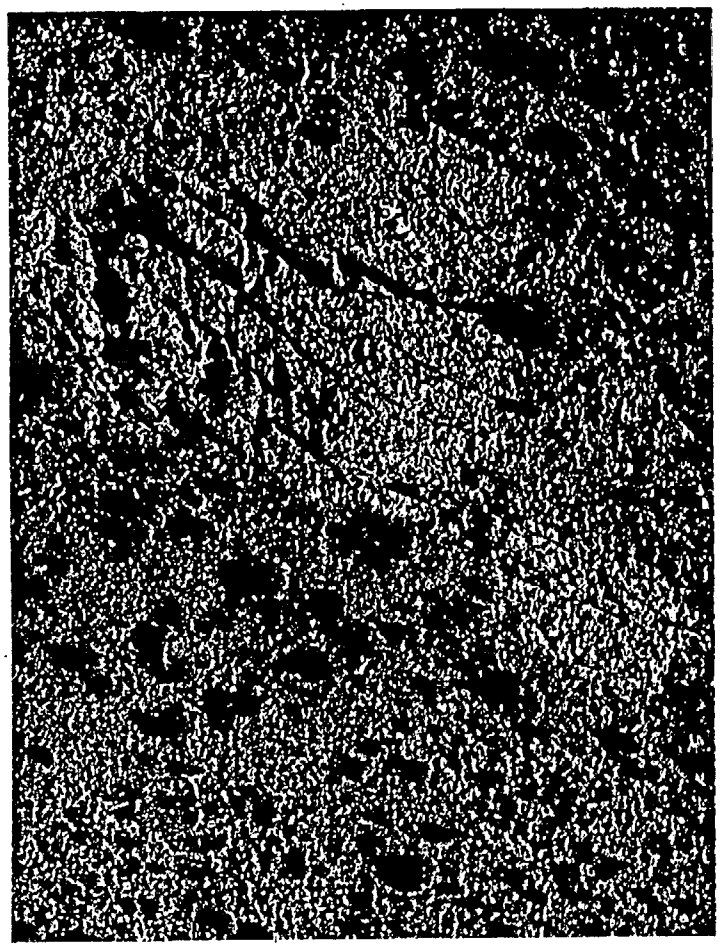

B.

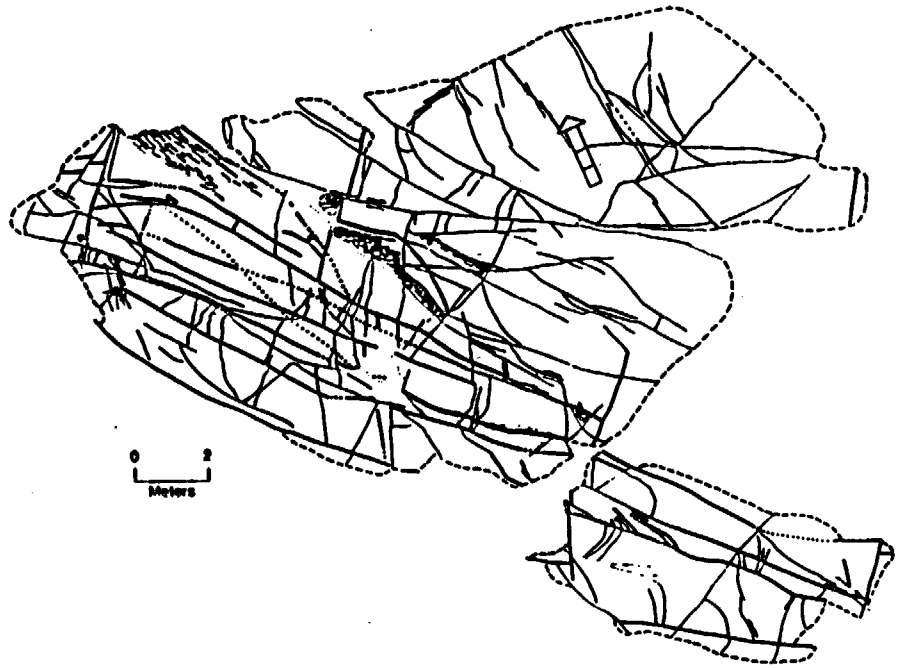

EXPLANATION

- Open joint with tubular structures, dashed where inferred, dotted where healed.
- Open fracture or fault without tubular structures, dashed where inferred, dotted where weathered; arrows showing direction of displacement on faults.
- Intense swarming of fractures less than 20cm long.
- Shallow dipping joint or fracture surface.
- Black hole.
- Vapor-phase silica mineralization along joint or fracture.
- Calcrete in joint, fracture, or fault zone.
- Pavement boundary.
- Fracture serving as part of pavement boundary.
- True-north arrow

Figure 9

B.

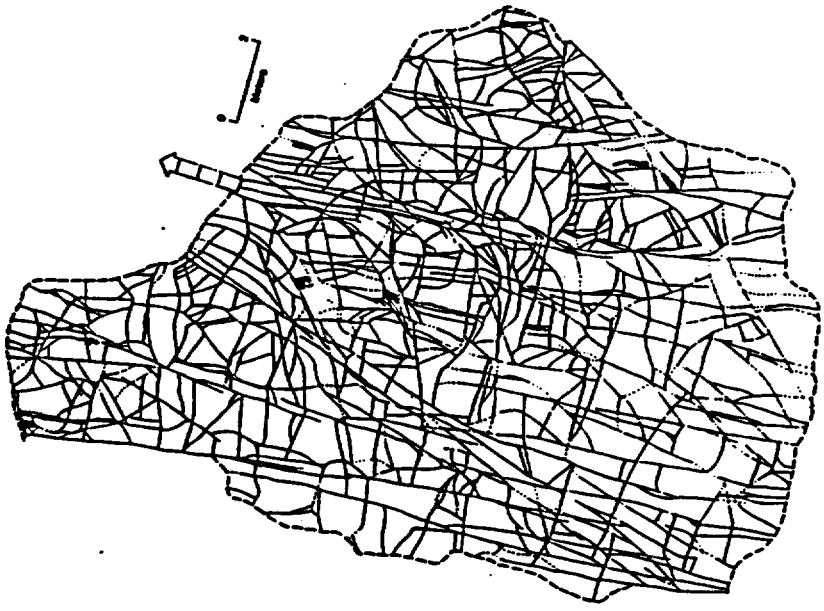

A.

Figure 10

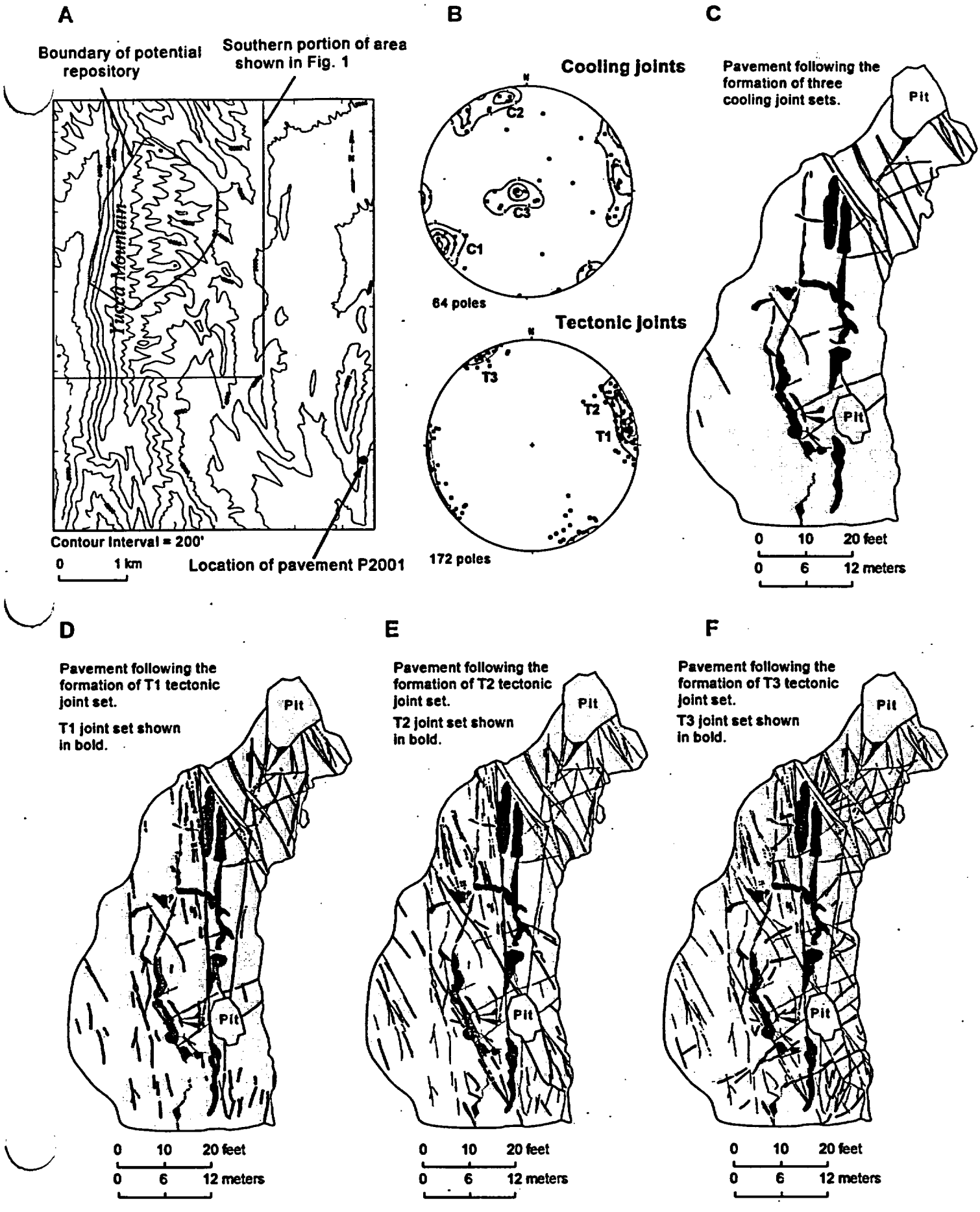
A
Boundary of potential repository
Southern portion of area shown in Fig. 1
Yucca Mountain
Contour Interval = 200'
0 1 km
Location of pavement P2001
B
Cooling joints
C2
C3
C1
64 poles
Tectonic joints
T3
T2
T1
172 poles
C
Pavement following the formation of three cooling joint sets.
Pit
Pit
0 10 20 feet
0 6 12 meters
D
Pavement following the formation of T1 tectonic joint set.
T1 joint set shown in bold.
Pit
Pit
0 10 20 feet
0 6 12 meters
E
Pavement following the formation of T2 tectonic joint set.
T2 joint set shown in bold.
Pit
Pit
0 10 20 feet
0 6 12 meters
F
Pavement following the formation of T3 tectonic joint set.
T3 joint set shown in bold.
Pit
Pit
0 10 20 feet
0 6 12 meters

Figure 11.

A

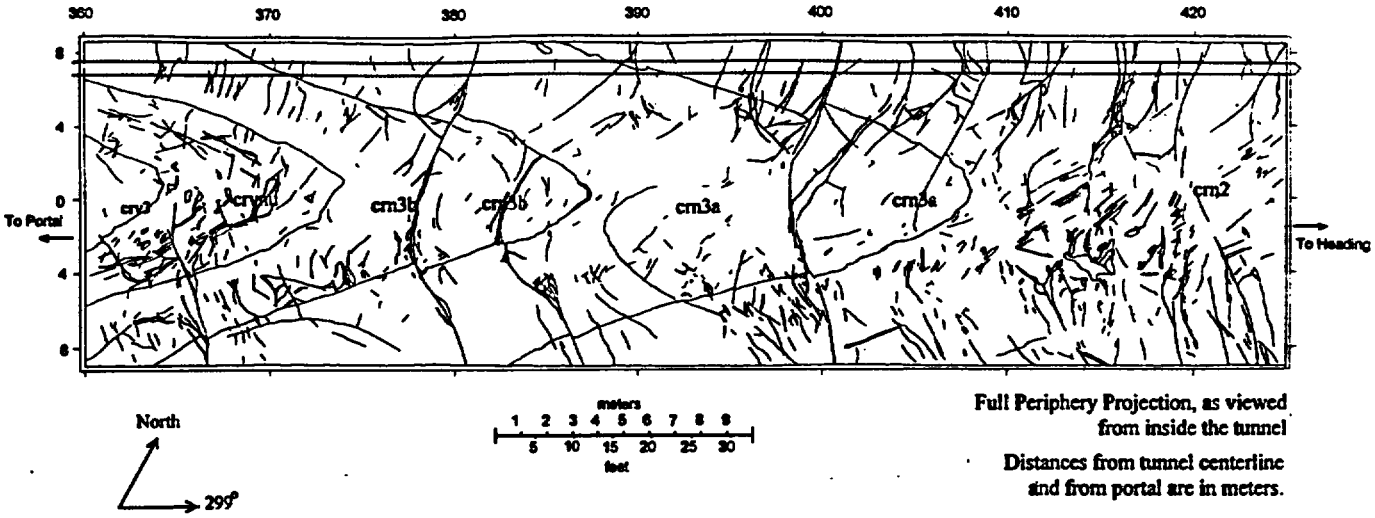

Full Periphery Projection, as viewed from inside the tunnel

Distances from tunnel centerline and from portal are in meters.

EXPLANATION OF MAP SYMBOLS

TIVA CANYON TUFF

Crystal-rich member, vitric zone

- crv3 — Nonwelded to partially welded subzone
- crvnu — Densely welded vitrophyre and subvitrophyre transition

Crystal-rich member, nonlithophysal zone

- crm3b — Pumice-poor subzone
- crm3a — Pumice-poor to mixed-pumice transition subzone
- crv2 — Mixed-pumice subzone

Trace of fracture or fault

Exposed fracture face

Location of detailed line survey

Conceptual development of the full periphery projection.

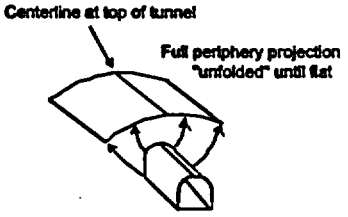

B

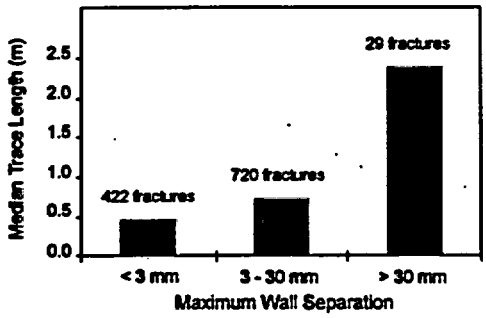

C

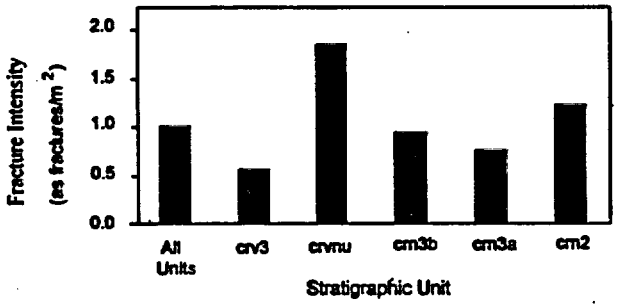

D

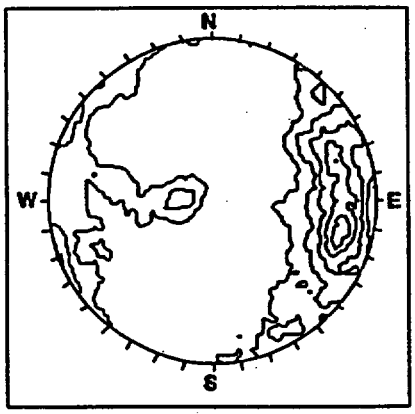

Contoured stereonet based on 978 poles to fractures planes, plotted on lower hemisphere, equal area projection.

Contours are drawn based on percentage of poles per one percent area.

Contour interval 1 percent, maximum concentration is 5.83 percent.

Figure 12

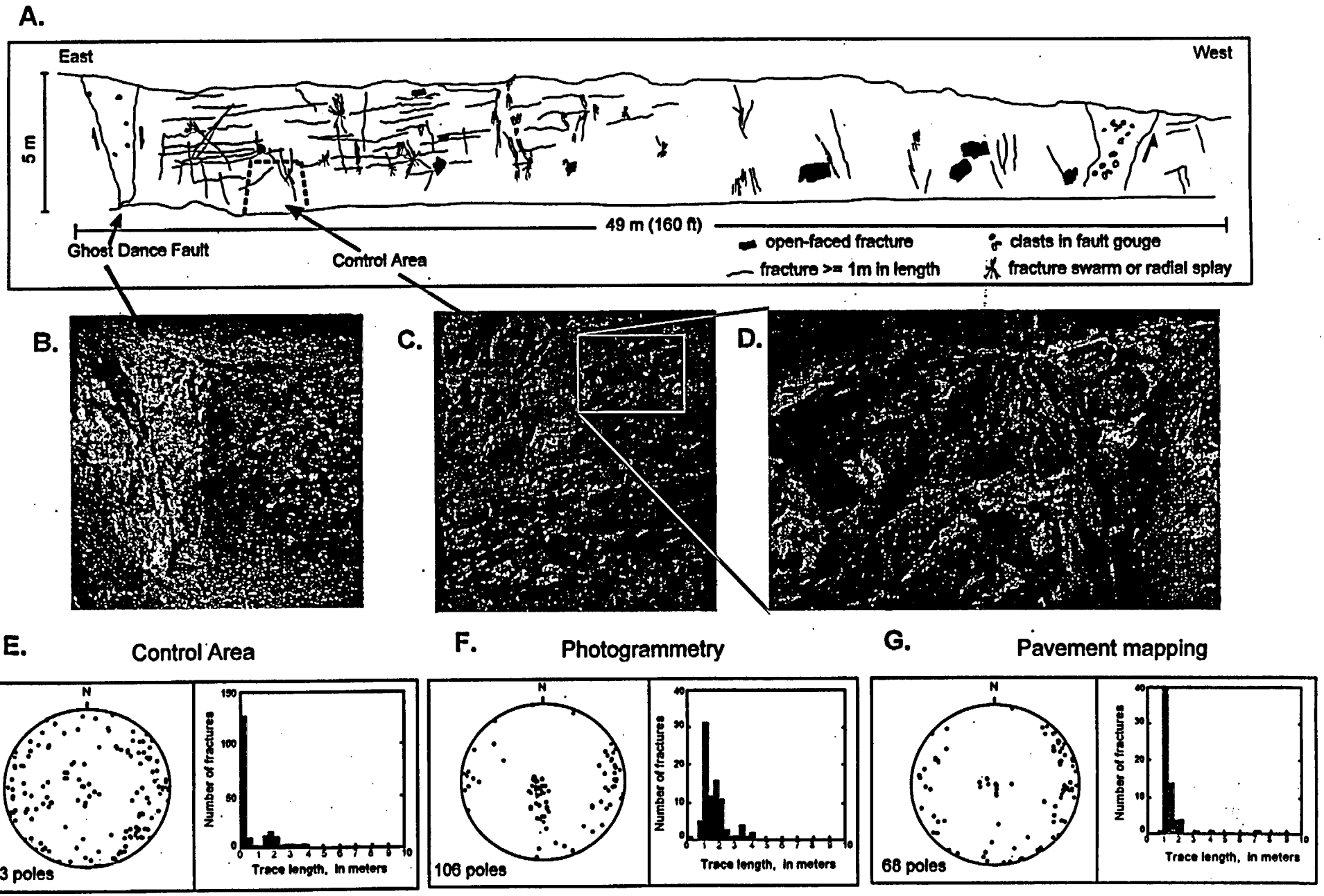
A.
East
West
5 m
49 m (160 ft)
Ghost Dance Fault
Control Area
open-faced fracture
fracture >= 1m in length
clasts in fault gouge
fracture swarm or radial splay
B.
C.
D.
E.
Control Area
F.
Photogrammetry
G.
Pavement mapping
N
143 poles
106 poles
68 poles
Number of fractures
Trace length, in meters

Figure 13.

Tiva Canyon Tuff - Crystal Rich Member

A. Qualified Surface Data

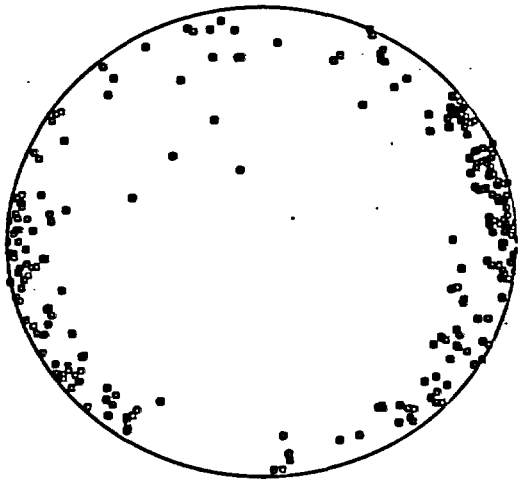

Number of points = 266

B. Qualified Subsurface Data: DLS

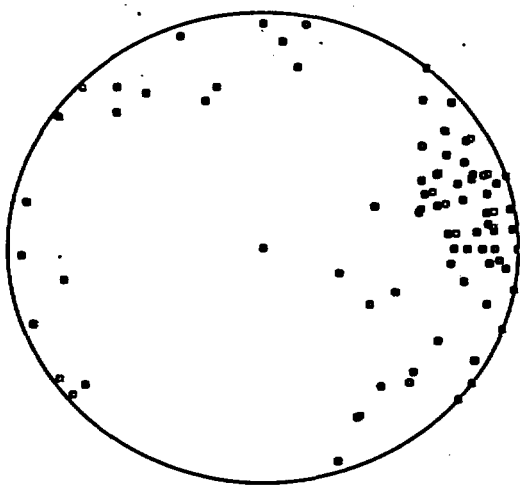

Number of points = 93

C. Qualified Subsurface Data: Photogrammetry

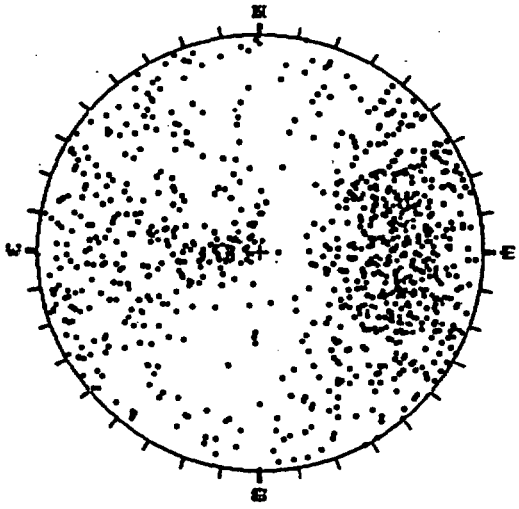

Figure 14

Tiva Canyon Tuff Crystal-Poor Member

A. Upper Lithophysal Zone

Qualified Surface Data

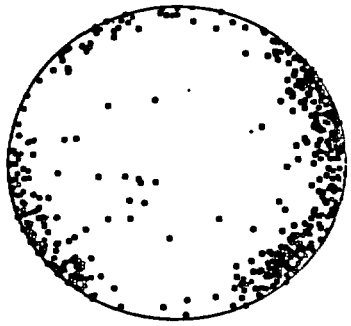

Number of points = 591

Qualified Subsurface Data

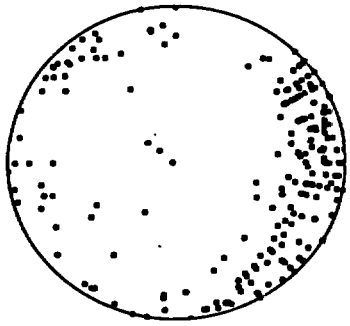

Number of points = 228

Non-qualified Surface Data

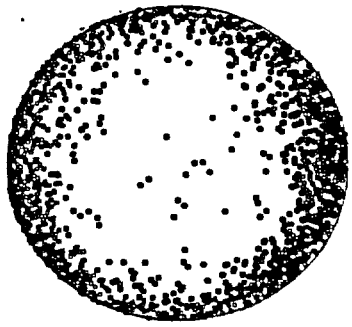

Number of points = 2088

B. Middle NonLithophysal Zone

Qualified surface data (Global Inventory)

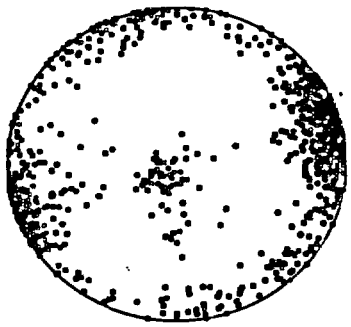

Number of points = 1069

Qualified Subsurface Data

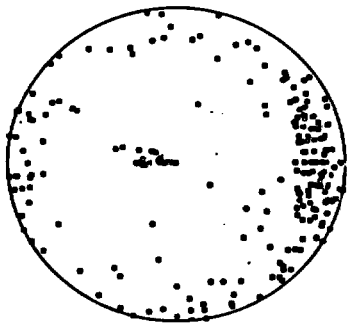

Number of points = 267

Qualified surface data (Selective Inventory)

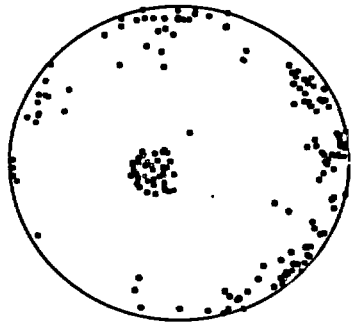

Number of points = 186

Figure 15

Tiva Canyon Tuff Crystal-Poor Member

C. Lower Lithophysal Zone

Qualified surface data (Global Inventory)

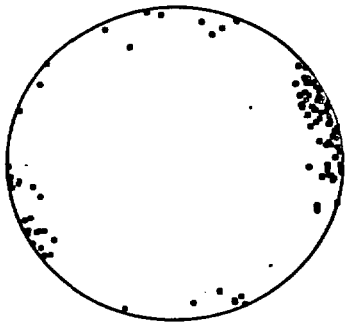

Number of points = 113

Qualified Subsurface Data

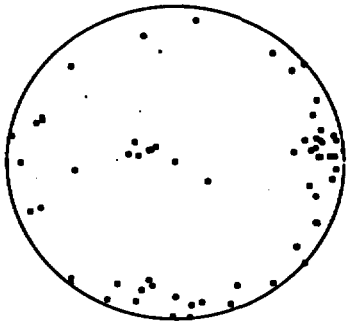

Number of points = 67

Qualified surface data (Selective Inventory)

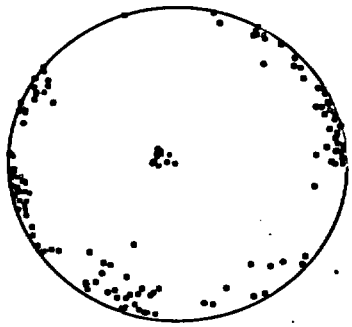

Number of points = 158

D. Lower Nonlithophysal Zone

Qualified surface data (Global Inventory)

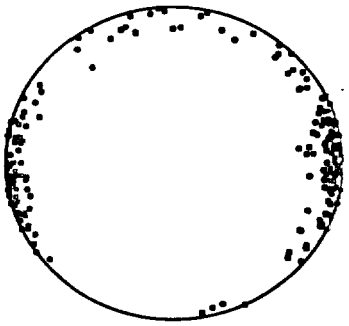

Number of points = 266

Qualified Subsurface Data

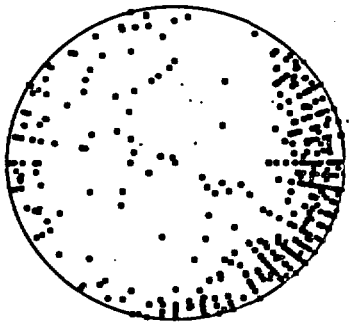

Number of points = 507

Qualified surface data (Selective Inventory)

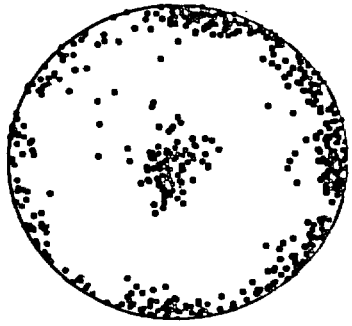

Number of points = 592

Figure 15
(continued)

Lithostratigraphic Units Within the PTn Hydrologic Unit

A. Qualified Surface Data

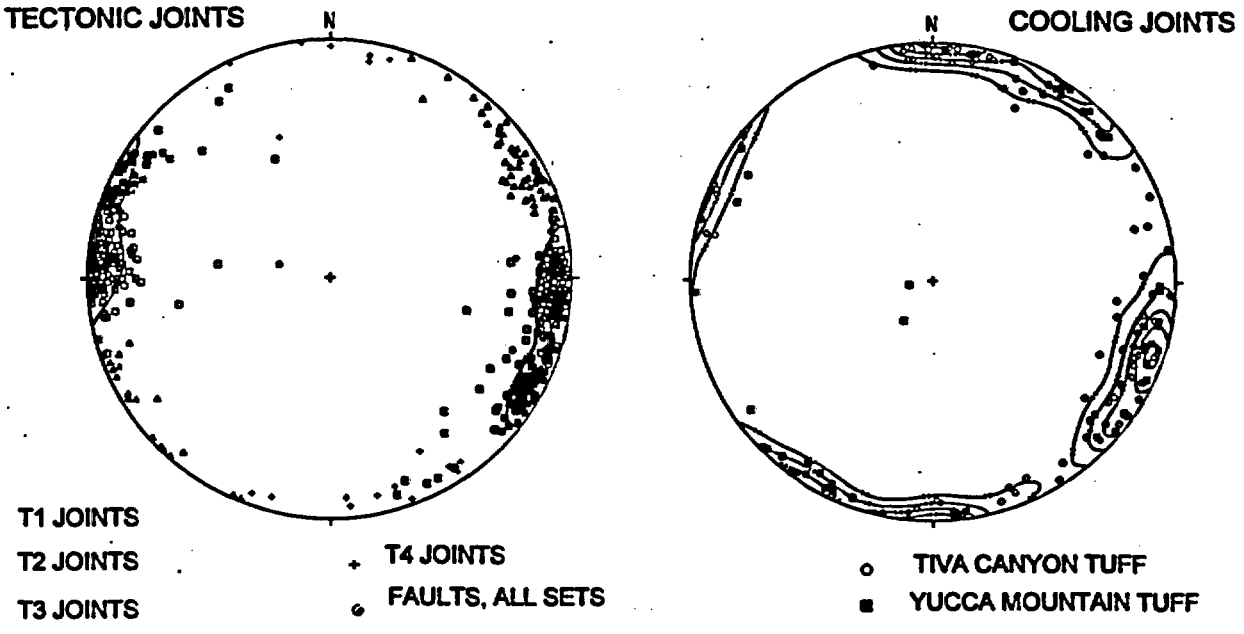

B. Qualified Subsurface Data

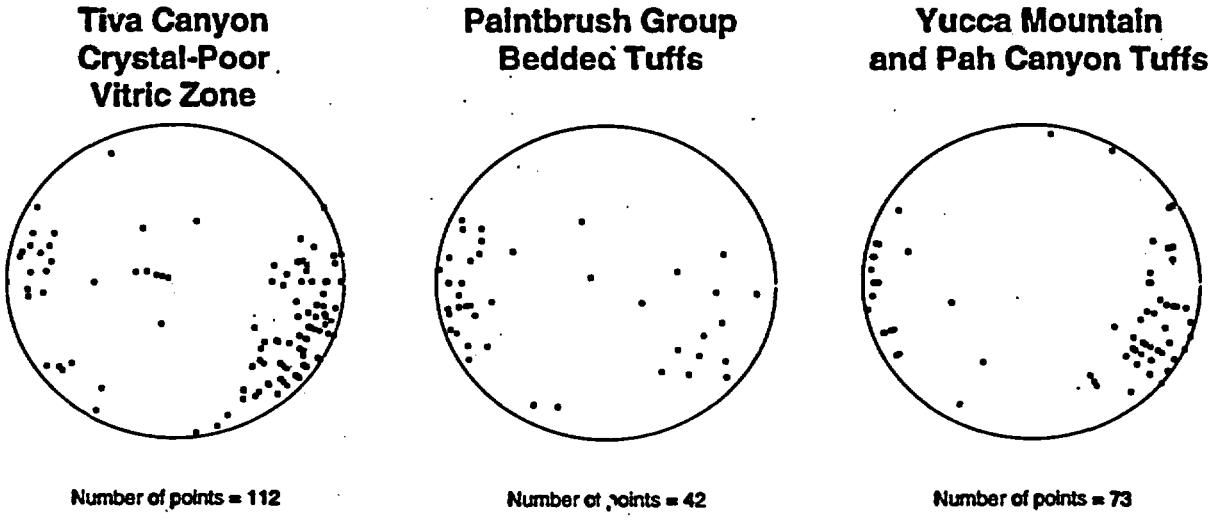

Figure 16

Topopah Spring Tuff

Crystal-Rich Member

Qualified Subsurface Data

Vitric Zone

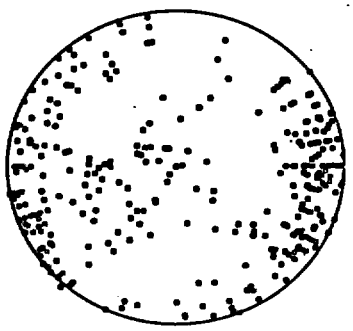

Number of points = 358

Nonlithophysal Zone

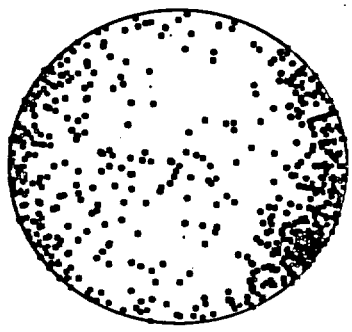

Number of points = 819

Figure 17

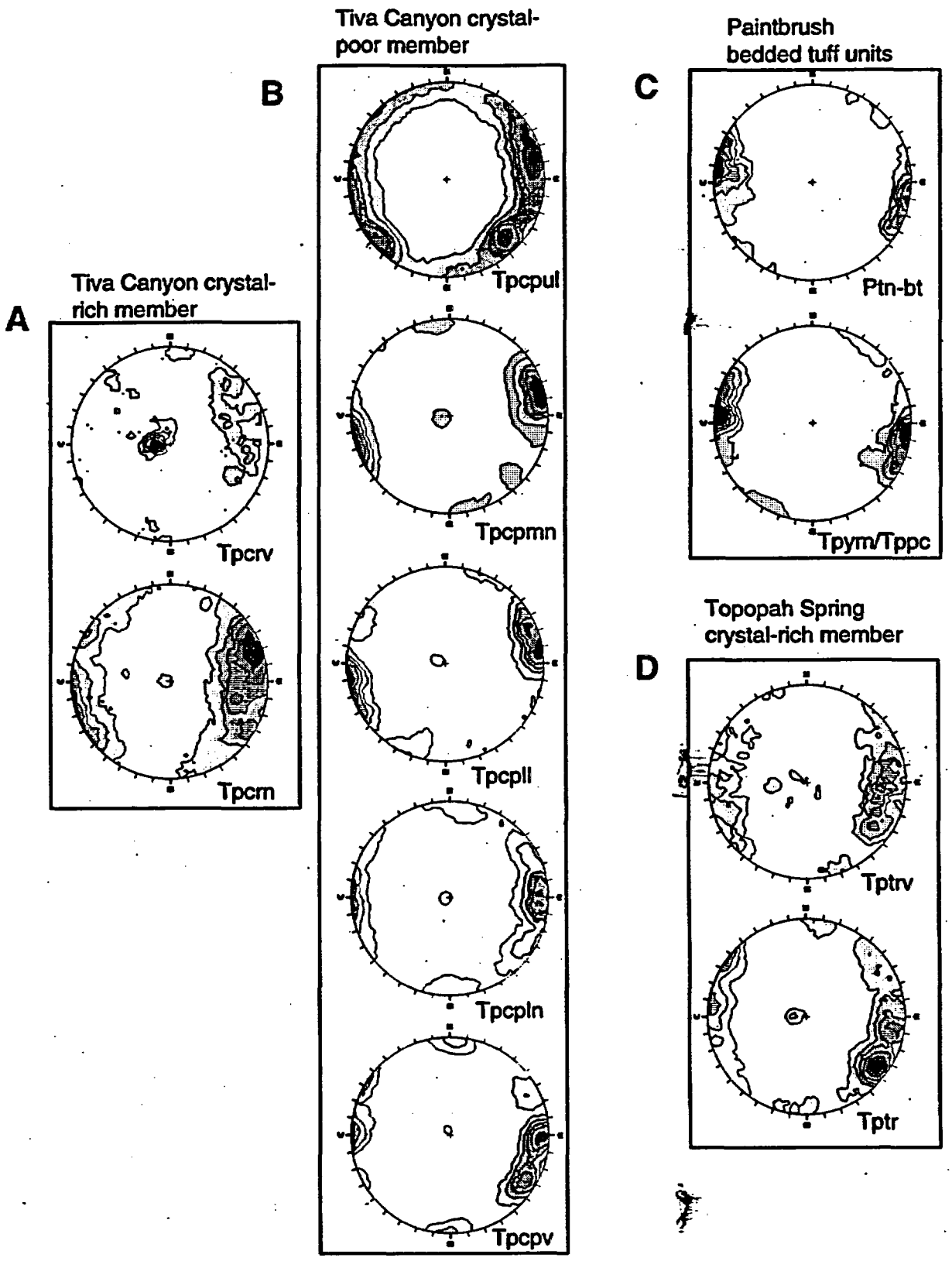
A
Tiva Canyon crystal-rich member
Tpcrv
Tpcm
B
Tiva Canyon crystal-poor member
Tpcpul
Tpcpmn
Tpcpll
Tpcpln
Tpcpv
C
Paintbrush bedded tuff units
Ptn-bt
Tpym/Tppc
D
Topopah Spring crystal-rich member
Tptrv
Tptr

Figure 18

Possible cooling joints, selected on the basis of roughness
(Joint roughness coefficient less than 3)

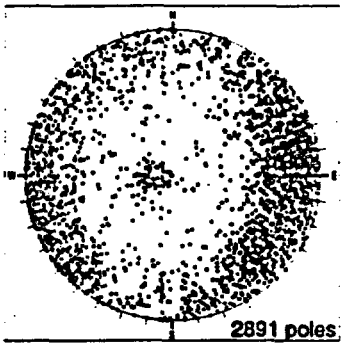

Pole plot of fractures. Lower hemisphere projection.

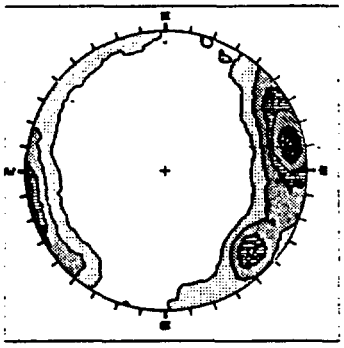

Contour plot of poles. Max. concentration = 8.86%

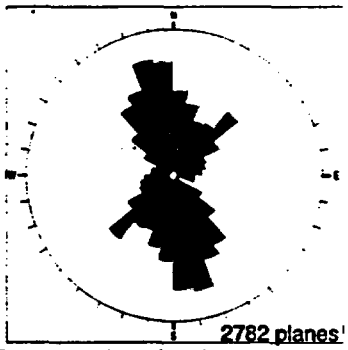

Rosette plot of strike azimuths.

A

Fractures definitively identified as cooling joints by the observer

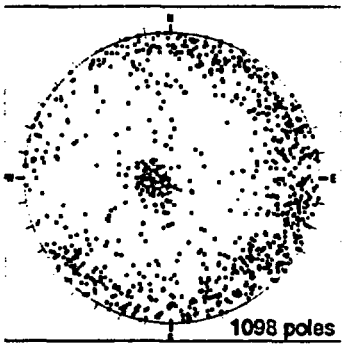

Pole plot of fractures. Lower hemisphere projection.

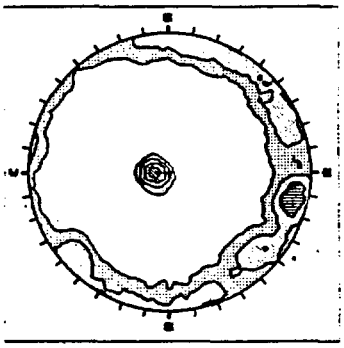

Contour plot of poles. Max. concentration = 7.65%.

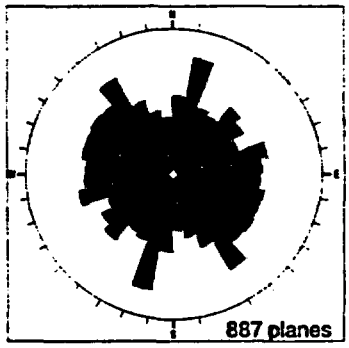

Rosette plot of strike azimuths.

B

Figure 19

Possible tectonic joints, selected on the basis of roughness
(Joint roughness coefficient greater than 2)

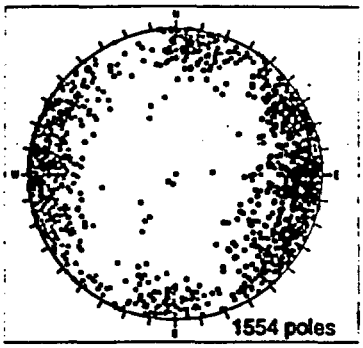

Pole plot of fractures. Lower hemisphere projection.

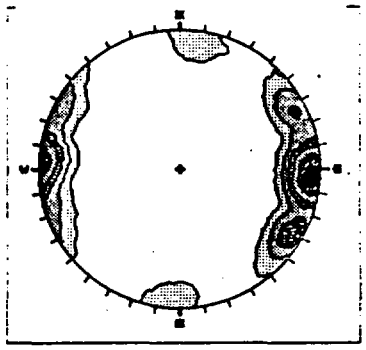

Contour plot of poles. Max. concentration = 13.51%

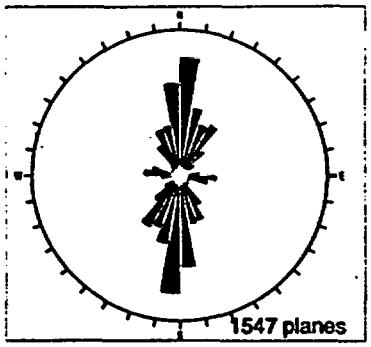

Rosette plot of strike azimuths.

A

Fractures definitively identified as tectonic joints by the observer

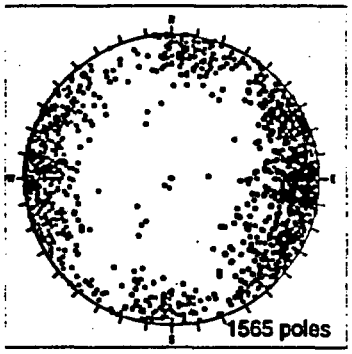

Pole plot of fractures. Lower hemisphere projection.

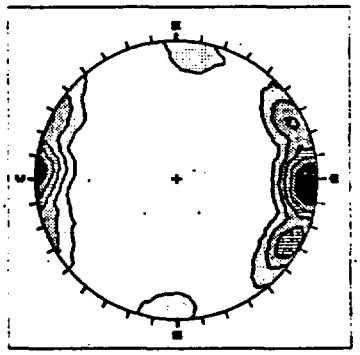

Contour plot of poles. Max. concentration = 13.42%

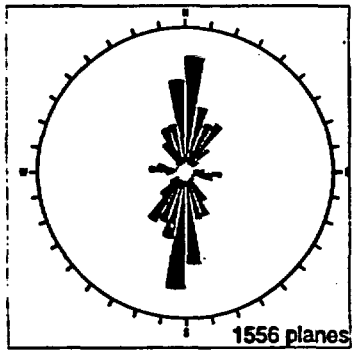

Rosette plot of strike azimuths.

B

Figure 20

A. TOPOPAH SPRING TUFF - PAVEMENT P2001, FRAN RIDGE

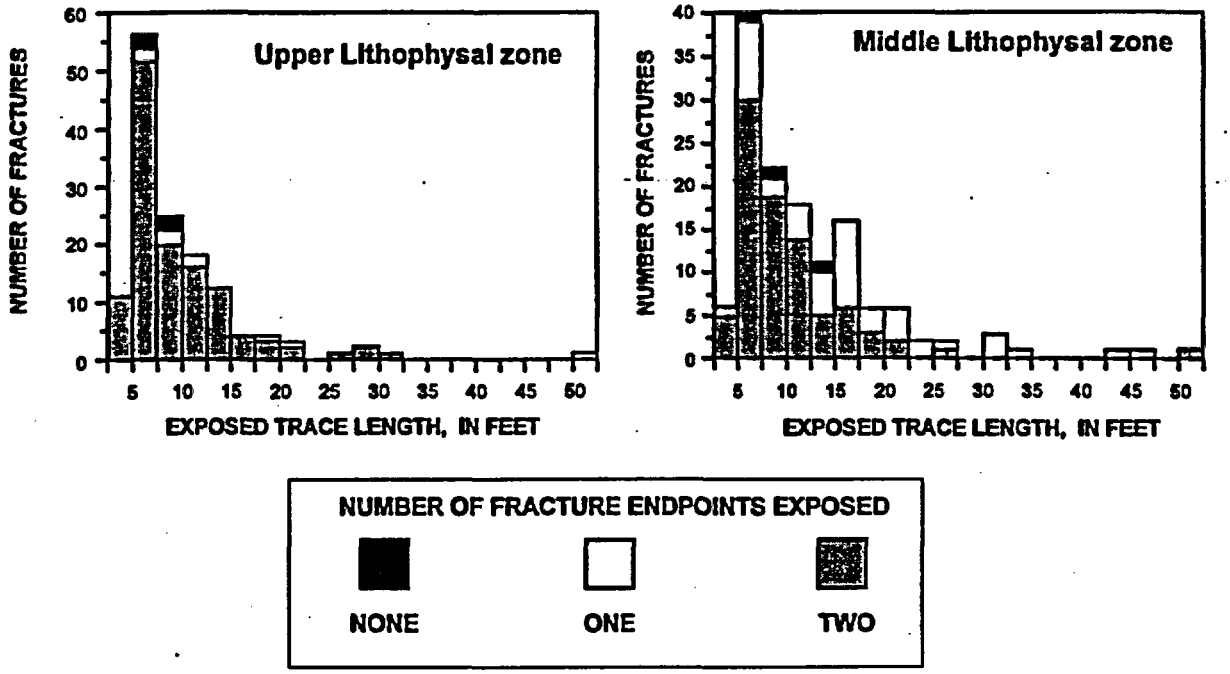

B. LITHOSTRATIGRAPHIC UNITS WITHIN THE PTn HYDROLOGIC UNIT

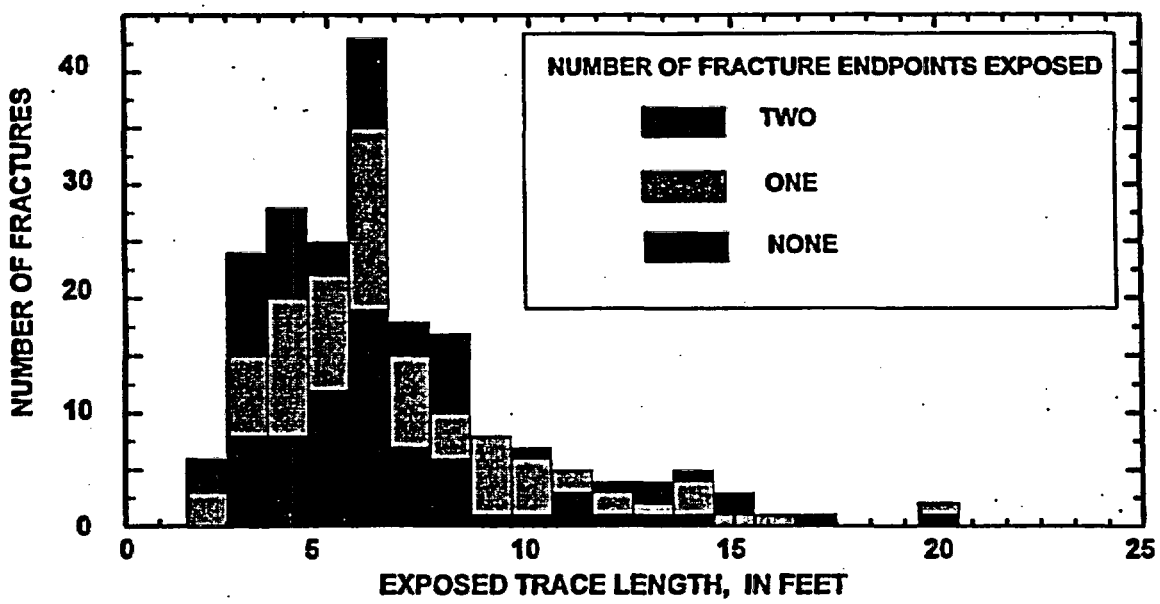

Figure 21

Fracture trace lengths, ESF detailed line survey

Tiva Canyon Tuff
Crystal-rich
nonlithophysal zone

Tpcrn

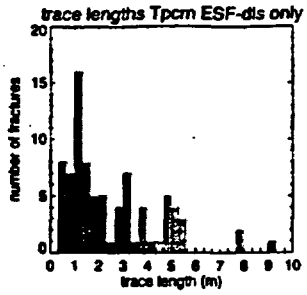

Tiva Canyon Tuff
upper lithophysal zone

Tpcpul

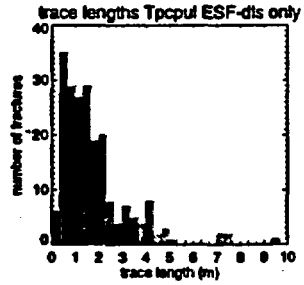

Tiva Canyon Tuff
middle nonlithophysal zone

Tpcpmn

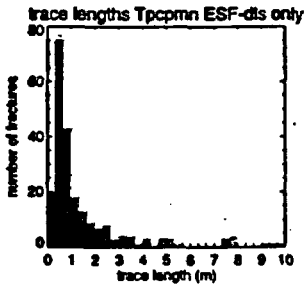

Tiva Canyon Tuff
lower lithophysal zone

Tpcpll

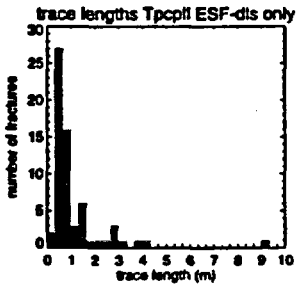

Tiva Canyon Tuff
lower nonlithophysal zone

Tpcpln

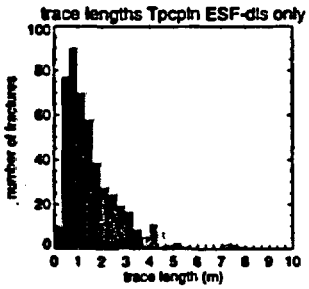

Tiva Canyon Tuff
crystal-poor vitric zone

Tpcpv

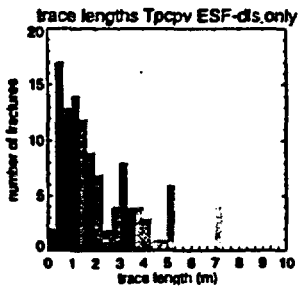

Pah Canyon Tuff,
Yucca Mountain Tuff

Tpp/Tpy

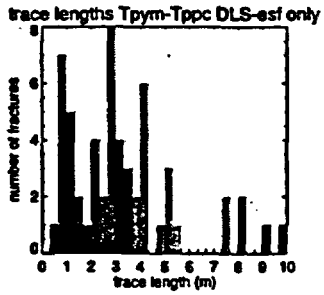

Paintbrush Group
bedded tuffs

Tpbt

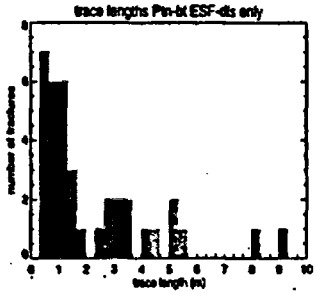

Topopah Spring Tuff
Crystal-rich member

Tptr

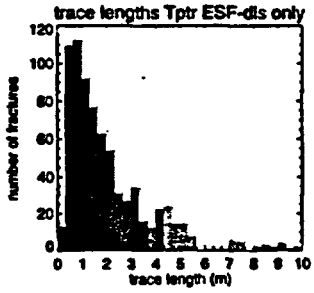

Figure 22

Fracture trace lengths, qualified and nonqualified surface data

Tiva Canyon Tuff
Crystal-rich
nonlithophysal zone

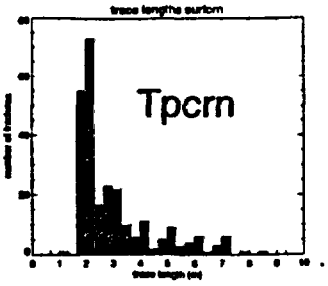

Tiva Canyon Tuff
upper lithophysal zone

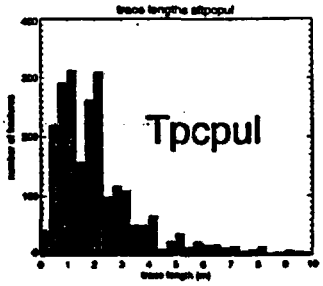

Tiva Canyon Tuff
middle nonlithophysal zone

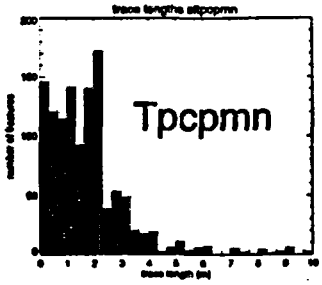

Tiva Canyon Tuff
lower lithophysal zone

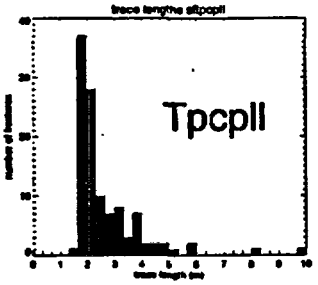

Tiva Canyon Tuff
lower nonlithophysal zone

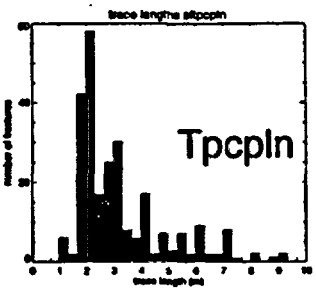

Tiva Canyon Tuff
crystal-poor vitric zone

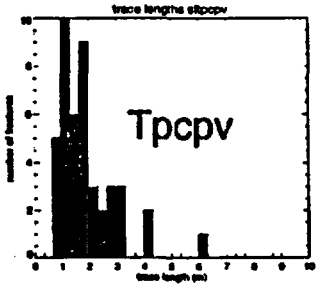

Pah Canyon Tuff,
Yucca Mountain Tuff

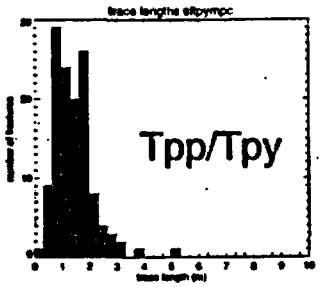

Paintbrush Group
bedded tuffs

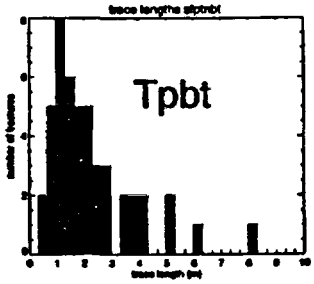

Topopah Spring Tuff
Crystal-rich member

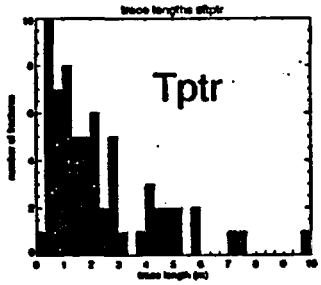

Topopah Spring Tuff
upper lithophysal zone

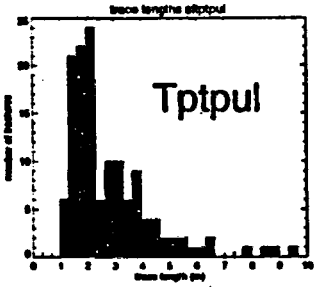

Topopah Spring Tuff
middle nonlithophysal
zone

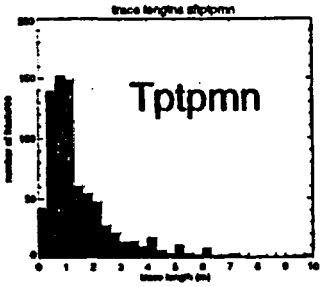

Figure 23

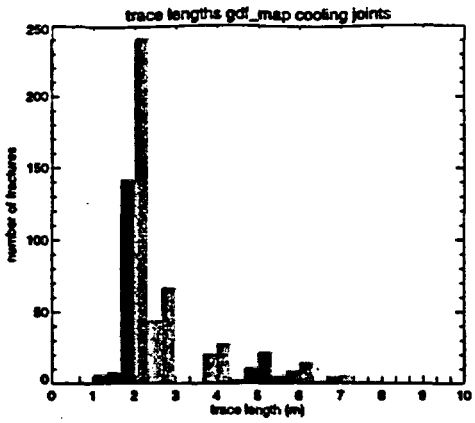

Fractures with roughnes <3 from the Ghost Dance fault mapping data set.

A

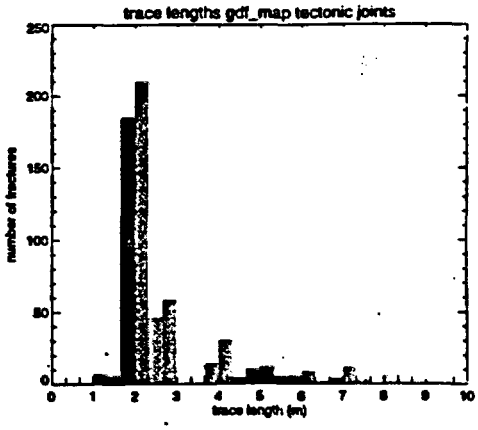

Fractures with roughness >2 from the Ghost Dance fault mapping data set

B

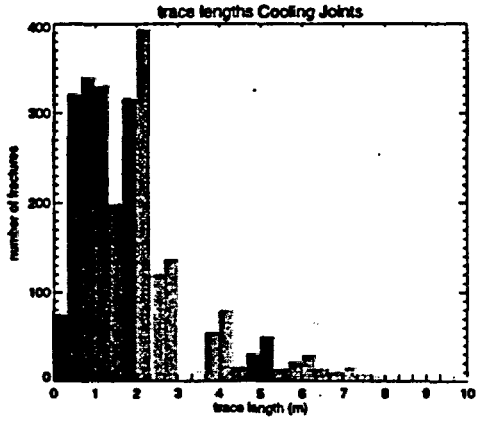

All fractures with joint roughness coefficient less than 3

C

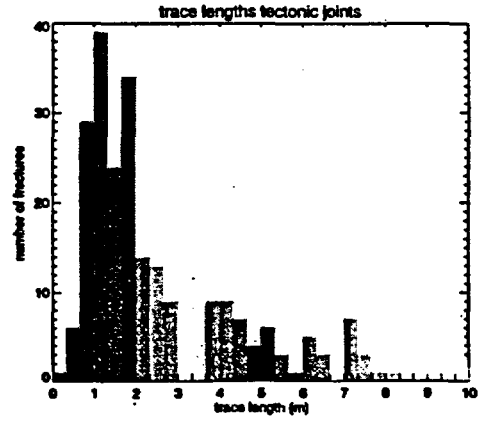

All fractures with joint roughness coefficient greater than 2

D

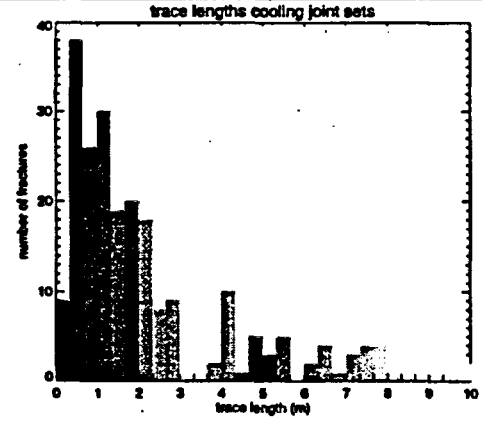

All fractures definitively identified as cooling joints by the observer

E

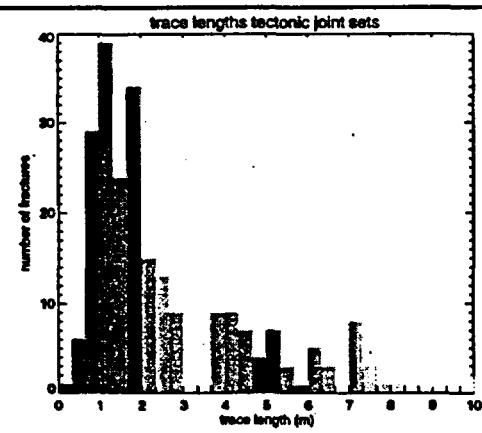

All fractures definitively identified as tectonic joints by the observer

F

Figure 24

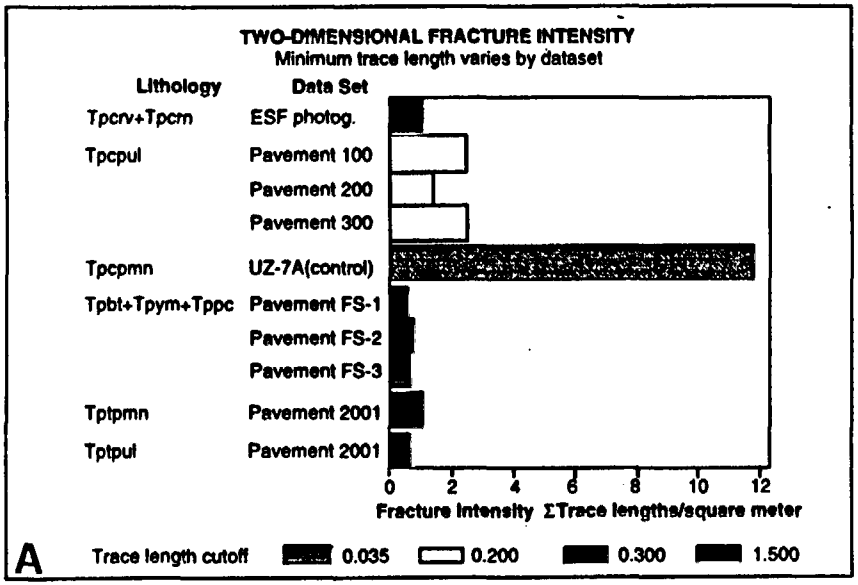
TWO-DIMENSIONAL FRACTURE INTENSITY
Minimum trace length varies by dataset
Lithology
Data Set
Tpcrv+Tpcrn
ESF photog.
Tpcpul
Pavement 100
Pavement 200
Pavement 300
Tpcpmn
UZ-7A(control)
Tpbt+Tpym+Tppc
Pavement FS-1
Pavement FS-2
Pavement FS-3
Tptpmn
Pavement 2001
Tptpul
Pavement 2001
0 2 4 6 8 10 12
Fracture Intensity ΣTrace lengths/square meter
A
Trace length cutoff
0.035
0.200
0.300
1.500

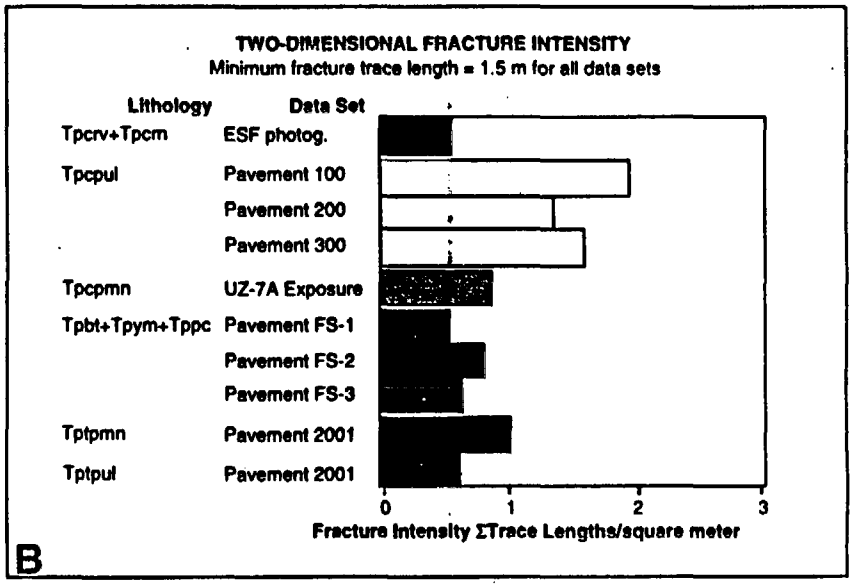
TWO-DIMENSIONAL FRACTURE INTENSITY
Minimum fracture trace length = 1.5 m for all data sets
Lithology
Data Set
Tpcrv+Tpcrn
ESF photog.
Tpcpul
Pavement 100
Pavement 200
Pavement 300
Tpcpmn
UZ-7A Exposure
Tpbt+Tpym+Tppc
Pavement FS-1
Pavement FS-2
Pavement FS-3
Tptpmn
Pavement 2001
Tptpul
Pavement 2001
0 1 2 3
Fracture Intensity ΣTrace Lengths/square meter
B

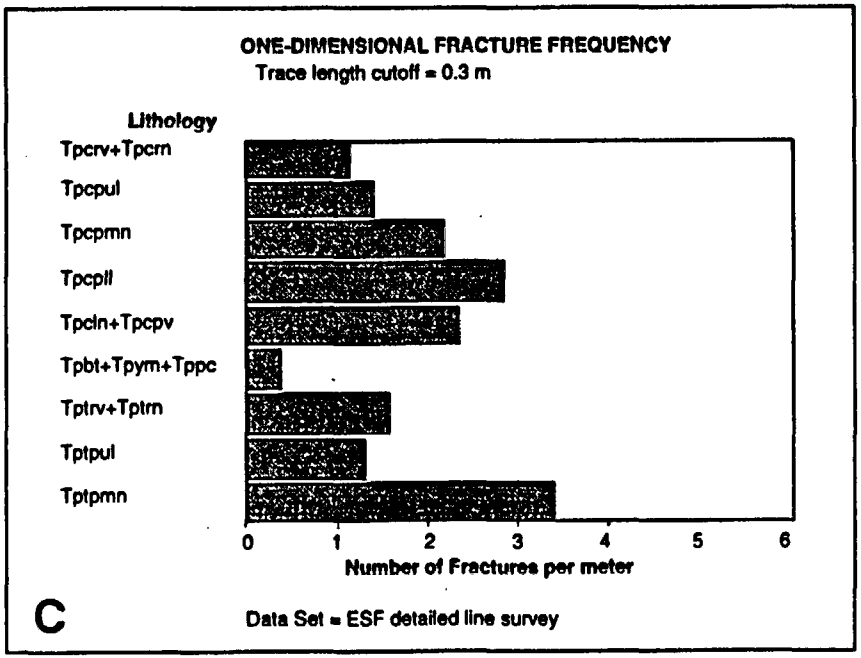
ONE-DIMENSIONAL FRACTURE FREQUENCY
Trace length cutoff = 0.3 m
Lithology
Tpcrv+Tpcrn
Tpcpul
Tpcpmn
Tpcpll
Tpcln+Tpcpv
Tpbt+Tpym+Tppc
Tptrv+Tptrn
Tptpul
Tptpmn
0 1 2 3 4 5 6
Number of Fractures per meter
C
Data Set = ESF detailed line survey

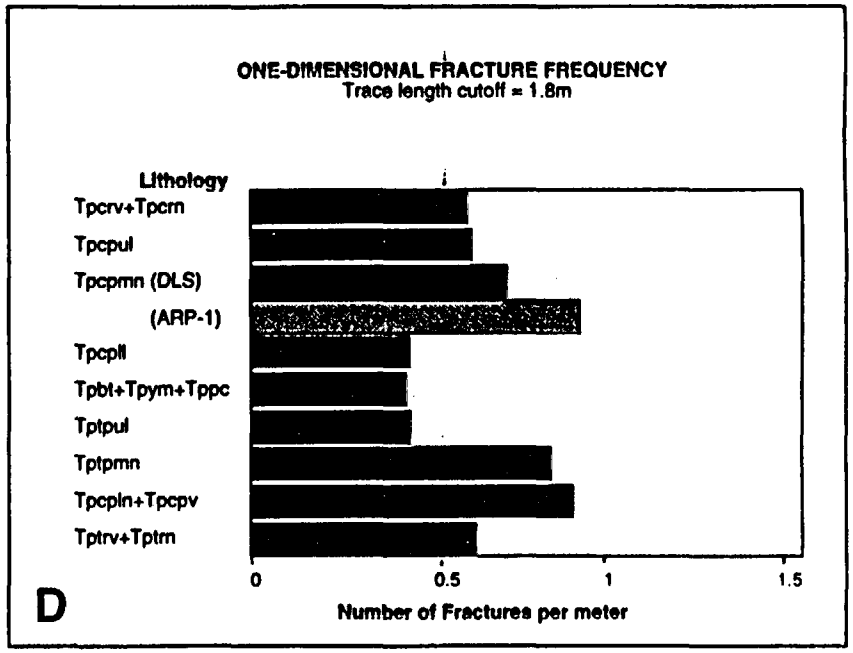
ONE-DIMENSIONAL FRACTURE FREQUENCY
Trace length cutoff = 1.8m
Lithology
Tpcrv+Tpcrn
Tpcpul
Tpcpmn (DLS)
(ARP-1)
Tpcpll
Tpbt+Tpym+Tppc
Tptpul
Tptpmn
Tpcpln+Tpcpv
Tptrv+Tptrn
0 0.5 1 1.5
Number of Fractures per meter
D

Figure 25

A

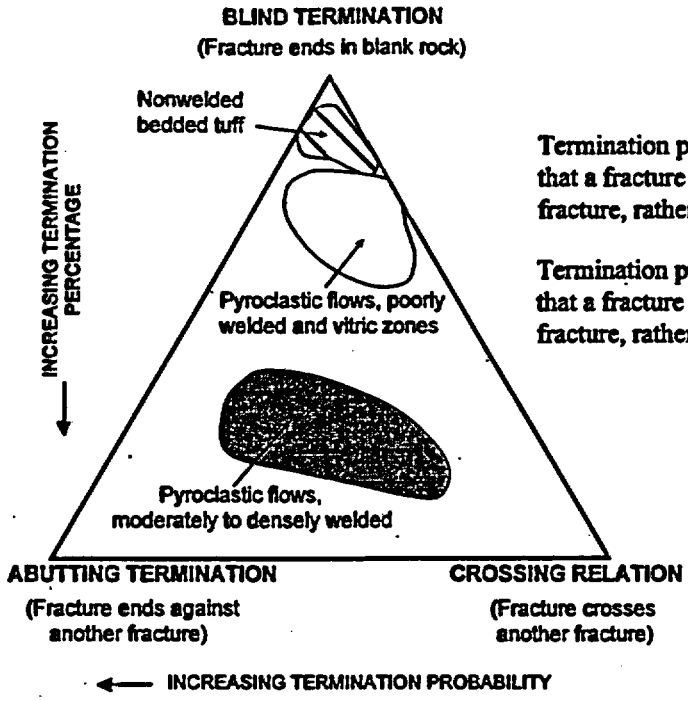

Termination percentage is the liklihood that a fracture will interact with another fracture, rather than end in blank rock.

Termination probability is the liklihood that a fracture will abut an earlier formed fracture, rather than cross it.

B

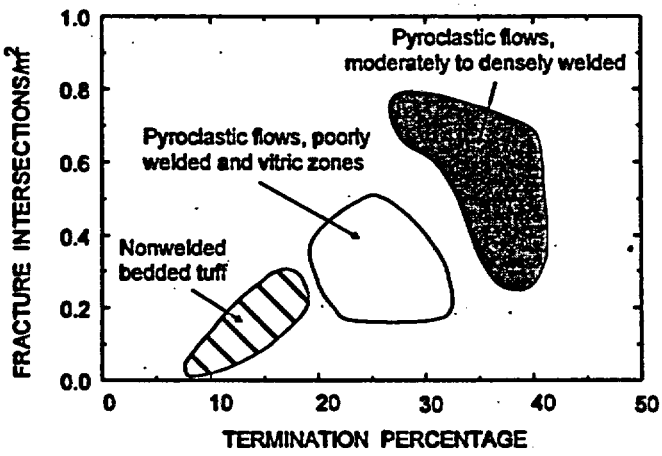

DATA SOURCES FOR THE ABOVE DIAGRAMS

Data for moderately to densely welded pyroclastic flows are from geometric analysis of three cleared exposures constructed in the upper lithophysal zone of the Tiva Canyon Tuff (Barton et al., 1993) and from pavement P2001in the middle nonlithophysal and upper lithophysal zones of the Topopah Spring Tuff (Sweetkind, Verbeek, Singer and others, 1995).

Data for poorly welded pyroclastic flows, vitric zones of pyroclastic flows, and bedded tuffs are from geometric analysis of maps of three natural exposures in the interval separating the Topopah Spring and the Tiva Canyon Tuff (Sweetkind, Verbeek, Geslin and Moyer, 1995). Poorly welded pyroclastic flows include the Pah Canyon and Yucca Mountain Tuffs (Sawyer et al., 1993). The vitric zone is the vitric base of the Tiva Canyon Tuff.

Figure 26.

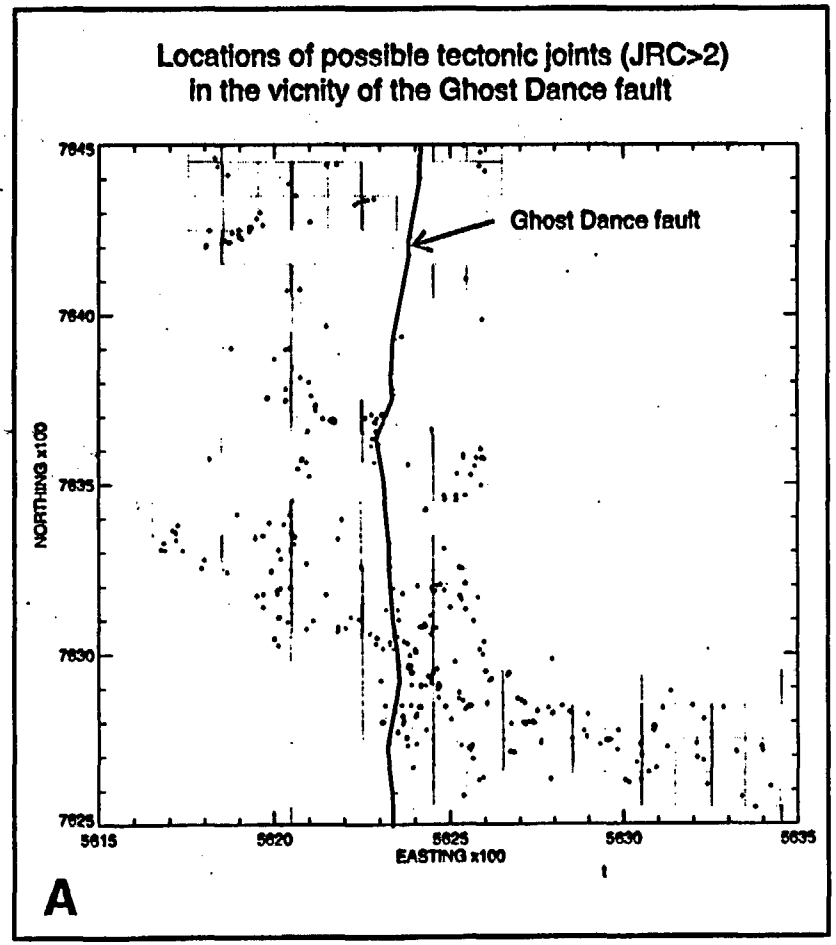
Locations of possible tectonic joints (JRC>2)
in the vicnity of the Ghost Dance fault
Ghost Dance fault
NORTHING x100
7645
7640
7635
7630
7625
5615
5620
5625
5630
5635
EASTING x100
A

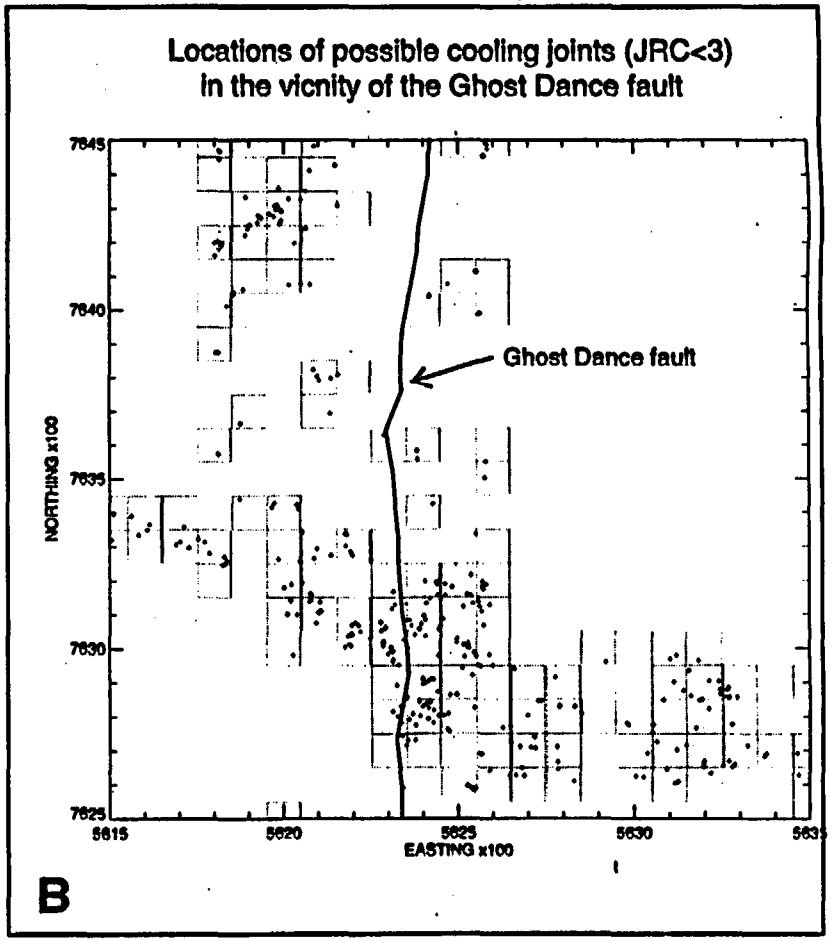
Locations of possible cooling joints (JRC<3)
in the vicnity of the Ghost Dance fault
Ghost Dance fault
NORTHING x100
7645
7640
7635
7630
7625
5615
5620
5625
5630
EASTING x100
B

Figure 27

Possible cooling joints (Joint roughness coefficient < 3)
Measured during 1:240 mapping near the Ghost Dance fault

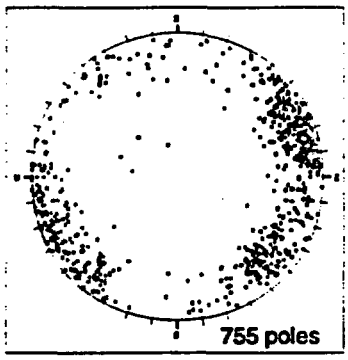

Pole plot of fractures. Lower hemisphere projection.

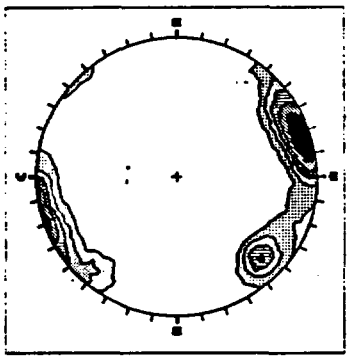

Contour plot of poles. Max. concentration = 15.89%

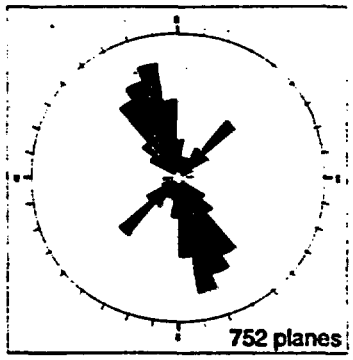

Rosette plot of strike azimuths.

A

Possible tectonic joints (Joint roughness coefficient > 2)
Measured during 1:240 mapping near the Ghost Dance fault

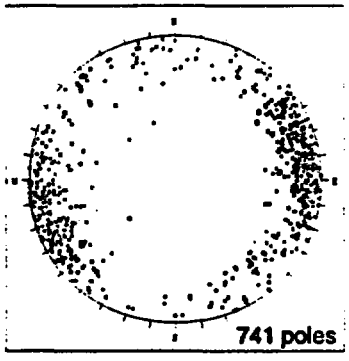

Pole plot of fractures. Lower hemisphere projection.

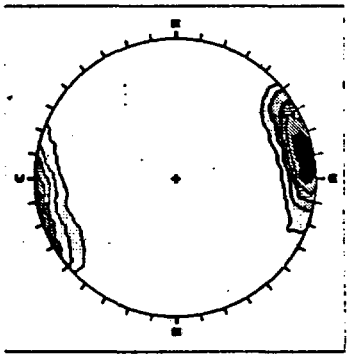

Contour plot of poles. Max. concentration = 18.49%

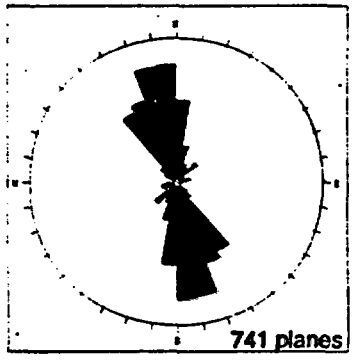

Rosette plot of strike azimuths.

B

Figure 28